

Alma Mater Studiorum – Università di Bologna

DOTTORATO DI RICERCA IN
Scienze Biochimiche e Biotecnologiche

Ciclo XXIX

Settore Concorsuale di afferenza: 07/H1
Settore Scientifico disciplinare: VET/02

**Early markers of microglia activation
in inflammatory diseases**

Presentata da

Nozha Borjini
Ph.D. candidate

Relatore

Prof. Laura Calzà

Co-Relatore

Prof.Dr. Lydia Sorokin

Coordinatore Dottorato

Prof. Santi Mario Spampinato

Esame finale anno 2017

*« Life is not easy for any of us. But what of that? We must have pre-severance
and above all confidence in ourselves. We must believe that we are
gifted for something and that thing must be attained. »*

Marie Skłodowska Curie (1867-1934)

ACKNOWLEDGEMENTS

This thesis is the culmination of my journey of Ph.D which was just like climbing a high peak step by step accompanied with encouragement, hardship, trust, dedication and sacrifice of many people to whom I would like to express my deepest gratitude for helping me directly or indirectly to make this thesis possible.

Special thanks are extended to:

Prof. Laura Calzà and **Prof. Luciana Giardino** for giving me the opportunity to work with them in such interesting project, for their highly scientific guidance and also for their enormous kindness and helpful.

Dr. Fabrizio Facchinetti for being part of such huge team of Chiesi Farmaceutici spA, for his support and encouragement during the difficult moments.

I have truly enjoyed the atmosphere of solidarity, friendship, happiness and support which is characteristic of IRET's Lab. Many thanks to **Mercy, Roby, Anto, Sandra, Alessandro, Chiara, Alessandra, Luca, Marco, Andrea** and **Maura**.

Prof. Dr. Lydia Sorokin my co-supervisor, for giving me the opportunity to realize my secondment in the Institute of Physiological Chemistry and Pathobiochemistry - Universität Münster. It was very exciting to be part of such an excellent lab. I would like also to thank all the members, **Omar, Eva, Hanna, Miriam** and **Mélanie** for their expertise, help and constructive comments.

I would like to express my most sincere gratitude to all my friends in Tunisia, Germany and Montpellier especially **Dr. Bénédicte Fauvel** and **Dr. Bénédicte Cazal** for their contribution, support and encouragement. A big Thank you goes also to my **Marie Curie Network – nEUROinflammation**. Being part of such network is really a two way street: giving and receiving. I have watched and been inspired by so many people in the network that have given me the courage, strength and power of example to keep going and get through.

Family is the most important thing in the world. And I have been blessed by a good one! I owe thanks to a very special person, my beloved partner **Amine**, for being a constant source of support and encouragement. I am truly thankful for having you in my life, you have been patient with me when I'm frustrated, you celebrate with me

when even the littlest things go right, and you are there whenever I need you.

To my sisters **Angel** and **Nadia**, for their selfless love, care and dedicated efforts which contributed a lot for completion of my thesis. To my nephew **Souma** and my niece **Sirina** who have brought great joy to my life.

Finally, my deepest gratitude goes to **mom Latifa** and **dad Kacem** that always believed in me and supported me with their love. You made me live the wonderful childhood that has made me who I am now. Words alone can't express how much I owe you. I consider myself the luckiest in the world to have such a lovely and caring family, for giving me the strength and patience to work through all these years so that today I can stand proudly with my head held high.

My sincere apologies and many thanks to those I have missed in this section.

To my parents,

List of abbreviations

ADAMs: anchored disintegrin metallo-proteinases

APC: antigen-presenting cell

ATP: adenosine triphosphate

BMs: basement membranes

BBB: blood brain barrier

βA: β-amyloid

CCA: common carotid artery

CFA: complete Freund's adjuvant

CNS: central nervous system

COX: cyclooxygenase

CSF1: colony stimulating factor 1

CSF: cerebrospinal fluid

CXCL: C-X-C motif chemokine

CCL: C-C-L motif chemokine

DA: dark agouti

D.P.I.: day post-immunization

EAE: experimental allergic encephalomyelitis

ECs: endothelial cells

ECM: extracellular matrix

ERKs: extracellular-signal-regulated kinases

FN: fibronectin

GFAP: glial fibrillary acidic protein

HI: hypoxia ischemia

ICAM1: intercellular adhesion molecule 1

IC: inhibitory concentration

IFN-γ: interferon-γ

IL: interleukin

IR: immunoreactivity

JNKs: Jun amino-terminal kinases

LFA-1: Leukocyte function antigen-1
LPS: Lipopolysaccharide
LSC: lumbar spinal cord
MAPKs: mitogen activated protein kinases
MBP: myelin basic protein
MOG: myelin oligodendrocyte glycoprotein
MMP: matrix metalloproteinase
MS: multiple sclerosis
MWM: Morris water maze
NO: nitric oxide
NSAIDs: Non-steroidal anti-inflammatory drugs
PBS: phosphate buffered saline
PLP: proteolipid protein
RORgt: receptor-related orphan receptor gt
ROS: reactive oxygen species
RRMS: relapsing-remitting multiple sclerosis
SAPKs: stress-activated protein kinases
SC: spinal cord
TJs: tight junctions
TGFβ: transforming growth factor β
TLR: toll like receptor
TNF: tumor necrosis factor
Treg: regulatory T cells
TREM-2: triggering receptor expressed on myeloid cells 2
VCAM1: vascular cell adhesion molecule 1

TABLE OF CONTENTS

ABSTRACT	4
GENERAL INTRODUCTION	5
1. Neuroinflammation	5
1.1. Neuroinflammation: physiological vs pathological response	5
1.1.1. Acute neuroinflammation	6
1.1.2. Chronic neuroinflammation	7
1.2. Cytokines and chemokines in neuroinflammation	7
1.2.1. Cytokines	8
1.2.2. Chemokines	11
2. Microglia and its role in neuroinflammation	13
2.1. Microglia in the brain	13
2.2. Activation of microglia in neuroinflammation	14
2.3. Pathways mediating microglial activation	15
2.4. Release of noxious mediators by activated microglia	15
2.5. Microglial phagocytosis	16
2.6. Targeting microglial activation as therapeutic strategy	17
3. Neuroinflammation in neurodegenerative diseases	18
3.1. Experimental Allergic Encephalomyelitis as multiple sclerosis animal model	19
3.1.1 Multiple sclerosis	19
3.1.2 Experimental Allergic Encephalomyelitis	21
3.2. Blood-brain barrier and extracellular matrix in neuroinflammation	21
3.2.1. Blood brain barrier disruption	23
3.2.2. Extracellular matrix	24
3.2.3. Metalloproteinases	25
3.3. Neonatal hypoxia-ischemia	26
3.3.1. Hypoxic-ischemic neuronal injury	26
3.3.2 Inflammation and immune dysregulation after HI	27
MAIN OBJECTIVES	29

GENERAL EXPERIMENTAL PROCEDURES	30
1. Animals	30
2. Surgical procedures	30
2.1. EAE induction	30
2.2. Disease follow-up	30
2.3. GW2580 treatment	31
2.4. Neonatal hypoxia-ischemia injury model.....	31
3. Examination of neurobehavioral development	32
3.1. Neurological reflexes	32
3.2. Behavioral assessment.....	33
4. Immunohistochemistry on slides	35
5. Histology	35
6. Microscopy.....	36
7. In Vitro Experiments	38
7.1. Preparation of CNS Tissue Lysates.....	38
7.2. Determination of Protein Concentrations.....	38
7.3. Gelatin Zymography.....	38
8. mRNA analysis	39
8.1. Spinal cord mRNA analysis	39
9. CSF and plasma biomarker analysis.....	39
10. Functional pathway and network analysis.....	40
11. Statistical Analysis	40
RESULTS AND GENERAL DISCUSSION	42
CHAPTER I.....	44
Cytokine and chemokine alterations in tissue, CSF, and plasma in early presymptomatic phase of experimental allergic encephalomyelitis (EAE), in a rat model of multiple sclerosis.....	44

CHAPTER II	64
Effect of CSF1R inhibition on Blood-Brain Barrier Disruption and temporal evolution of experimental allergic encephalomyelitis in rats.	64
CHAPTER III.....	89
Biomarkers of inflammation during neonatal hypoxia/ischemia and their correlation with the neurological symphoms.....	89
CONCLUSION	120
REFERENCES	122

ABSTRACT

The last two decades has witnessed many achievements in our understanding of the molecular-mechanisms underlying various neuroinflammatory-disorders. Microglia activation is thought to be a driving force of neurodegeneration that follows neuroinflammation in many neurological disorders, but confirmatory evidence is still elusive. In particular, the possible relationship between cause and consequence for microglia activation and pathological landmarks, such as neuronal demyelination and cell death in adult vs neonatal age is still disputed. In this thesis we tried to highlight the potential of early biomarkers for microglia-activation, using two rat models of diseases where microglia activation and neurodegeneration interact.

In the paper included in **chapter I**, we performed a time-course investigation of neuroinflammation and demyelination biomarkers in the spinal cord, cerebrospinal fluid and blood in EAE induced in Dark-Agouti female rats compared with controls and adjuvant, focusing on the time-course between immunization and clinical-onset. We demonstrate that CSF1 was the first up-regulated protein at 1 DPI, in blood, cerebrospinal fluid and spinal cord. A treatment with GW2580, a selective CSF1R inhibitor, slowed the disease progression, significantly reduced the severity and prevented the relapse phase. Moreover, both pro-and anti-inflammatory cytokines were regulated starting from 8 DPI.

In the manuscript included in **chapter II**, we investigated the effect of GW2580 on blood brain barrier disruption with the temporal evolution of EAE. We demonstrated that GW2580 treatment had a therapeutic effect in EAE rats, through reduction of BBB leakage by inhibiting activities of MMP-9 and consequent reduction of microglia activation, IgG-extravasation, and T-cell infiltration.

In the manuscript included in **chapter III**, we investigated plasma and CSF-contents of inflammatory biomarkers after neonatal-HI on acute and chronic phases and their correlation with neurological disorders in rat model of HI. Our data revealed that several inflammatory modulators were most affected at the acute-phase and stabilized at the chronic-phase.

Key words: Neuroinflammation, Multiple sclerosis, Experimental allergic encephalomyelitis, Biomarkers, microglia, CSF1, Blood brain barrier, MMPs, Neonatal Hypoxia Ischemia, neurobehavioral tests

GENERAL INTRODUCTION

The present thesis is dedicated to study two rat models of diseases in which microglia activation and neurodegeneration interact, to try to identify a very early marker for microglia activation as compared to neural distress markers. We performed a time-course investigation based on a discovery strategy of inflammation using high-throughput technologies in order to highlight the potential of novel early biomarkers in adult experimental allergic encephalomyelitis (EAE) and neonatal hypoxia ischemia (HI) models. In the following, such knowledge will be discussed to provide a framework for the different observations made in this thesis.

1. Neuroinflammation

1.1. Neuroinflammation: physiological vs pathological response

Neuroinflammation process plays a significant role in health and diseases of the central nervous system (CNS) (Gendelman and Masliah, 2017; McFarland et al., 2014). Brain inflammatory response appears to be a double edged sword promoting both reparation and damaging of neural tissue in brain and spinal cord injuries, as well as in other CNS pathologies. Neuroinflammation includes adaptive and reparative mechanism, hence, its neurotoxic effect could result from deregulation of underlying biochemical processes (Amor et al., 2010; Nencini et al., 2013). In other words, perturbation of normal physiological mechanisms of neural tissue protection or reparation results in absolute or relative hyperproduction of certain neuroinflammatory mediators which causes neuronal damages or death (Becher et al., 2017a). These responses are mediated by two types of immune cells: the hematopoietic system cells (lymphocytes, monocytes and macrophages) and glial cells of the CNS: astrocytes and microglia (Stoll and Jander, 1999).

In response to a brain insult, glial cells are the first to be activated. Astrocytes upon activation increase expression of the intermediate filament glial fibrillary acid protein (GFAP), and produces cytokines, also contributing to the formation of the glial scar, which isolates the damaged area. These reactive astrocytes also produce neurotrophic factors including nerve growth factor and brain-derived growth factor which favors the blood brain barrier (BBB) repair and remyelination (Faulkner et al., 2004). On the other hand, within any scenario of immune-mediated brain injury, microglia qualifies as the main intrinsic immune effector cells

of the brain. They are potentially phagocytic cells, have a pronounced cytotoxic potential (reviewed by (Banati et al., 1993)), may express several immunomolecules on their surface, may effectively present antigen to T-lymphocytes (Matsumoto et al., 1992; Wang et al., 2016) and are capable of releasing a plethora of mediator substances such as inflammatory cytokines and chemokines.

Most inflammatory mediators have relatively few actions in healthy CNS tissue, where are expressed at very low or undetectable levels. Nevertheless some cytokines and chemokines also modulate neuronal activities in the mature CNS and participate in the neuroendocrine communication. However, their expression is rapidly induced in response to tissue injury or infection; certain inflammatory mediators appear in the affected brain region and the cerebrospinal fluid (CSF) when the CNS homeostasis is disturbed as a result of trauma, stroke, ischemia, infection, or degenerative processes. This increased cytokines and chemokines levels in the CNS may result also from BBB disruption that allows cells of the hematopoietic immune system to leave the blood stream and reach the injury site (Lossinsky and Shivers, 2004). The immune cells respond to injuries by eliminating debris, and synthesizing and releasing a host of powerful regulatory substances, like complements, cytokines, chemokines, glutamate, interleukins, nitric oxide, reactive oxygen species and transforming growth factors which in turn start the cycle all over of responding cells (Barker and Cicchetti, 2014; Hensley et al., 2006; Jana et al., 2016). Neuroinflammation can be further explained as two distinct responses, during acute and chronic conditions.

1.1.1. Acute neuroinflammation

Acute neuroinflammation is often associated to CNS injury or insult. CNS tissue responses to injury is referred to as “reactive gliosis”, which is the accumulation of hypertrophic glial cells (microglia and astrocytes) at the CNS injury site (Streit et al., 2004). Glial “reactivity” is majorly a passive response to injury whereas glial “activation” implies a more aggressive role in responding to activating stimuli. Activated glial cells release factors that act on and generate responses in target cells equivalent to the responses of activated immune cells in the periphery; however, peripheral immune cells activation leads to leukocyte infiltration, which is notably absent in the brain unless there has been a transient lesion or a permanent destruction of the BBB (Minagar, 2015). When peripheral immune cells enter the CNS, they do produce a scenario similar to that seen in inflammatory responses in the periphery.

1.1.2. Chronic neuroinflammation

Chronic inflammation is often associated to CNS chronic diseases, and several hypothesis support a major role in neurodegenerative diseases onset and progression (Cherry et al., 2014; Streit et al., 2004). The immune cells and pro-inflammatory chemicals involved in neuroinflammation would underlie the mechanisms of diseases and neurodegeneration. The general framework is that activation, or over activation, of immune cells involved in neuroinflammation and the release of pro-inflammatory substances would result in reduced neuroprotection and neuronal repair, and increased neurodegeneration (Nathan and Ding, 2010). In particular, the inflammatory responses damage the BBB, increase oxidative stress and release pro-inflammatory and pro-apoptotic cytokines and other neurotoxic factors that affect neuronal viability. The damage and stress signals enhance microglial activation, resulting in positive feedback in the release of chemokines and cytotoxic cytokines that cause further ingress of immune cells into the brain and expand inflammatory responses.

1.2. Cytokines and chemokines in neuroinflammation

Biomarkers are measurable indicators of normal biological and pathogenic processes, or pharmacological responses to a therapeutic intervention (Santonen et al., 2015). A good biomarker should be precise and reliable, distinguishable between healthy and pathological state (Piskunov, 2010). Clinical biomarkers can be detectable molecules from blood, urine or other biological fluids that refer to measurable indicators used to predict physiological states of a disease. To be used in clinics, biomarkers should fulfill certain requirements; their measurements should be accurate, precise and reproducible. Moreover, biomarkers should also present high sensitivity and specificity, be relatively easy to interpret by clinicians and add information on top of clinical variables (Bustamante et al., 2016; Mayeux, 2004; Piskunov, 2010).

Inflammatory mechanisms appear to be universal; hence, neuroinflammation biomarkers can be studied in any acute or chronic brain disease related to neuroinflammation (Muneer, 2016; Vezzani and Friedman, 2011). Such universality results from the fact that microglia activation is a programmed response consisting in stereotypic changes in gene expression and enzyme activity, which are independent from initial stimuli. Therefore, regardless of disease, neuroinflammation is characterized by a dramatic increase in pro-inflammatory cytokines production, induction of adhesion molecules expression, and

activation of proteases and enzymes generating low molecular inflammatory mediators (Brown et al., 2010; Wang et al., 2015b). Classically defined neuroinflammatory conditions, as observed in inflammatory demyelinating diseases (for example, multiple sclerosis) and infections (bacterial and viral encephalitis), are characterized by leukocytes invading the CNS parenchyma and a drastic loss of BBB integrity (Becher et al., 2017b; da Fonseca et al., 2014). Lymphocytes and myeloid cells are the main mediators of tissue damage and deliver cytokines to the tissue, fuelling the inflammatory cascade (Figure 1).

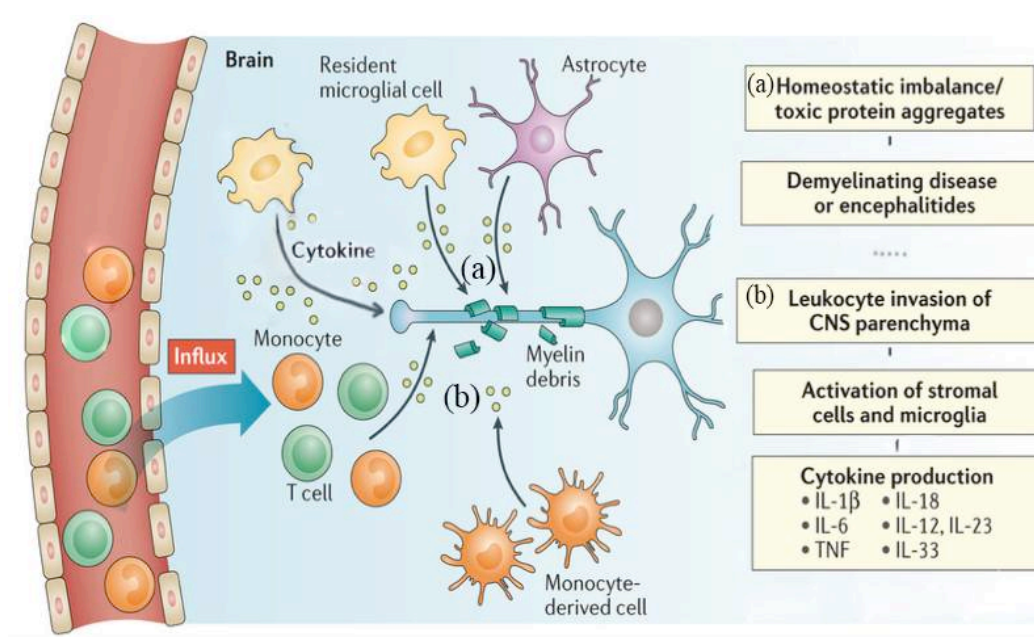


Figure 1. Neuroinflammation cascade in demyelinating diseases. (a) In response to homeostatic unbalance and (b) as observed in inflammatory demyelinating diseases and infections. *Source:* adapted from (Becher et al., 2017a).

Classically defined neuroinflammatory conditions, as observed in inflammatory demyelinating diseases (for example, multiple sclerosis) and infections (bacterial and viral encephalitis), are characterized by leukocytes invading the CNS parenchyma and a drastic loss of BBB integrity. Lymphocytes and myeloid cells are the main mediators of tissue damage and deliver cytokines to the tissue, fuelling the inflammatory cascade (Figure 1).

1.2.1. Cytokines

Cytokines are small multifunctional glycoprotein mediators whose biological actions are mediated locally by specific receptors and which are linked to most processes in the body. Cytokines are mainly released from immune cells such as monocytes, macrophages and

lymphocytes, in addition to microglia and astrocytes (Kim et al., 2016). Both pleiotrophy and redundancy exist within the cytokine families, and several different cytokines often exert similar and overlapping functions on certain cells. Their receptors also often display redundancy and utilize different signal transduction pathways (Robertson, 1998).

Cytokines are activated during situations in which inflammation, infection and/or immunological alterations occur and are mainly involved in the repair of damaged tissues and the restoration of homeostasis (Nathan, 2002 and Woodroffe, 1995). Cytokines mediate signals between immune cells and are generally divided into pro-inflammatory and anti-inflammatory cytokines, which facilitate and inhibit inflammatory responses, respectively.

As shown in Table 1, some cytokines act primarily as T-lymphocyte or B-cell growth factors, others function as prominent mediators of inflammation, whereas yet others suppress inflammation as well as immune responses (Dinarello, 2007; Turner et al., 2014). In some cases, the cytokine receptor is found primarily on one type of cell, accounting for its primary function, for example, IL-33 receptor is expressed on mast cells (Schmitz et al., 2005). In other cases, the receptor is found on nearly every cell, for example, IL-1 and TNF α . In these cases, the cell type defines the property of the cytokine.

Table 1. Functional Classes of Cytokines.

Functional Class	Primary Property	Other Effects	Examples
lymphocyte growth factors	clonal expansion	Th1/Th2/Th17 polarization	IL-2, IL-4, IL-7, IL-17, IL-15
Th1 cytokines	↑ Th1 response	clonal expansion of cytotoxic T-cell	IFN γ , IL-2, IL-12, IL-18
Th2 cytokines	↑ Th2 responses	↑ antibody production	IL-4, IL-5, IL-18, IL-25, IL-33
Th17 cytokines	↑ Th17 responses, IFN γ	autoimmune responses	IL-17, IL-23, IFN γ
pro-inflammatory cytokines	↑ inflammatory mediators	↑ innate immune responses	IL-1 α , IL-1 β , TNF α , IL-12, IL-18, IL-23
			MIF, IL-32, IL-33, CD40L
anti-inflammatory cytokines	↓ inflammatory genes	↓ cytokine-mediated lethality	IL-10, IL-13, TGF β , IL-22, IL-1Ra, IFN α/β
adipokines	pro-inflammatory	↓ autoimmune disease pro-atherogenic	IL-1 α , TNF α , IL-6, leptin, adiponectin
gp130 signaling cytokines	growth factors	B-cell activation, acute phase	IL-6, CNTF, IL-11, LIF, CT-1
nerve growth factors	↑ nerve/Schwann cells	B-cell activation	BDNF, NGF
osteoclast activating cytokines	bone resorption	immune stimulation	RANK L
colony stimulating factors	hematopoiesis	pro and anti-inflammatory	IL-3, IL-7, G-CSF, GM-CSF, M-CSF
angiogenic cytokines	neovascularization	pro-metastatic	VEGF, IL-1, IL-6, IL-8
mesenchymal growth factors	fibrosis	pro-metastatic	FGF, HGF, TGF β , BMP
type II interferon	macrophage activation	increase class II MHC	IFN γ
type I interferons	anti-viral; ↑ class I MHC	anti-inflammatory, anti-angiogenic	IFN α , IFN β

1.2.2. Chemokines

Chemokines belong to a large superfamily of structurally and functionally related cytokines with chemotactic activity, they are involved in chemotaxis of monocytes, lymphocytes, neutrophils, eosinophils, basophils, natural killer cells, dendritic cells, and endothelial cells (Proost et al., 1996). More than 50 chemokines have been identified to date, but there is a large degree of redundancy and overlap of functions (Bacon et al., 2002; Murphy et al., 2000). As shown in Table 2, there are four major subfamilies of chemokines, based on the relative positions of their cysteine residues (CC, CXC, C and CX3C) (Luster, 1998). Chemokines perform a variety of functions aside from chemotaxis, including T helper cell differentiation and function, as well as angiogenesis (Turner et al., 2014).

Chemokines can have direct effects on T cell differentiation through direct interactions on the developing cell or indirectly by altering antigen-presenting cell (APC) trafficking or cytokine secretion. For example, it was recently found that the chemokine receptor, CXCR3, was upregulated on CD4 + T cells and this was associated with cytokine expression and differentiation of these cells to type 1 (Th1) cells (Groom et al., 2012). Chemokines play an important role in angiogenesis, although this function lies with a subclass of the CXC chemokines. The CXC chemokines can be subdivided into two categories, those with a specific amino acid or motif of Glu-Leu-Arg (or ELR for short) immediately before the first cysteine of the CXC motif (ELR-positive), and those without an ELR motif (ELR-negative). ELR-positive CXC chemokines are angiogenic and specifically induce the migration of neutrophils, and interact with chemokine receptors CXCR1 and CXCR2 (Baggiolini, 2001). By contrast, the non-ELR chemokines are angiostatic and act mainly through the CXCR3B receptor. The exception to this is CXCL12, which is a non-ELR chemokine but is angiogenic and exerts its effects on the vasculature primarily by binding to CXCR4 and CXCR7 (Kryczek et al., 2007).

Table 2. Chemokine families and their functions.

Chemokine families	Main function	Examples
CC chemokine	Recruitment of monocytes/macrophage Recruitment of T-lymphocytes Recruitment of eosinophils	CCL2, CCL3, CCL5, CCL7, CCL8, CCL13, CCL17 and CCL22. CCL2, CCL1, CCL22 and CCL17 CCL11, CCL24, CCL26, CCL5, CCL7, CCL13, and CCL3
C chemokine	Recruitment of T-lymphocytes	XCL1 (Lymphotactin) and XCL2 (SCM1-b)
CXC chemokine		
- non-ELR ^(a)	Angiostatic	CXCL4, CXCL9, CXCL10, CXCL11 and CXCL17
- ELR	Angiogenic and chemoattractant for neutrophils	CXCL1, CXCL2, CXCL3, CXCL5, CXCL6, CXCL7, and CXCL8/IL-8
CX3C chemokine	Serve as a chemoattractant and as an adhesion molecule	CX3CL1 (Fractalkine)

^(a) ELR is a conserved amino acid motif (Glu-Leu-Arg) immediately preceding the first cysteine amino acid in the CXCL chemokine

2. Microglia and its role in neuroinflammation

2.1. Microglia in the brain

Microglia are tissues-resident cells of the brain, that regulates tissues homeostasis during normal physiology as well as in CNS pathologies (Prinz and Priller, 2014). Microglia are of myeloid origin, invade the CNS from the yolk sac during development and are maintained by self-renewal throughout the animal's lifespan (Ginhoux et al., 2013; Hashimoto et al., 2013; Ikezu and Gendelman, 2017). They are distributed throughout the parenchyma and account for approximately 10% to 20% of the total glial cell population in the brain (Karperien et al., 2013). Research on microglia biology often focuses on cellular behaviors during tissue injury or disease (Hilaire and Gendelman, 2017). Interestingly, microglia exhibit dynamic behavior in the CNS under normal physiological conditions and they do have a critical role for the development and maintenance of the neural environment (Butovsky et al., 2017; Nathan, 2002). A CNS injury can trigger “resting microglia” to become activated, thus showing different morphology according to the state (Figure 2).

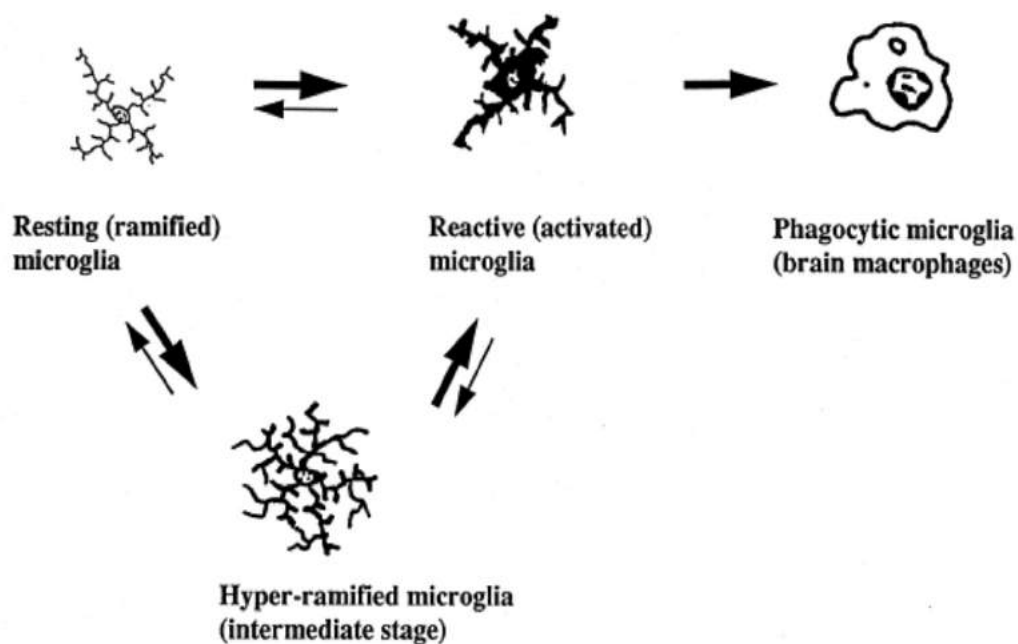


Figure 2. Microglial morphology in adult CNS (human). *Source:* adapted from (Streit et al., 1999).

Neurons may also activate microglia, and the degree of microglial activation varies with the severity of neuronal injury. The mildest injuries may only cause hyper-ramification of microglia (Wilson and Molliver, 1994), but most types of neuronal damage will cause resting microglia to become reactive microglia. If neurons die, microglia transform into brain macrophages (phagocytic microglia) and remove the dead cells and debris. If an injured neuron recovers, hyper-ramified and reactive microglia may revert back to the resting form (Kettenmann et al., 2011; Ling, 1976).

Microglia are present throughout the CNS, including the spinal cord, although some regions are more populated than others, with the white matter generally containing fewer microglia than the grey matter (Graeber et al., 2011). In the prenatal brain, the amoeboid phagocytic microglia are the predominant form, with a large spherical cell body and short processes (Hess et al., 2004). During postnatal maturation, amoeboid microglia transform into ramified resting microglia, and these cells remain a semi-permanent population with relatively slow turnover rates when compared to peripheral macrophages (Hess et al., 2004; Kennedy and Abkowitz, 1997). Resting ramified microglia monitors the microenvironment, adapting their morphology and expressing cell surface markers accordingly (Butovsky et al., 2017; Lawson et al., 1992).

2.2. Activation of microglia in neuroinflammation

As microglia have been recognized as the major components of the intrinsic brain immune system they have become a main focus in cellular neuroimmunology and therefore in neuroinflammation. There are various stimuli that could activate microglial cells and cause neuroinflammation (Shimizu et al., 2016; Tang and Le, 2016). *In vivo* studies identified stimuli associated to neural infections, ischemia, neurodegeneration and prion diseases. *In vitro*, lipopolysaccharide (LPS), thrombin, interferon- γ (IFN- γ), β -amyloid (β A) and some proinflammatory mediators produce microglia activation (Dheen et al., 2007; Nayak et al., 2014). The response to these different stimuli include changes in morphology, proliferation and upregulation of surface markers.

The magnitude of microglial activation depends on the type of insult, potency and distance of the stimulus, immediate microenvironment and the state of microglia that have been exposed to prior and existing stimuli (Lue et al., 2010). The activation of microglia by these stimuli exerts cytotoxic effects through two different processes, they either act as

phagocytes, which implicate a direct contact cell-to-cell or release of large noxious factors (Lull and Block, 2010; Schmitt et al., 2014).

2.3. Pathways mediating microglial activation

Several intrinsic factors such as Irf8 and Pu.1 and extrinsic like TREM2, CX3CR1 and CD200 regulate the transition of microglia cells from homeostatic phenotype to an activated stage in response to neuronal injury. Kinase and phosphate cascades mediate microglial response to extracellular stimuli.

Some reports have demonstrate that p38 mitogen-activated protein kinases, which are a class of mitogen-activated protein kinases (MAPKs) and p44/42 families of mitogen activated protein kinase pathways, play an important role in activation of microglial cells which in turn leads to neuroinflammation and the release of neurotoxic mediators in acute brain injury and chronic neurodegenerative diseases (Harry and Kraft, 2008; Lee et al., 2015). In mammals MAPKs can be grouped into three main families, these are ERKs (extracellular-signal-regulated kinases), JNKs (Jun amino-terminal kinases), and p38/SAPKs (stress-activated protein kinases). Microglia activation could effect through any these if not all of the MAPK pathways (Morrison, 2012). A major role of the macrophage colony-stimulating factor CSF1/MAPKs in microglia activation and disease progression has been also described. In neuropathic pain induced by peripheral nerve injury, CSF1 is produced and retrograde transported to the spinal cord by sensory neurons (Guan et al., 2016).

Other proinflammatory pathways that could respond to microglia activation is the NF κ B and Wnt pathway (Du and Geller, 2010). Indeed, any of the microglia mediated pro-inflammatory stimuli can activate NF κ B expression (Sparacio et al., 1992), which can further induce target genes that in turn regulate the expression of inflammation genes, thus leading to a self-maintaining process producing the elevation of inflammatory proteins. Wnt pathway can instruct pro-inflammatory microglia transformation and emphasize the pathogenic significance of β -catenin signaling networks in this cell type (Halleskog et al., 2011).

2.4. Release of noxious mediators by activated microglia

Upon activation, microglia cells express wide array TLRs and initiates innate responses with the production of a large number of neuroactive substances, cytokines and chemokines. On the basis of *in vitro* evidence, microglia are considered the major CNS sources of pleiotropic cytokines that stimulate humoral and cell-mediated immune responses

(Aloisi, 2001). These include IL-1 and TNF- α , the two master proinflammatory cytokines with largely overlapping functions during CNS inflammation; IL-18 (Klapal et al., 2016), which have a critical role in the stimulation of NK and Th1 cells; IL-6, a cytokine with pro- and anti-inflammatory actions, which promotes B-cell growth and differentiation (CHEN et al., 2016; Stone and Flamme, 2016); IL-15, which selectively activates NK and CD8⁺ T cells (Hanisch et al., 1997).

Activated microglial cells release also radicals, such as superoxide and nitric oxide, that are products of the enzymes nicotinamide adenine dinucleotide phosphate (NADPH) oxidase and inducible nitric oxide synthase, respectively (Butovsky et al., 2017; Ikezu and Gendelman, 2017). Microglial cells contain glutathione, substantial activities of the antioxidative enzymes, superoxide dismutase, catalase, glutathione peroxidase and glutathione reductase as well as NADPH-regenerating enzymes that provide an efficient antioxidative defense mechanisms for microglia against oxidative stress (Dringen, 2005). Activated microglia cells triggers and maintains an inflammatory response, deluging neurons with a whole host of inflammatory mediators that may eventually lead to cell death. Consequently, the activation of microglia cells and chronic inflammation thereafter is the initiation of the release of panoply of neurotoxic mediators that are believed to contribute to neurodegenerative processes (Harry and Kraft, 2008; Lull and Block, 2010).

2.5. Microglial phagocytosis

Microglia cells are able to phagocytes particles and debris via different phagocytic receptors and digest the taken-up material by proficient lysosomal mechanism. Depending on the type of the phagocytic receptor, microglia responds differently in their downstream cytokine signaling, either pro- or anti-inflammatory (Moller 2000; Wu et al., 2002).

Microglial phagocytosis (Figure 3) may need different types of receptors to initiate function (Aderem and Underhill, 1999). In general, there are two distinctive types of receptors, one with a high affinity to bind to foreign microbial pathogens, such as Toll-like receptors (TLRs), and another recognizing apoptotic cellular substances, such as triggering receptor expressed on myeloid cells 2 (TREM-2) (Fu et al., 2014; Nayak et al., 2014). Besides these two types, some receptors such as Fc receptors, pyrimidinergic receptor P2Y₆, G-protein coupled-6 (P2RY6), macrophage antigen complex 2 (MAC-2), also participate in microglial phagocytosis (Smith, 1999). Microglia are able to engulf whole neurons within hours (Neher

et al., 2011). In order too reduce inflammation, microglia cells phagocyte dead and dying neurons, neuronal and myelin debris (Sierra et al., 2013).

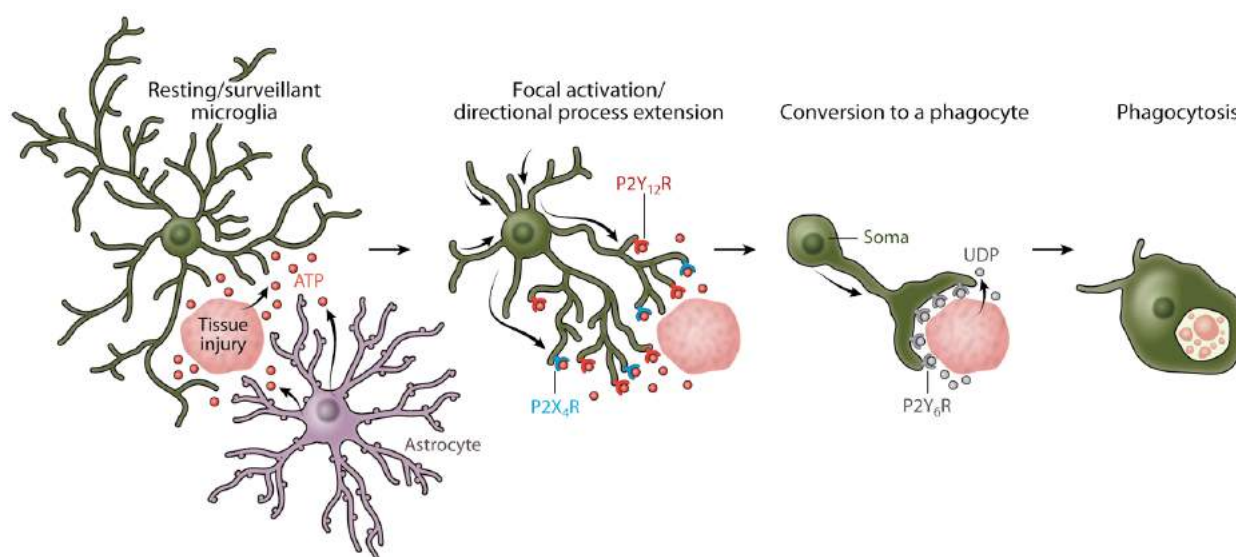


Figure 3. Microglia (green) detects a tissue injury and springs to action. Its extended processes detect signs of damage and trigger the cell’s transformation into a big blob that engulfs the debris. *Source:* adapted from (Nayak et al., 2014).

However, microglia could also cause death of the engulfed cell by phagocytosing live neurons (Fricker et al., 2012; Fu et al., 2014; Hoeppner et al., 2001), live neutrophils (Neumann et al., 2008) and live glioma cells under certain conditions (Kopatz et al., 2013).

2.6. Targeting microglial activation as therapeutic strategy

So far, the development of effective neuroprotective therapies is impeded by our limited knowledge of the pathogenesis of neurodegenerative diseases. Since its role in neuroinflammation and thereby neurodegenerative diseases progression, microglia has been put in focus as intervention targets (Kim, 2015; Wang et al., 2015a). Many reports about neuroinflammation, proposes that the inhibition of microglial activation and suppression of inflammatory mediators production will avoid the escalation of CNS inflammatory processes, thus resulting in neuroprotection (McCarty, 2006). This may be possible through the identification of agents that target over-activated microglial cells and the determination of their anti-inflammatory mechanisms (Glass et al., 2010).

Several anti-inflammatory drugs have been shown to diminish neuroinflammation, such as glucocorticoids, minocyclines, vitamin E, D, endocannabinoids and several synthetic

drugs (Dheen et al, 2007), but a very few have demonstrated a direct functional effects on microglial activity (Lleo et al., 2007).

Non-steroidal anti-inflammatory drugs (NSAIDs), which include ibuprofen, naproxen, and many other generic drugs, have been identified with huge list of undesirable and severe side effects (Silverstein et al., 2000). Though, synthetic cyclooxygenase-2 (COX-2) selective NSAIDs were brought into the market as alternatives highlighting its association with less toxicity than nonselective NSAIDs, recent studies have shown that they cause more serious adverse effects like cardiovascular events and other life threatening side effects (Mukherjee et al., 2001). Moreover, the BBB is little permeable to most of these compounds. Therefore, there is an urgent need to develop drugs that have wide spectrum anti-inflammatory effects, accumulate the brain in appropriate concentration, and are able to slow down or curtail the progression of the degenerative process without causing any debilitating side effects.

In the recent decade, there has been a widespread surging interest in naturally occurring plants and plant derived compounds that prove to be highly efficacious drugs with less adverse side effects. With the great strides in the technology of extraction, isolation and activity detection, natural product studies are being propelled as alternatives to synthetic drugs (Newman and Cragg, 2007). In this encouraging scenario, any naturally occurring medicinal compound, which can efficaciously inhibit microglial activation, could open avenues for better ameliorating microglia-associated neurodegenerative and neuroinflammatory diseases.

All the drugs and molecules described above attempt to suppress the neurotoxic effect of microglial cells in CNS diseases. It should be emphasized that the neuroinflammation in CNS diseases is amplified considerably by the rapid influx of microglial cells to injury sites in CNS (Thameem Dheen et al., 2007). The migration of microglia is regulated by various chemokines. Recently, it has been shown that expression of chemokines such as MCP-1 and IFN- inducible protein-10 (IP-10) by astrocytes plays a role in migration and activation of microglial cells and subsequent neurodegeneration in secondary progressive multiple sclerosis (Tanuma et al., 2006). Therefore, targeting chemokines may be one of the therapeutic options to inhibit neuroinflammation caused by proinflammatory cytokines released by microglial cells.

3. Neuroinflammation in neurodegenerative diseases

Neurodegenerative diseases are characterized by the chronic progressive loss of the structure and functions of neurons, resulting in functional and mental impairments. While the

causes associated with neuronal degeneration remain poorly understood, the emerging evidence on the contribution of microglia and astrocytes in sustaining inflammatory response associated with in disease progression, suggest that effectors of neuroinflammation contribute in neuronal dysfunction and death (Campbell et al., 1999; Chen et al., 2016) Rm et al., 2015). Actually, some diseases debut as inflammatory disease, thus turning to neurodegeneration during the disease progression.

3.1. Experimental Allergic Encephalomyelitis as multiple sclerosis animal model

3.1.1 Multiple sclerosis

Multiple sclerosis (MS) is an immune-mediated demyelinating disease of the CNS, where the pathological hallmarks are inflammation, demyelination and axonal loss (Lassmann, 2009; Stadelmann, 2011; Trapp and Nave, 2008). MS is characterized by a variable clinical course and complex pathology and pathogenesis. There are three clinical subtypes of MS according to the clinical course: relapsing-remitting MS (RRMS), secondary progressive MS (SPMS) and primary progressive MS (PPMS) (Koudriavtseva and Mainero, 2016). RRMS is the most diffuse form, and is characterized by an acute begin followed by subsequent improvement and a further relapse after a disease-free interval. A minority of patients, about 15% suffer from PPMS from onset. This subtype of the disease progresses slowly without relapses (Compston and Coles, 2002). Although MS is considered to be as a white matter disease, grey matter is also extensively affected (Enzinger and Fazekas, 2015; Messina and Patti, 2014).

MS lesions are characterized by the infiltration of lymphocytes, antibody-producing plasma cells and a plethora of recruited macrophages that from the periphery enter the perivascular region of the brain and spinal cord (Hemmer et al., 2002; Zigmond et al., 2014), cross the BBB, cause microglial and astrocytes hyper activation that trigger a cascade of inflammatory mediators and ultimately lead to severe demyelination and axonal loss (Figure 4) (Lassmann et al., 2001, 2012). Oligodendrocytes are in fact cells highly sensitive to inflammatory stimuli, such as denuded axons. In the progressive phase of MS, deposition of antibodies and complement around demyelinated lesions and axonal degeneration have been observed (Frohman et al., 2006; Trapp and Nave, 2008). When damage is not too extensive and the ensuing inflammatory response is transient, remyelination took place as part of the normal repair. However, in the presence of chronic inflammation, remyelination is severely

impaired and leads to axon degeneration and the eventual neuronal death (Glass et al., 2010; Podbielska et al., 2013). Cytokines and chemokines play a key role in these processes by regulating cell migration, proliferation and activation of resident and infiltrating cells (Dendrou et al., 2015).

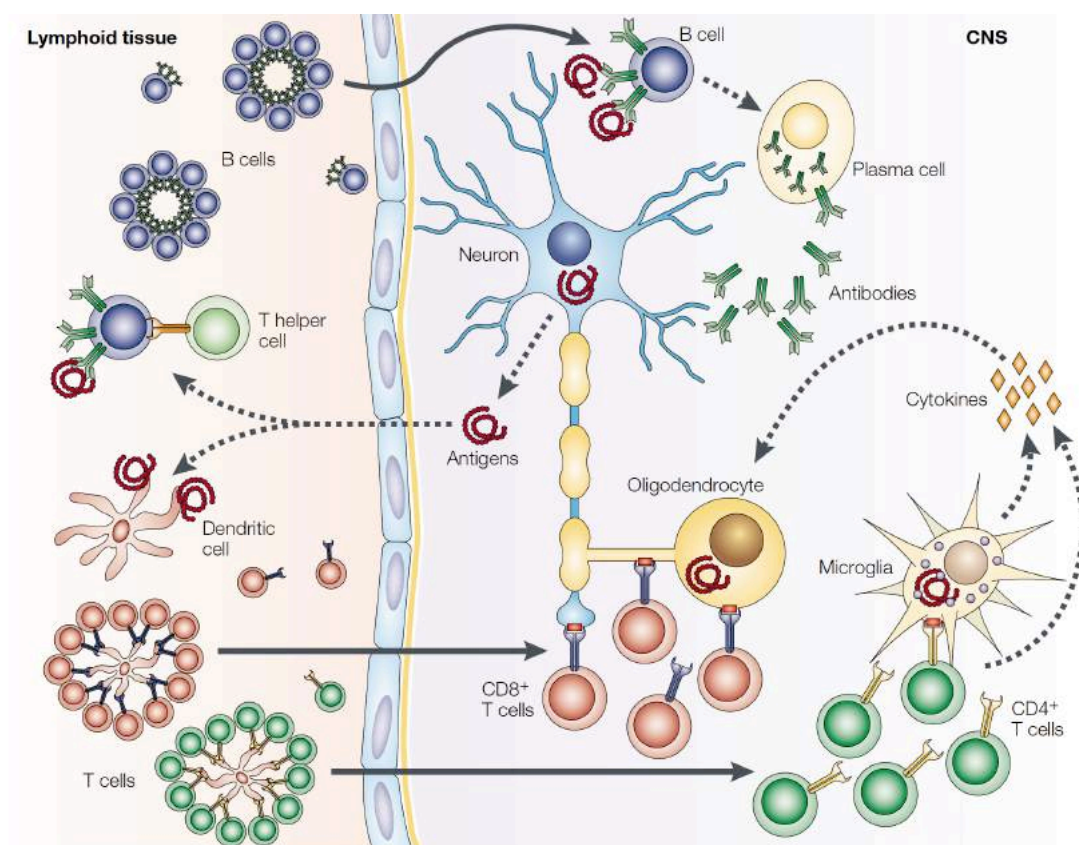


Figure 4. Inflammatory components in multiple sclerosis. Hypothetical view of immune responses in acute multiple sclerosis lesions. *Source:* adapted from (Glass et al., 2010).

Thus, there are four key pathological features in MS: (a) inflammation, which is generally believed to be the main trigger of the events leading to CNS tissue damage in the majority of cases, although recent evidence suggests that initial damage to neuroglial elements can trigger secondary inflammation in some cases (Barnett and Prineas, 2004); (b) demyelination, the hallmark of MS, where the myelin sheath or the oligodendrocyte cell body are destroyed by the inflammatory process; (c) axonal damage and loss; and (d) gliosis, the astrocytic reaction to CNS damage (Constantinescu et al., 2011a).

Despite the intensive efforts and the major progress achieved in understanding the inflammatory process and pathogenetic mechanisms within this heterogeneous disease entity

to date the many aspects of the of MS pathogenesis remain elusive. An important contribution to MS studies has been made by experimental allergic encephalomyelitis (EAE), the most widely used animal model for MS (Aharoni, 2013), in which the interaction between a variety of immunopathological and neuropathological mechanisms affords an approximation of the key pathological features of MS pathology, including inflammation and immune reaction, demyelination, axonal loss and gliosis (Guerreiro-Cacais et al., 2015; Robinson et al., 2014). EAE has been also used to develop and validate all approved therapies for MS (Constantinescu et al., 2011a), thus confirming the good correlation between animal and human pathology (Ben-Nun et al., 2014; 't Hart et al., 2015).

3.1.2 Experimental Allergic Encephalomyelitis

EAE is the most widely used animal model for MS, reproducing inflammation and immune reaction, demyelination, axonal loss and gliosis (Aharoni, 2013), (Constantinescu et al., 2011b). EAE may be induced by active or passive immunization. Active immunization is induced by injecting susceptible animals with CNS extract, purified myelin components, or synthesized specific peptides such as, derived from myelin oligodendrocyte glycoprotein (MOG), proteolipid protein (PLP), or myelin basic protein (MBP), emulsified in an adjuvant (Lorentzen et al., 1995; O'Brien et al., 2010).

The Dark Agouti (DA) rat model of EAE mimics certain aspects of the clinical course of disease in people with RRMS (Skundric, 2005), typified by progressive, sustained demyelination, and associated axonal loss (Barnett and Prineas, 2004; Bjartmar et al., 2003; Stadelmann, 2011). At disease onset, in DA rats, neurological impairments are observed, followed by an acute attack with ataxia and paralysis. Most animals recover from paralysis and experience remission, and then may undergo one or more relapses (Lorentzen et al., 1995). The neurological impairment in EAE is mediated by activation of autoimmune responses and is accompanied by infiltration of activated lymphocytes (T/B cells), NK cells, and monocytes into the affected CNS tissue (CHEN et al., 2016).

3.2. Blood-brain barrier and extracellular matrix in neuroinflammation

The microenvironment of the brain is strongly controlled to guarantee appropriate nervous system functions (Banks, 2016). The main layer of protection comes from the BBB at the capillary endothelium, and the blood-CSF barrier at the choroid epithelium and the arachnoid membrane. These barriers separate the blood from the CNS microenvironment

(Redzic, 2011). In vertebrates, the BBB consists primarily of endothelial cells (ECs) with specialized tight junctions (TJs) lining the blood vessels, astrocytic end-feet surrounding the blood vessels, and pericytes embedded in the basement membranes (BMs) between the ECs and the astrocytes (Figure 5) (Banerjee and Bhat, 2007; Varatharaj and Galea, 2017).

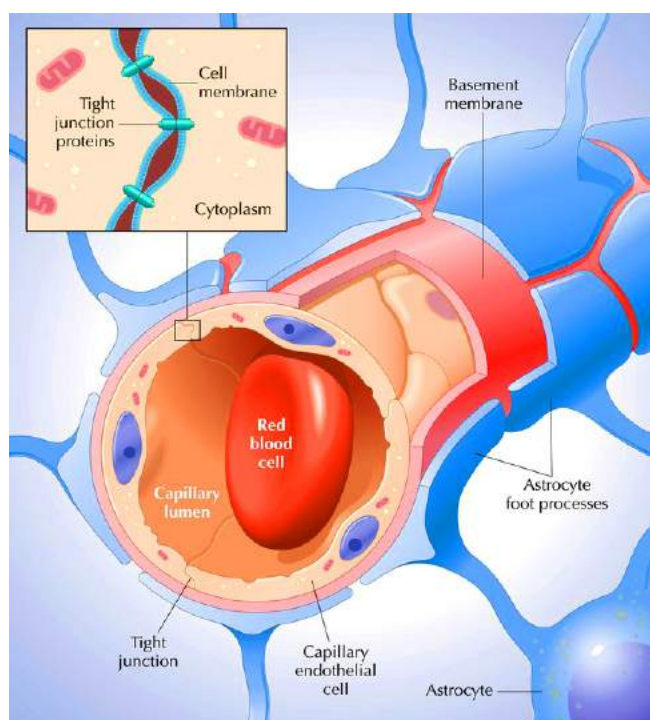


Figure 5. The barrier is formed by capillary endothelial cells, surrounded by basal lamina and astrocytic perivascular endfeet. Astrocytes provide the cellular link to the neurons. *Source:* adapted from (Hansen and Koeppen, 2002).

The BBB has multiple functions. As a physical barrier, it limits the paracellular transport of cells, proteins. As a transport barrier, it controls nutrient supply and waste removal, throughout specific transport systems. As a metabolic barrier, it contains enzymes that metabolize ATP and neuroactive compounds, allowing separation of the central and peripheral pools of neurotransmitters (Abbott et al., 2006; Baeten and Akassoglou, 2011). Nevertheless, the BBB is neither an absolute barrier nor is it immobile (Carvey et al., 2009; Neuwelt et al., 2011). Rather, this dynamic structure is highly regulated by interactions between its cellular and extracellular matrix (ECM) components along with integrin receptors.

3.2.1. Blood brain barrier disruption

The main functions of the BBB, namely maintenance of brain homeostasis, regulation of influx and efflux transport, and protection from harm, are determined by its specialized multicellular structure (Engelhardt and Liebner, 2014; Obermeier et al., 2013). Every constituent cell type makes an indispensable contribution to the BBB's integrity. But if one member of the BBB fails, and as a result the barrier breaks down, there can be dramatic consequences and neuroinflammation and neurodegeneration can occur.

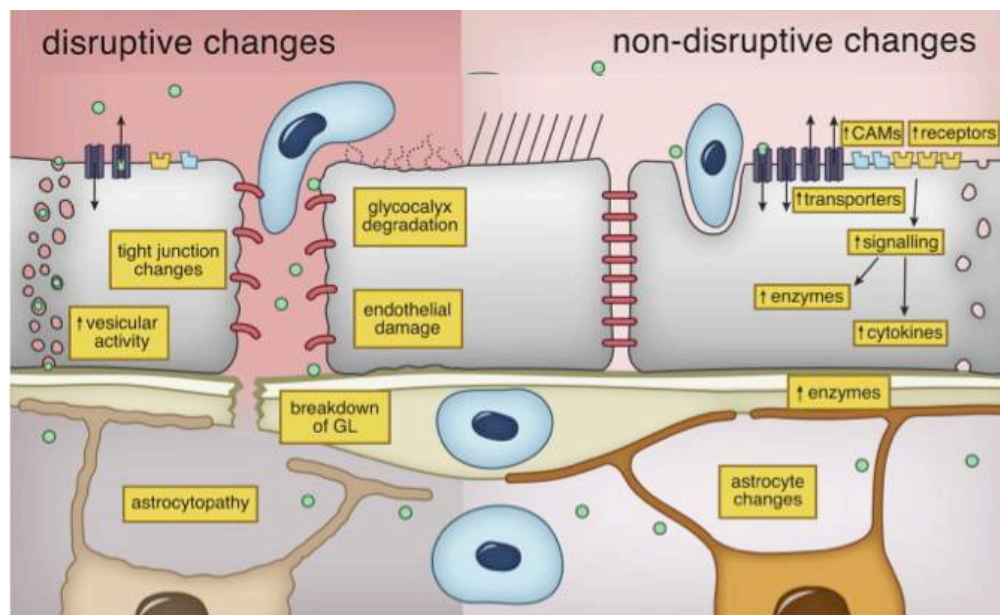


Figure 6. Schematic illustration of disruptive and non-disruptive BBB. CAMs, cellular adhesion molecules; GL, glia limitans. *Source:* adapted from (Varatharaj and Galea, 2017).

A common factor of the BBB fails, is the abundance of immune cells that infiltrate into the CNS (Carvey et al., 2009; Hallmann et al., 2015; Klein and Bischoff, 2011; Trapp and Nave, 2008). The process of leucocyte transmigration across a post-capillary venule into the CNS involves several important steps (Engelhardt, 2008; Larochelle et al., 2011). The first step is a slowing of leucocytes within the blood through the interaction and binding of integrin alpha 4 beta 1 receptors present on leucocytes plasma membrane with several cell adhesion molecules on the endothelium, including vascular cell adhesion molecule 1 (VCAM1), intercellular adhesion molecule 1 (ICAM1) and Leukocyte function antigen-1 (LFA-1) (Muller, 2009; Rezai-Zadeh et al., 2009). This is followed by leucocyte arrest to endothelial cells possibly due to a response to chemokines secreted by endothelial cells (Stamatovic et al., 2008). Once

leucocytes adhere, they migrate across the endothelial cell barrier and endothelial basement membrane to accumulate in the perivascular space and form an inflammatory perivascular cuff. The perivascular space have been defined as the space where leucocytes accumulate before entering the CNS parenchyma (Kivisäkk et al., 2009; Ransohoff et al., 2003).

Recent studies have demonstrated the important role of ECM components in the migration of leukocytes across the BBB, as the laminin composition of the vascular and possibly parenchymal BMs determine accessibility to the CNS (Wu et al., 2009).

3.2.2. Extracellular matrix

The ECMs (Figure 7) is secreted by cells, surrounds them in tissues and provide not only physical scaffolds into which cells are embedded but also regulate many cellular processes including growth, migration, differentiation, survival, homeostasis, and morphogenesis (Frantz et al., 2010; Theocharis et al., 2016). The ECMs consists of a complex assembly of several proteins and polysaccharides whose exact composition varies from tissue to tissue (Clause and Barker, 2013).

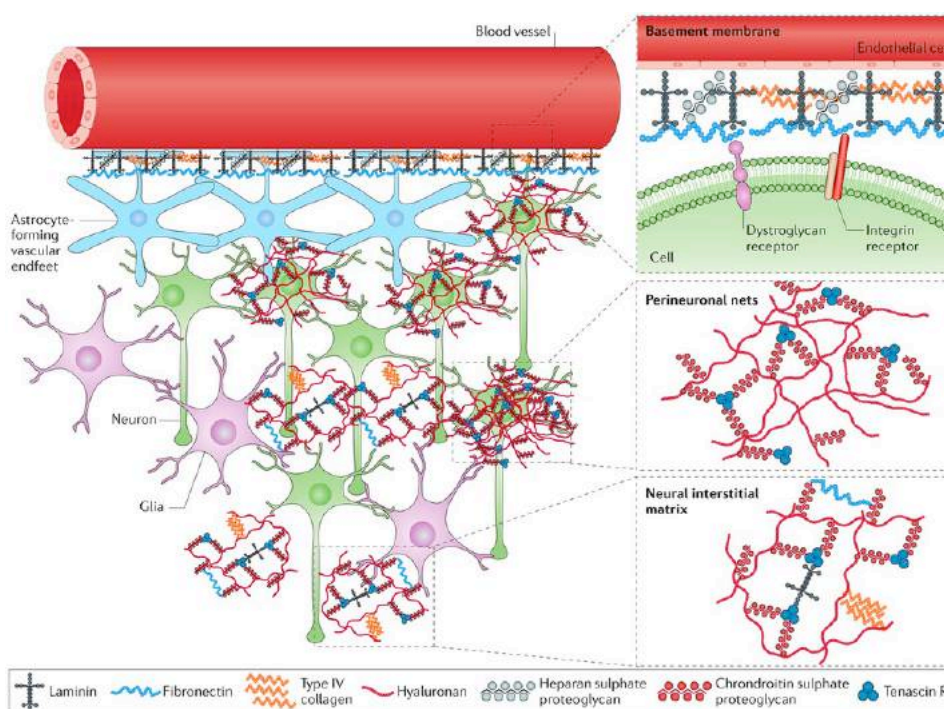


Figure 7. Extracellular matrix components. *Source:* adapted from (Lau et al., 2013).

BM proteins are degraded by proteolysis at certain conditions, mostly by matrix metalloproteinases (MMPs) and plasmin (Fukuda et al., 2004; Lu et al., 2011).

The major constituents of ECMs are fibrous-forming proteins, such as collagens and elastin, and glycoproteins, such as fibronectin (FN), laminins, formed by the assembly of different proteins with glycosaminoglycans (GAGs), which are highly acidic and hydrated molecules. There are two basic forms of the ECM, basement membranes (BM), the cellular matrix between epithelial and stromal layers of cells, and the interstitial matrix: the cellular matrix surrounding cells forming a porous 3-D lattice (Ingber, 2006; Sorokin, 2010). The BM is a thin layer of ECM below the epithelia and endothelia, that also surrounds muscle, fat and nerve cells. It provides mechanical structure, separates different cell types, and signals for cell differentiation, migration, and survival. The BM consist of four major components: type IV collagen, laminins, nidogen and the heparan sulphate proteoglycan perlecan (Sasaki et al., 2004; Sorokin, 2010).

3.2.3. Metalloproteinases

MMPs comprise a large group of endoproteinases that share some structural features in the N-terminal catalytic domains. MMPs can catalyze the degradation of all protein components to prevent tissue destruction. Recently, the spectrum of MMP substrates has been extended to enzyme inhibitors, cell membrane-bound adhesion molecules, cytokines precursors and cytokines receptors. MMPs are a family of 23 related either secreted or membrane bound endopeptidases catalyzing the hydrolysis of diverse biological macromolecules. The activation of MMPs is controlled at multiple levels. They are synthesized in a latent form and secreted as proenzymes that require extracellular activation.

During inflammation, the secretion of MMPs by tissue resident cells is controlled by the equilibrium of inflammatory mediators such as TGF- β , TNF- α and IFN- γ released by infiltrating immune cells (Song et al., 2015). This secretion is also controlled by growth factors and hormones (Benbow and Brinckerhoff, 1997; Sabeh et al., 2004). MMPs, together with membrane-anchored disintegrin metallo-proteinases (ADAMs) and meprins, target a wide range of ECM and other extracellular proteins involved in migration, survival and function of immune cells, thereby propagating or terminating immune signals (Malemud, 2006).

Notably, MMPs could alter the biological activity and the spatiotemporal distribution of growth factors and inflammatory mediators by cleaving their fragments (Van den Steen et al., 2003). By shedding of cell surface receptors, MMPs actively regulate the availability of both surface molecules and soluble effectors. For some proteins, this process is also a

prerequisite for intramembrane proteolysis, which releases the intracellular domain for translocation to the nucleus to direct gene expression. Altogether, these findings indicate that MMPs are a crucial component of the immune system and that tight control of MMP activity is essential for maintaining immune homeostasis.

During inflammation MMP play a critical role, at least on the chemotactic effects of certain chemokines such as CXCL12 which have been shown to be required for holding T cells in the perivascular cuff, and its proteolytic degradation by MMPs (MMP-9 and MMP-2) releases leukocytes to migrate into the CNS parenchyma (Chu et al., 2017; McCandless et al., 2008; Song et al., 2013).

3.3. Neonatal hypoxia-ischemia

3.3.1. Hypoxic-ischemic neuronal injury

Perinatal period is a critical period in the development of the CNS, and injuries in this period can cause severe damage with permanent disabilities. However, very little is known about the short-term effects of neuronal lesions, despite the prognostic significance of the early changes. Hypoxic-ischemic (HI) brain injury in human neonates is a rather common problem, having severe neurological sequelae that include cerebral palsy, mental retardation, high risk of mortality and long-term neurodevelopmental disability in survivors. This is especially true in infants and children. The injury is two staged. A certain amount of damage results from acute, primary neuronal death. This often is followed by a second, delayed period of neuronal loss. This pathology evolution provides a therapeutic window in which secondary damage might be prevented, and the huge potential of plasticity and regeneration of young age can limit the negative effects of neuronal damage.

The most commonly used rodent model of neonatal hypoxia ischemia is the unilateral ligation of the common carotid artery (CCA) followed by a period of hypoxic exposure. In rats, the first two weeks of age are the critical period of neuronal maturation and myelination. Injuries usually restricted to the hemisphere ipsilateral to the ligation and are primarily observed in the cerebral cortex, the deep gray matter (striatum of the basal ganglia and thalamus), the subcortical and periventricular white matter, and the hippocampus. Such neuropathological damage is rarely seen in the contralateral hemisphere and never in pups rendered hypoxic without carotid artery ligation.

3.3.2 Inflammation and immune dysregulation after HI

In the immature brain, HI injuries induce the expression of several genes related to immune responses and inflammation, including macrophages and microglial related genes, T-lymphocytes related genes, and cytokines (Albertsson et al., 2014; Hedtj rn et al., 2004).

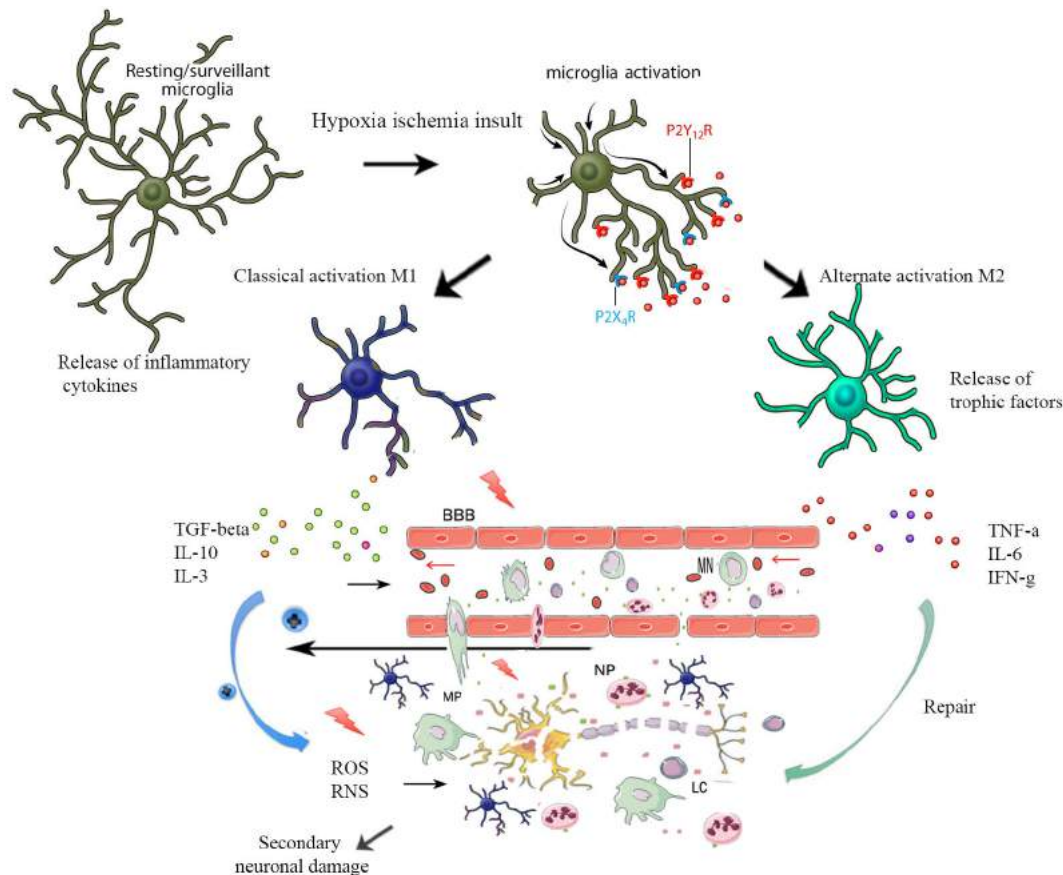


Figure 8. Cascade of inflammatory pathway in brain after acute HI. reactive oxygen species (ROS) and reactive nitrogen species (RNS), neutrophil (NP), leukocytes (LC), macrophage (MP).

This inflammatory mediators have been suggested to contribute to injury after HI, at a stage corresponding to human term and near-term infants (Saliba and Henrot, 2001). As already mentioned, microglia reveal a multifaceted response to injury (Figure 8), indeed they release inflammatory mediators which may aggravate injury (Hagberg et al., 2015; Liu and Mccullough, 2013), but also they express neutrophic and immunomodulatory factors which contribute to healing and recovery from injury (Lalancette-H bert et al., 2012). The exact contribution of these microglial responses depends on the mechanism, location, severity of the injury, and importantly, may also depend on the age at which the injury occurs (Albertsson et al., 2014; Gomes-Leal, 2012). Active microglia express receptors which play an important role

in microglial proliferation, such as IL-6, IL-3, and CSF1 (Denes et al., 2007; Sawada et al., 1990). At the site of injury, rapid increase in number of microglia was observed which might be related to influx of peripheral monocytes and movement of innate microglia from other parts of the brain (Hellström Erkenstam et al., 2016).

Cytokines and chemokines released by active microglia cells in response to an acute neurologic insult, modulate the influx of peripheral immune and inflammatory cells into the brain, contribute to secondary neuronal, oligodendrocyte, and axonal injury and ultimately promote tissue repair and recovery (Butt, 2006; Káradóttir and Attwell, 2007; Mesplès et al., 2005) (Figure 5). Inflammatory mediators released by peripheral immune cells also contribute to neuroinflammation (Albert-Weissenberger et al., 2013). For example, the tumor necrosis factor-related apoptosis inducing ligand (TRAIL) is expressed primarily on microglia and astrocytes and it has been shown to participate in neonatal brain injury after inflammation and HI and the reactive oxygen species (ROS) and nitrogen metabolites generated within the active microglia induce the release of proinflammatory cytokine (Eklind et al., 2001). In newborns' CSF, elevated levels of IL-6 and IL-8 have been correlated with an increased degree of encephalopathy and poor neurodevelopmental outcome.

MAIN OBJECTIVES

Due to the role of microglia in neuroinflammation, a strong effort in searching potential biomarker for microglia activation is in progress, also to monitor efficacy of therapeutic interventions.

In this frame, the main goals of this study were:

- To perform a time course investigation of potential neuroinflammation and demyelination biomarkers in the spinal cord, cerebrospinal fluid and blood in EAE induced in Dark-Agouti rat in order to try to identify novel early biomarkers for microglia activation. (**Chapter I**)
- To investigate the extracellular matrix components according to the temporal evolution of EAE focusing on very early stages, to clarify their contribution to the accumulation of the peripheral inflammatory cells in the perivascular space and their transmigration into the neural parenchyma (**Chapter II**)
- Identify novel early inflammatory biomarkers for microglia activation in neonatal hypoxic ischemic-related and their correlation with related neurological disorders (**Chapter III**)

GENERAL EXPERIMENTAL PROCEDURES

1. Animals

All animal protocols described herein were carried out in accordance with European Community Council Directives (86/609/EEC), approved by the intramural ethical committee for animal experimentation of Bologna University and the Ministry of Health (n° 158/2013-B and no. 607/2016-PR). The experiments were designed in compliance with the guidelines published in the *NIH Guide for the Care and Use of Laboratory Animals* (Louhimies, 2002) and the ARRIVE guidelines, randomizing the procedures and applying blinded analysis.

The animals used in the course of this thesis work were, Dark-Agouti (DA) female rats (151-167 g body weight), and Wistar rat pups of both sexes (12-14 g body weight). Animals were maintained in an animal room on a 12-h light/12-h dark cycle and at constant temperature ($22 \pm 2^\circ\text{C}$), food and water *ad libitum*.

During the surgical procedures, all animals were deeply anesthetized by isoflurane inhalation (Gas anesthesia system-21100- Ugo Basile, Varese – Italy).

2. Surgical procedures

2.1. EAE induction

DA rats were sensitized by a medium containing 0.15-g/ml guinea pig spinal cord tissues in complete Freund's adjuvant (CFA, Sigma, Saint Louse, USA), 50% v/v, to which 5 mg/ml of heat-inactivated *Mycobacterium tuberculosis* (Difco H37Ra, DB, Milan, Italy) was added. Sensitization was performed by injecting 100 μl in both hind pads. Control rats and adjuvant-injected rats (CFA, 50% v/v, heat-inactivated *Mycobacterium tuberculosis*, 5 mg/ml) were used.

2.2. Disease follow-up

Rats were weighed daily and examined for clinical signs of EAE, according to the following semi quantitative score for neurological disability: 0 = no signs, 1 = loss of tail tone, 2 = mono or bilateral weakness of hind legs or middle ataxia, 3 = ataxia or paralysis, 4 = severe hind legs paralysis, 5 = severe hind leg paralysis and urinary incontinence (Calza et al., 2002). In view of the animals' disability, wet food was included inside the cages to facilitate feeding.

2.3. GW2580 treatment

GW2580 (LC Laboratories, Boston, USA) was dissolved in 0.5% hydroxypropylmethylcellulose and 0.1% Tween 80 (Leblond et al., 2015a) (Conway et al., 2005). Experimental groups are: vehicle (0.5% hydroxypropylmethyl-cellulose / 0.1% Tween 80); control+GW2580; EAE and EAE+GW2580. Rats (control+GW2580 and EAE+GW2580 groups) were under GW2580 treatment at 80 mg/Kg (Dose calculation based on BSA (Value based on data from FDA Draft Guidelines), see calculation below) once daily by oral gavage using flexible plastic feeding tubes FTP-15-78-50 (Instech Laboratories, Netherlands) for one-day prior and eleven consecutive days following the immunization. Previous investigations have established that GW2580 administered in mice at 160 mg/kg once daily achieved GW2580 levels that peaked at approximately 9 μ M, and remained greater than 1 μ M for 24 hours, exceeding the estimated minimum plasma concentration to achieve a therapeutic effect (Leblond et al., 2015b).

All animals were weighed daily and EAE and EAE+GW2580 groups were examined for clinical signs of EAE till the 18 DPI (last day of the experiment) following the semi quantitative score for neurological disability as already explained in 2.2.

$$\text{Rat dose (mg/Kg)} = \text{mouse dose (160mg/kg)} \times \frac{\text{Mouse Km (3)}}{\text{Rat Km (6)}} = 80\text{mg/kg}$$

2.4. Neonatal hypoxia-ischemia injury model

At postnatal day 7 (P7), Wister rat pup was first weighed and then anesthetized with 3% isoflurane. The surgery was performed under surgical microscope and lasted less than 5 min. The rat pup was palced on surgical heating pad at 37°C, the skin was cleaned with 10% povidone iodide and a less than 1 cm longitudinal midline incision of the neck was performed to expose the right common carotid artery (CCA). In order to avoid an overextension of the nerve, the fibrous sheath that wraps together both the carotid and the vagus nerve was broken and separated. The CCA was permanently doubly ligated with a 5/0 silk suture. After the ligation few drops of surgical glue was used for the suture of the skin. Pups were placed above a heat mat at 37°C until awakening and recovering then were returned to their dam and were allowed to recuperate for 1.5 hours. Pups were then placed in a hypoxic chamber that contains 8% O₂ and 92% N₂ with a constant flow of 3L/min for 90 min, submerged in a water bath

maintained at 32°C, which is the usual temperature to which rat pups are exposed when huddling with their mother (Mortola and Dotta, 1992) (Hosono et al., 2010). After hypoxia, all pups were returned again to their dam for recovery.

Sham animals underwent the HI surgical procedures (i.e. exposure of the CCA) without artery ligation and without exposure to hypoxic conditions.

3. Examination of neurobehavioral development

3.1. Neurological reflexes

Examinations of neurobehavioral development were performed for all rat pups from P8 to the P21 after the hypoxic insult, and were carried out daily between 10 and 12 a.m. Rat were weighed daily. Pups were tested for the following neurological reflexes:

Righting reflex: this test is believed to be a reflection of subcortical maturation estimate, the generation of these movements from circuits in the spine connected to the supplementary motor area, the basal ganglia, and the reticular formation. The time (sec) used by the animal to go from a supine to a prone position by placing all four paws on the surface was recorded.

Negative geotaxis: this test examines the sensorimotor function of neonatal rats (Rumajogee et al., 2016). Rat pups were placed upside down in the middle of a slope (45°) of 30 cm. The latency to turned 180 degree to an upward direction was recorded. From the day when the animal turns to go up, the time (sec) it took to reach the upper side of the plane was recorded. The maximum duration of recording was 30 seconds otherwise the test was considered negative.

Sensory reflex: the ear and the eyelid of the pup were touched with a cotton swab and the first day of the ear twitch reflex and the contraction of the eyelid were recorded.

Auditory startle: the first day of the startle response to a clapping sound was recorded.

Crossed extensor reflex: the left hind paw was pinched and the possible extension of the right paw was recorded.

Limb placing: the back of the forepaw and hindpaw was touched with the edge of the bench while the animal suspended, and the first day of lifting and placing the paws on the table was noted.

Limb grasp: the forelimbs were touched with a thin rod, and the first day of grasping onto the rod was recorded.

Gait: the animals are placed at the center of a white plexiglass circle (diameter = 13cm). Register the day when they start to move out of the circle with both front paws, estimate the time (sec) that the animal uses to exit out of the circle. In the case in which the animal does not leave the circle within 30 seconds, the test is considered negative.

In order to assess the development of neurological reflex, rats are given a score the to the corresponding time (sec). The higher score indicates greater capacity for development of neurological reflexes (See table 3)

Table 3. Neurological reflex score and the corresponding time.

Time (sec)	Score
0-10	3
11-20	2
21-30	1
>30	0

3.2. Behavioral assessment

Three weeks after (P28), the assessment of long-term neurofunctional handicap were performed in sham and HI groups. These tasks consisted of the open field, Rota-rod, Catwalk and Morris water maze.

3.2.1. Open field

Animals were observed for locomotor behavior in an open-field. Pups were placed in an open-field consisting of a 46x46 cm wooden chamber with 21 cm high walls around, with a dark gray floor divided into 16 fields. Rats were placed individually in the center, always facing the same direction, in the center of the chamber and the latency to leave this first square will be recorded. The following parameters were measured: distance travelled, rearing, grooming and ambulation frequency. Speed was calculated from the ambulatory time and the total travelled distance. Animals were video-recorded for 10 min (Balduini et al., 2000)

3.2.2. Rota-rod

The rotarod test (LE 8500 RotaRod : 2Biological Instruments, Varese, Italy) consist on two days test. Animals were exposed to one habituation session during 3 min in the apparatus on slow velocity (20 rpm). In the test session, 24 h later, animal's motor ability was evaluated. The rotarod test was performed by placing rats on rotating drums and measuring the time each animal was to maintain its balance on the rod. The speed of the rotarod accelerated from 16 to 40 rpm over a 6 min period. Variables recorded were: latency of the first downfall,

number of falls (maximum 3) and time of permanence in the apparatus (Rojas et al., 2013) (Rojas et al., 2013; Takao et al., 2010).

3.2.3. CatWalk

Cerebellar function was analysed by CatWalk (Noldus Information Technology, Wageningen, The Netherlands), a quantitative gait analysis system.

Each rat ran across a glass walkway transversely and three complete runs were recorded using a camera positioned below, and the average will be calculated. If an animal failed to complete a run within 5 s, walked backwards or reared during the run, the process was repeated. The experiment was performed in the dark; the glass walkway was illuminated with beams of light, thereby allowing the animals' paws to reflect light as they touched the glass floor. Each paw was labeled on the recorded video in order to calculate paw-related parameters. The gait-related parameters measured using the CatWalk system was the following: *maximum contact area*: the maximum area of a paw that comes into contact with the glass plate, *stand*: stance phase is the duration in seconds of contact of a paw with the glass plate and swing speed: is the speed (Distance Unit/second) of the paw during Swing. The formula of *Swing Speed* is: $\text{Swing (s) Phase} \times \text{Swing Speed}$ which is the duration in seconds of no contact of a paw with the glass plate. The Stride Length which is the distance (in Distance Units) between successive placements of the same paw, the calculation of Stride Length is based on the X-coordinates of the center of the paw print of two consecutive placements of the same paw during Max contact and taking into account Pythagoras' theorem (Hattori et al., 2015).

3.2.4. Morris Water Maze

The spatial memory performance was evaluated 3 week after HI lesion using an MWM (180 cm diameter, 45 cm high) conceptually divided in four equal imaginary quadrants. The water of the pool was made opaque by using non-toxic grey tempera paint. Training on spatial version of the MWM was carried out over 4 consecutive days. On each day, rats received four training trials in which a randomly starting point was used, such that 2 successive trials never began from the same position. The training consisted of a swim followed by a 30 s seconds platform sit. The escape latency to find the platform was measured for individual animals on each day. Rats that did not find the platform within 120 seconds were guided to it by the experimenter. To assess long-term memory, 24 hours after the final trial, the platform was removed from the maze and a 2-minute free swim will be conducted, and time (seconds) spend

during the first 20 seconds and the entire swim in the quadrant formerly occupied by the platform will be recorded (Chou et al., 2001).

4. Immunohistochemistry on slides

Spinal cord tissues were fixed in 4% paraformaldehyde and picric acid saturated aqueous solution in 0.1 M Sörensen buffer pH 7 for 24 h and then washed with 5% sucrose solution every day till the fixative was completely removed. Tissues were frozen with CO₂ gas and kept at -80°C until processed. Coronal sections (14µm thickness) were then prepared (Microm HN550, Bio-Optica, Milan, Italy) and processed for morphological studies. For immunohistochemistry, sections were first rehydrated and then incubated for 1 h with PBS-0.3% Triton X-100, 2% normal serum goat, 1% BSA, followed by incubation with the primary antibodies (table 4) diluted in the pre-absorption solution overnight at 4°C. After rinsing in PBS, the sections were incubated at 37°C for 30 min with the secondary antibodies (table 5) diluted in PBS-0.3% Triton X-100. Sections were then rinsed in PBS and mounted in phenylendiamine solution (0.1% 1,4-phenylendiamine, 50% glycerine, carbonate/bicarbonate buffer pH 8.6, Sigma, Saint Louse, USA). Control slices were incubated with the secondary antibodies only and processed in parallel.

Cerebellum tissues were fixed in 1.5% paraformaldehyde saturated aqueous solution in 0.1 M Sörensen buffer pH 7 for 4 h then embedded in Tissue-Tek® O.C.T.™ Compound (Sakura Finetek Europe, Alphen aan den Rijn, Netherlands), (Leica CM1950, Walldorf, Germany). Tissues were frozen and kept at -80°C until processed. For immunohistochemistry, sections (10µm thickness) were incubated for 1 h with PBS-0.5% Triton X-100, 1% BSA, followed by incubation with the primary antibodies (table 4) diluted in the pre-absorption solution overnight at 4°C. After rinsing in PBS, the sections were incubated at 37°C for 2 h with the secondary antibodies (table 5) diluted in the pre-absorption solution. Sections were then rinsed in PBS and mounted in Evanol solution.

5. Histology

To analyze the inflammatory infiltration, spinal cord sections were stained with toluidine blue and evaluated on 3 replicate sections per animal, counting the number and severity of cellular infiltrates over each whole coronal section. Cellular infiltrates were scored as follows: 0, none; 1, a few inflammatory cells; 2, organization of perivascular infiltrates; 3, increasing severity of perivascular cuffing with extension into the adjacent tissue (Hickey et

al., 1987). The inflammation score derives from the sum of infiltration scores in each cellular infiltrate.

To analyze the cerebellum's perivascular cuffs, tissues were cut into 10 µm thickness sections on the cryostat (Leica CM1950), and stained with hematoxylin and eosin (H&E) according to standard procedures.

6. Microscopy

Sections destined for quantification were examined under bright field in a Nikon Eclipse E-600 microscope equipped with appropriate filters for the visualization of fluorescence produced by FITC, RRX, TMR, Texas Red or Nikon Microphot-FXA or Zeiss AxioImager equipped with epifluorescent optics

Photographs were taken with digital CCD camera Q Imaging Retiga-2000RV (Q Imaging, Surrey, BC, Canada) or digital camera DXM1200F or Hamamatsu ORCA ER camera. Images were captured and analyzed using NIS software 4.30 or Volocity 5.1 software (Improvision).

Table 4. List and characteristics of primary antibodies used in this thesis

<i>Antibody</i>	<i>Species of origin</i>	<i>Dilution</i>	<i>Reference</i>
Cluster of differentiation 44 (CD44)	Rabbit	1:100	Acris Antibodies, Inc, San Diego, USA
CD163	Rabbit	1:100	Bioss Inc, Woburn, USA
Neurofilament (NF200)	Mouse	1:800	Sigma, Saint Louse, USA
Colony Stimulating Factor 1 (CSF1)	Rabbit	1:100	Novus Biologic
OX42	Mouse	1:250	AbD Serotec Inc., Raleigh, USA
Membrane-spanning chondroitin sulphate proteoglycan (NG2)	Mouse	1:100	Millipore, Merck S.p.a., Milan, Italy
2', 3'-cyclic nucleotide 3'-phosphodiesterase (CNPase)	Mouse	1:250	Millipore, Merck S.p.a., Milan, Italy
Glial Fibrillary Acidic Protein (GFAP)	Rabbit	1:500	Dako, Milan, Italy
GFAP	Mouse	1:500	Sigma, Saint Louse, USA
FluoroMyelin TM Fluorescence Myelin Staining	-	1:300	Molecular Probes, Eugene, OR
Ionized calcium binding adaptor molecule 1 (Iba 1)	Rabbit	1 :100	Wako
Neuronal Nuclei (NeuN)	Mouse	1 :400	Millipore
Cluster of differentiation 3 (CD3)	Rabbit	1 :500	Abcam
Pan-Laminin (Pan LM)	Human	1 :1000	L.M.Sorokin Lab
C-X-C motif chemokine 12 (CXCL12)	Rabbit	1 :400	AHP794, AbD Serotec

Table 5. List and characteristics of secondary antibodies used in this thesis

<i>Antibody</i>	<i>Species of origin</i>	<i>Dilution</i>	<i>Reference</i>
Anti-mouse IgG DyLight 488	Rabbit	1:100	ThermoScientific, Milano, Italy
Anti-rabbit IgG Rhodamine Red TM -X	Donkey	1:100	Jackson ImmunoResearch, West Grove, PA, USA
Anti-rabbit IgG DyLight 488	Donkey	1:100	ThermoScientific, Milano, Italy
Anti-goat IgG Red TM -X	Donkey	1:100	Jackson ImmunoResearch, West Grove, PA, USA
Anti-mouse IgG Alexa Fluor 488	Rabbit	1:1000	Molecular Probes/Invitrogen
Anti-rat IgG Alexa Fluor 594	Donkey	1:1000	Invitrogen
Anti-rabbit IgG Alexa Fluor 594	Donkey	1:1000	Invitrogen
Anti-GFAP Alexa Fluor 488	Mouse	1:1000	eBioscience
Anti-mouse IgG Cy3	Goat	1:400	Jackson ImmunoResearch

7. In Vitro Experiments

7.1. Preparation of CNS Tissue Lysates

Crude CNS samples from Controls and EAE rats were frozen in liquid nitrogen, weighed and homogenized in PBS with 0.37 mg/ml proteinase inhibitor-EDTA cocktail tablets (Roche) on ice. For 1 mg tissue, 500 μ l PBS was used. Extracts were centrifuged for 10 min at 12,000g at 4°C and supernatants were collected.

7.2. Determination of Protein Concentrations

Protein concentrations of brain lysates were determined using the BCATM Protein Assay Kit (Pierce, Rockford; USA) according to the manufactures' instructions. Photometric analysis was performed using a BioPhotometer (Eppendorf) with a BSA standard curve utilizing the internal, pre-programmed BCA protein concentration determination algorithm.

7.3. Gelatin Zymography

Cerebellum tissue lysates were used. Prepurification of tissue lysates was carried out by incubation with gelatin-Sepharose 4B for 20 min (Descamps et al., 2002). Equal amounts of total protein were mixed with SDS sample buffer without reducing agent and run on a 4% stacking and 12% separating SDS-polyacrylamide gel, containing 1 mg/ml gelatin to detect pro- and activated-forms of MMP-2 and MMP-9 (Masure et al., 1991). After electrophoresis, gels were washed with 2.5% Triton X-100 in H₂O for 30 minutes at room temperature to remove SDS and to renature MMP-2 and MMP-9. Gels were then incubated in developing buffer (50 mM Tris base, 50 mM Tris-HCL, 0.2 M NaCl, 5 mM CaCl₂, 0.02% NP-40, dH₂O) for an optimized length of time (overnight) at 37°C to induce gelatin cleavage by the renatured MMPs. After overnight incubation, proteins in the gels were fixed in acetic acid:ethanol:dH₂O [10:50:40] for 30 minutes and then washed in acetic acid:methanol:H₂O [10:50:40] mixture also for 30 minutes. Subsequently, the zymogram was stained with Coomassie Brilliant Blue and destained in acetic acid: methanol: dH₂O [10:50:40] solution at room temperature for 1 h. Areas of cleaved gelatin appear as clear bands against a dark blue stained background. Human recombinant MMP-9 and mouse recombinant MMP-2 were used as controls.

8. mRNA analysis

8.1. Spinal cord mRNA analysis

Rats were sacrificed and total LSC was dissected, snap frozen and stored at -80°C until used. Total RNA was prepared from spinal cord using QIAzol Reagent, cleaned with RNeasy Mini kit (Qiagen; Milano- Italy) and eluted in RNase Free Water and purity and concentration were evaluated by spectrophotometry using NanoDrop ND-2000 (ThermoScientific, Milano, Italy). cDNA synthesis was performed using RT² First Strand kit following the manufacturer's instructions. In brief, after incubation for 5 min at 42°C with Genomic DNA elimination mix in order to avoid any DNA contamination, a reverse-transcription mix of BC3, P2, RE2 and H₂O was used and the transcription performed in a final volume of 20 µl by heating first at 42°C for 15 min, then at 95°C for 5 min. Real-time PCR amplification was performed using the Stratagene Mx3005P multiplex quantitative PCR system (Agilent Technologies). The expression of genes involved in MS progression was carried out using RT² SYBR Green qPCR Mastermix (Qiagen). These genes were grouped according to: T Cell Activation/Signaling, Adaptive Immunity, Cytokine/Chemokine Inflammation, demyelination and cellular stress. The raw data obtained was uploaded into GeneGlobe Data Analysis software (SABiosciences, Qiagen) for analysis. Relative quantification of mRNA expression was calculated using the comparative cycle threshold (C_T) method and is expressed as Log 2 Fold Change of expression. The Fold Change ($2^{(-\Delta\Delta Ct)}$) is the normalized gene expression ($2^{(-\Delta Ct)}$) in the test sample divided by the normalized gene expression ($2^{(-\Delta Ct)}$) in the control sample.

9. CSF and plasma biomarker analysis

CSF sampling was adapted from the method of Liu, L. and Duff, K (Liu and Duff, 2008). Briefly, rats were anesthetized and placed prone on the stereotaxic instrument letting the body of the rat laid down. A sagittal incision of the skin was made below the occiput and the subcutaneous tissue and neck muscles through the midline were separated and held apart using a microretractor. The dura mater of the cisterna magna was then penetrated by an 8 cm long glass capillary, which had a narrowed tip with an inner diameter of about 0.5 mm so that the CSF flowed into the capillary. After collection, each sample was centrifuged at 2000xg for 10 minutes at 4°C, and the supernatant aliquoted and stored at -80°C for biochemical assays. Blood was collected from the abdominal aorta in EDTA-K2 Vacutainer tubes, centrifuged at

3000xg for 10 min at 4°C and the plasma collected, aliquoted and stored at -80°C until used. Proteins known to play key roles in neuroinflammation pathways were selected. For this purpose Bio-Plex Pro™ Rat Cytokine 24-plex Assay (Bio-Rad; Milano- Italy) was used. The kit included EPO, G-CSF (CSF3), GM-CSF (CSF2), GRO/KC, IFN- γ , IL-1 α , IL-1 β , IL-2, IL-4, IL-5, IL-6, IL-7, IL-10, IL-12p70, IL-13, IL-17A, IL-18, M-CSF (CSF1), MCP-1 (CCL2), MIP-1 α (CCL3), MIP-3 α (CCL20), RANTES (CCL5), TNF- α and VEGF.

The simultaneous quantification of the different proteins in CSF and plasma was performed using xMAP technology and a MAGPIX Luminex platform. This technology makes use of different populations of color-coded beads of monoclonal antibodies specific to a particular protein, thus allowing simultaneous capture and detection of specific analytes from a sample. All the beads from each set are read off, which further validates the results. Using this process, xMAP Technology allows multiplexing of up to 50 unique bioassays within a single sample, both rapidly and precisely (Houser, 2012), (Blankesteyn and Altara, 2014). In brief, after the incubation of a specific monoclonal antibody conjugated bead population with 50 μ l of CSF/plasma samples for 1 hour at RT, washed beads were incubated with detection antibody solution at RT for 30 min, then with the streptavidin–phycoerythrin conjugated solution (RT, 10 min). After washing, beads were resuspended in the assay buffer, shaken for 1 min and then a reading performed on the MAGPIX instrument. The results were analyzed with xPONENT 4.2 ® software and expressed as pg/mL.

10. Functional pathway and network analysis

A pathway analysis approach in an exploratory study was implemented. We proceed through the web-software STRING 10.0 (<http://string-db.org/>) and Gene Ontology databases. Protein–protein interaction analysis (both physical and functional interactions) was performed using default parameters (high confidence: 0.7) and *R.norvegicus* as the organism of interest. The software allows the net of interactions including other proteins closely linked to the one analyzed to be extended, in order to obtain a better understanding of the possible pathways affected by the disease.

11. Statistical Analysis

Student's *t* test was used to compare means of two groups and one-way ANOVA followed by Dunnett's multiple comparison tests. Data are presented as mean \pm standard error

of the mean and significance was set at $P \leq 0.05$. All statistical analyses were performed using GraphPad Prism 6.0 (GraphPad Software).

In order to calculate the number of animals needed to study the effect of the treatment with GW2580, we performed a power analysis using the G*Power 3.1 software. To reach a power of 0.9, based on retrospective analysis of recent research done by others (Gómez-Nicola et al., 2013; Olmos-Alonso et al., 2016), we needed a minimum of $n = 6$ animals per experimental group.

For the normalization of gene expression on the RT² PCR Profiler Array, five housekeeping genes, Ribosomal protein, large, P1, Hypoxanthine phosphoribosyltransferase 1, Ribosomal protein L13A, Lactate dehydrogenase A, Actin beta were used. The CT was determined for each sample and normalized to the average CT of the five housekeeping genes. A comparative CT method was used to calculate relative gene expression. Data are represented as Log 2 Fold Change relative to control. The P -values were calculated on the basis of a Student's t -test of the replicate $2^{(-\Delta Ct)}$ values for each gene in the control group and treatment groups, and P values less than 0.05 was considered significant.

RESULTS AND GENERAL DISCUSSION

During this study we came across some results that are interesting from a methodological point of view. Part of these results presented in this thesis has been already published (Chapter I), or are in manuscript form (Chapter II and III). Data included in this paper or manuscripts, are only briefly described in this section.

In **chapter I**, using high-throughput technologies for gene expression and protein assays, and focusing on the time-course between immunization and the clinical onset, we performed a time course investigation of neuroinflammation and demyelination biomarkers in the CNS tissue (spinal cord, SC), and biological fluids (CSF and plasma) in EAE induced in Dark-Agouti female rats compared with controls and adjuvant injected rats. In this study, we demonstrate that the CSF1 was the first up-regulated protein as soon as 1 DPI, not only in blood but also in CSF and SC. A treatment with GW2580, a selective CSF1R inhibitor, slowed the disease progression, significantly reduced the severity and prevented the relapse phase. Moreover, both pro-inflammatory (IL-1 β , TNF- α) and anti-inflammatory cytokines (IL-5, IL-10, VEGF) were upregulated starting from 8 DPI. Myelin genes were down-regulated starting from 8 DPI, especially MAL, MBP, PMP22 while an opposite expression profile was observed for inflammation-related genes, such as CXCL11 and CXCL10.

In **chapter II**, we investigated the effect of CSF1R inhibition using the small molecule, GW2580, on BBB disruption with the temporal evolution of EAE. We have shown that GW2580 treatment had a therapeutic effect in EAE rats. Our findings prove that GW2580 down regulates microglia activation, reduce IgG extravasation and T-cell recruitment and more important, CSF1R inhibition, reduces BBB leakage by inhibiting activities of MMP-9. Those findings identify a novel mechanism underlying the effect of GW2580 that could be a novel therapy for MS.

In **chapter III**, we investigated plasma and CSF contents of biomarkers after neonatal HI during the acute (24 and 72 hours) and chronic (44 days) phases and their correlation with neurological disorders in rat model of HI. In this study, both male and female Wistar rats were used and underwent ischemia procedure, where the right carotid artery permanently was

doubly ligated, and exposed to 8% oxygen for 90 min; control rats received sham surgery. Sensory and cognitive parameters were assessed by the use of open field, rotarod, CatWalk and Morris water maze test. After behavioral testing, plasma and CSF were used to investigate proinflammatory and immunoregulatory biomarkers at different time points. Our data suggest that HI induced an early activation of the inflammatory cascade leads to increased production of a large number of proinflammatory mediators that could be the cause of tissue loss of hypoxic hemisphere, which in his turn might leads to short-term- as well as long-lasting behavioral- deficits.

CHAPTER I


Cytokine and chemokine alterations in tissue, CSF, and plasma in early presymptomatic phase of experimental allergic encephalomyelitis (EAE), in a rat model of multiple sclerosis.

RESEARCH

Open Access



Cytokine and chemokine alterations in tissue, CSF, and plasma in early presymptomatic phase of experimental allergic encephalomyelitis (EAE), in a rat model of multiple sclerosis

Nozha Borjini^{1,2,3*} , Mercedes Fernández⁵, Luciana Giardino^{2,3,4} and Laura Calzà^{2,3,5}

Abstract

Background: Experimental allergic encephalomyelitis (EAE) is the most commonly used experimental animal model for human multiple sclerosis (MS) that has been used so far to study the acute and remission-relapsing phases of the disease. Despite the vast literature on neuroinflammation onset and progression in EAE, important questions are still open regarding in particular the early asymptomatic phase between immunization and clinical onset.

Methods: In this study, we performed a time-course investigation of neuroinflammation and demyelination biomarkers in the spinal cord (SC), cerebrospinal fluid (CSF), and blood in EAE induced in dark agouti (DA) female rats compared to the controls and adjuvant-injected rats, using high-throughput technologies for gene expression and protein assays and focusing on the time-course between immunization, clinical onset (1, 5, 8 days post-immunization (DPI)), and progression (11 and 18 DPI). The expression profile of 84 genes related to T cell activation/signaling, adaptive immunity, cytokine/chemokine inflammation, demyelination, and cellular stress were analyzed in the tissue; 24 cytokines were measured in the CSF and plasma.

Results: The macrophage colony-stimulating factor (CSF1) was the first up-regulated protein as far as 1 DPI, not only in blood but also in CSF and SC. A treatment with GW2580, a selective CSF1R inhibitor, slowed the disease progression, significantly reduced the severity, and prevented the relapse phase. Moreover, both pro-inflammatory (IL-1 β , TNF- α) and anti-inflammatory cytokines (IL-5, IL-10, VEGF) were up-regulated starting from 8 DPI. Myelin genes were down-regulated starting from 8 DPI, especially MAL, MBP, and PMP22 while an opposite expression profile was observed for inflammation-related genes, such as CXCL11 and CXCL10.

Conclusions: This early cytokine and chemokine regulation indicates that novel biomarkers and therapeutic options could be explored in the asymptomatic phase of EAE. Overall, our findings provide clear evidence that CSF1R signaling regulates inflammation in EAE, supporting therapeutic targeting of CSF1R in MS.

Keywords: Neuroinflammation, Multiple sclerosis, Experimental allergic encephalomyelitis, Biomarkers, Plasma, CSF1

* Correspondence: n.borjini@chiesi.com

¹Research and Development, Chiesi Farmaceutici S.p.A, Via Palermo 26/A, Parma 43100, Italy

²Health Science and Technologies Interdepartmental Center for Industrial Research (HST-ICIR), University of Bologna, Via Tolara di Sopra 41/E, Bologna, Ozzano Emilia I 40064, Italy

Full list of author information is available at the end of the article



Background

Inflammation and demyelination are the primary pathological events in multiple sclerosis (MS), the most diffuse inflammatory demyelinating disease of the central nervous system (CNS) [1]. The progressive failure of remyelination leads to the cumulative loss of axons, gray matter atrophy, and the prevalent neurodegeneration responsible for chronic disability and cognitive defects [2]. Despite the intensive efforts and the major progress achieved in understanding the inflammatory process and pathogenetic mechanisms within this heterogeneous disease entity to date, the exact pathophysiological process of MS remains elusive.

Both humoral and the cell-mediated immune reactions having peripheral macrophages and central microglia as key players take part in the neural-immune mechanisms underlying MS [3]. Indeed, MS pathogenesis has been believed to be derived from autoreactive lymphocytes (T/B cells) and a plethora of macrophages recruited from the periphery. Both cell classes are able to cross the blood–brain barrier (BBB) [4] and to engage microglia, the resident immune cells in the CNS [5], ultimately leading to severe demyelination and neuronal degeneration. Cytokines and chemokines play a key role in these processes by regulating cell migration, proliferation, and activation of resident and infiltrating cells [6].

An important contribution to MS studies has been made by experimental allergic encephalomyelitis (EAE), the most widely used animal model for MS [7], in which the interaction between a variety of immunopathological and neuropathological mechanisms affords an approximation of the key pathological features of MS pathology, including inflammation and immune reaction, demyelination, axonal loss, and gliosis [8, 9]. EAE has been also used to develop and validate all approved therapies for MS [10], thus confirming the good correlation between animal and human pathology [11, 12].

In particular, the EAE model allows a hitherto poorly studied phase of the disease to be investigated, i.e., the preclinical asymptomatic phase. This time window could be particularly interesting for the discovery of novel early biomarkers and novel therapeutic target. According to recent reports, in the MS murine model, a significant T cell mobilization was observed at 2 days post-immunization (DPI), thus an asymptomatic stage of the disease [13]. Furthermore, a transient vessel leak in the cortical gray matter has been described at the same time window [14]. Moreover, pain associated with microglia and astrocyte activation occurs in EAE prior to the onset of clinical signs [15, 16].

It is worthy of note that few studies to date have been devoted to the investigation of this asymptomatic phase of the disease. In order to elucidate very early molecular alterations occurring in the CNS of EAE animals before

the clinical onset of the disease and to link tissue alterations to potential CSF and plasma biomarkers, in the present study, we investigated molecular mediators of neuroinflammation and demyelination in the tissue (SC), CSF, and plasma during early presymptomatic EAE using high-throughput technologies for gene expression and protein assays. The results indicate that the profile of neuroinflammation and demyelination biomarkers is dramatically changed during the early phase of EAE. Consequently, we have identified the regulation of the chemokine macrophage colony-stimulating factor (CSF1) already 24 h after immunization, which indicates the occurrence of microglia activation. Interestingly, we found that a selective inhibition of CSF1R significantly reduced the severity of the disease and prevented the relapse phase in EAE rats, suggesting the importance of CSF1-CSF1R signaling in microgliosis and inflammation in MS.

Methods

Animals, EAE induction, and disease follow-up

Dark agouti (DA) (Harlan, Italy) female rats, 151–167-g body weight, were used in the first part of the study, placed on ad libitum food and water, and housed three per cage on a 12-h light/dark cycle. The DA rat model of EAE mimics certain aspects of the clinical course of the disease in people with RRMS [17–19], typified by progressive, sustained demyelination, and associated axonal loss [20, 21]. The disease onset in this strain bears is characterized by neurological impairments, manifested as a flaccid tail followed by an acute attack with disturbed gait and paralysis. Most DA animals recover spontaneously from paralysis and experience remission and may then undergo one or more relapses.

A group of 42 rats was sensitized (considering group composition and two extra animals) by a medium containing 0.15 mg/ml guinea pig spinal cord tissue in complete Freund's adjuvant (CFA, Sigma, Saint Louis, USA), 50% v/v, to which 5 mg/ml of heat-inactivated *Mycobacterium tuberculosis* (Difco H37Ra, DB, Milan, Italy) was added. Sensitization was performed by injecting 100 µl in both hind pads. Control rats ($n = 8$) and adjuvant-injected rats (CFA, 50% v/v, heat-inactivated *M. tuberculosis*, 5 mg/ml) ($n = 15$) were used. The rats were weighed daily and examined for clinical signs of EAE, according to the following semi quantitative score for neurological disability: 0 = no signs, 1 = loss of tail tone, 2 = mono or bilateral weakness of hind legs or middle ataxia, 3 = ataxia or paralysis, 4 = severe hind legs paralysis, and 5 = severe hind leg paralysis and urinary incontinence [22]. In view of the animals' disability, wet food was included inside the cages to facilitate feeding. At 1, 5, 8, 11, and 18 DPI, eight EAE rats were randomly sacrificed. From each experimental group, five animals were used for proteomic and molecular biology experiments and three for

morphology and immunohistochemistry. All animal protocols described herein were carried out in accordance with the European Community Council Directives (86/609/EEC), approved by the intramural ethical committee for animal experimentation of Bologna University and the Ministry of Health (no. 158/2013-B) and comply with the guidelines published in the *NIH Guide for the Care and Use of Laboratory Animals* [23].

GW2580 treatment and CSF1R inhibition

In order to calculate the number of animals needed to study the effect of the treatment with GW2580, we performed a power analysis using the G*Power 3.1 software. To reach a power of 0.9, based on retrospective analysis of recent research done by others [24, 25], we needed a minimum of $n = 6$ animals per experimental group.

The experiments were designed in compliance with the ARRIVE guidelines, randomizing the procedures and applying blinded analysis.

GW2580 (LC Laboratories, Boston, USA) was dissolved in 0.5% hydroxypropyl methylcellulose and 0.1% Tween 80 [26, 27]. The experimental groups made of $n = 6$ animals each were as follows: vehicle (0.5% hydroxypropyl methylcellulose/0.1% Tween 80); control + GW2580; EAE; and EAE + GW2580. The rats (control + GW2580 and EAE + GW2580 groups) were under GW2580 treatment at 40 mg/kg once daily by oral gavage using flexible plastic feeding tubes FTP-15-78-50 (Instech Laboratories, Netherlands) for 1 day prior and 11 consecutive days following the immunization. All animals were weighed daily and the EAE and EAE + GW2580 groups were examined for clinical signs of EAE till the 18 DPI (last day of the experiment) following the semi quantitative score for neurological disability as already explained in the first part of the study. Animal protocols described herein were carried out in accordance with the European Community Council Directives (86/609/EEC), approved by the intramural ethical committee for animal experimentation of Bologna University and the Ministry of Health (no. 607/2016-PR).

Histology and immunohistochemistry

On post-immunization days 1, 5, 8, 11, and 18, three rats were sacrificed and the lumbar spinal cord (LSC) tissues of the control, EAE, and adjuvant groups were fixed in 4% paraformaldehyde and picric acid and saturated aqueous solution in 0.1 M Sørensen buffer pH 7 for 24 h and then washed with 5% sucrose solution every day till the fixative was completely removed. The tissues were frozen with CO₂ gas and kept at -80°C until processed. Coronal sections (14- μm thickness) were then prepared (Microm HN550, Bio-Optica, Milan, Italy) and processed for morphological studies. For immunohistochemistry, the sections were first rehydrated and then

incubated for 1 h with PBS–0.3% Triton X-100, 2% normal serum goat, and 1% BSA, followed by incubation with the primary antibodies diluted in the pre-absorption solution overnight at 4°C . The primary antibodies and dilutions used were as follows: rabbit anti-CD44 (1:100, Cluster of differentiation 44, Acris Antibodies, Inc, San Diego, USA), rabbit anti-CD163 (1:100, Cluster of differentiation 163, Bioss Inc, Woburn, USA), mouse anti-CD86 (1:250, Cluster of differentiation 86, Novus Biological Europe, Cambridge, UK), mouse anti-NF200 (1:200, Neurofilament, Sigma, Saint Louse, USA), rabbit anti CSF1 (1:100, colony-stimulating factor 1, Novus Biological), mouse anti-OX42 (1:250, AbD Serotec Inc., Raleigh, USA), mouse anti-NG2 (1:100, membrane-spanning chondroitin sulfate proteoglycan, Millipore, Merck S.p.a., Milan, Italy), mouse anti-CNPase (1:250, 2', 3'-cyclic nucleotide 3'-phosphodiesterase, Millipore, Merck S.p.a., Milan, Italy), rabbit anti-GFAP (1:500, glial fibrillary acidic protein, Dako, Milan, Italy), and mouse anti-GFAP (1:500, Sigma, Saint Louse, USA). FluoroMyelin™ Fluorescence Myelin Staining (Molecular Probes, Eugene, OR) was also performed to stain the myelin sheaths, following the manufacturer's specifications. After rinsing in PBS, the sections were incubated at 37°C for 30 min with the secondary antibodies: DyLight488-conjugated affinity-pure goat anti-mouse IgG (ThermoScientific, Milano, Italy), Rhodamine Red™-X-conjugated affinity-pure donkey anti-rabbit IgG (Jackson ImmunoResearch, West Grove, PA, USA), DyLight488-conjugated affinity-pure donkey anti-rabbit IgG (ThermoScientific, Milano, Italy), and Red™-X-conjugated affinity-pure donkey anti-goat IgG (Jackson ImmunoResearch, West Grove, PA, USA) diluted in PBS–0.3% Triton X-100, 1:100. The sections were then rinsed in PBS and mounted in phenylenediamine solution (0.1% 1,4-phenylenediamine, 50% glycerine, carbonate/bicarbonate buffer pH 8.6, Sigma, Saint Louse, USA). The control slices were incubated with the secondary antibodies only and processed in parallel. Images were captured using a Nikon Eclipse E600 microscope equipped with digital CCD camera Q Imaging Retiga-2000RV (Q Imaging, Surrey, BC, Canada). To analyze the inflammatory infiltration, the sections were stained with toluidine blue and evaluated on three replicate sections per animal, counting the number and severity of cellular infiltrates over each whole coronal section. Cellular infiltrates were scored as follows: 0, none; 1, a few inflammatory cells; 2, organization of perivascular infiltrates; and 3, increasing severity of perivascular cuffing with extension into the adjacent tissue [28]. The inflammation score derives from the sum of infiltration scores in each cellular infiltrate.

Spinal cord mRNA analysis

At post-immunization days 1, 5, 8, 11, and 18, five rats were sacrificed and the total LSC was dissected, snap frozen, and stored at -80°C until used.

The total RNA was prepared from the spinal cord using QIAzol Reagent, cleaned with RNeasy Mini kit (Qiagen; Milano- Italy), and eluted in RNase Free Water, and purity and concentration were evaluated by spectrophotometry using NanoDrop ND-2000 (ThermoScientific, Milano, Italy). Complementary DNA (cDNA) synthesis was performed using RT² First Strand kit following the manufacturer's instructions. In brief, after incubation for 5 min at 42 °C with genomic DNA elimination mix in order to avoid any DNA contamination, a reverse-transcription mix of BC3, P2, RE2, and H₂O was used and the transcription was performed in a final volume of 20 µl by heating first at 42 °C for 15 min, then at 95 °C for 5 min. Real-time PCR amplification was performed using the Stratagene Mx3005P multiplex quantitative PCR system (Agilent Technologies). The expression of genes involved in MS progression was carried out using RT² SYBR Green qPCR Mastermix and the Multiple Sclerosis RT2 Profiler PCR Array (Qiagen). The genes are grouped according to the following: T cell activation/signaling, adaptive immunity, cytokine/chemokine inflammation, demyelination, and cellular stress. The raw data obtained was uploaded into GeneGlobe Data Analysis software (SABiosciences, Qiagen) for analysis. Relative quantification of messenger RNA (mRNA) expression was calculated using the comparative cycle threshold (C_T) method and is expressed as Log2 fold change of expression. The fold change ($2^{-(\Delta\Delta C_T)}$) is the normalized gene expression ($2^{-\Delta C_T}$) in the test sample divided by the normalized gene expression ($2^{-\Delta C_T}$) in the control sample.

CSF and plasma biomarker analysis

CSF sampling was adapted from the method of Liu and Duff [29]. Briefly, the rats were anesthetized by isoflurane inhalation (Gas Anesthesia System-21100, Ugo Basile, Varese, Italy) and placed prone on the stereotaxic instrument letting the body of the rat laid down. A sagittal incision of the skin was made below the occiput, and the subcutaneous tissue and neck muscles through the midline were separated and held apart using a microretractor. The dura mater of the cisterna magna was then penetrated by an 8-cm long glass capillary, which had a narrowed tip with an inner diameter of about 0.5 mm so that the CSF flowed into the capillary. After collection, each sample was centrifuged at 2000×g for 10 min at 4 °C, and the supernatant aliquoted and stored at -80 °C for biochemical assays.

Blood was collected from the abdominal aorta in EDTA-K2 Vacutainer tubes and centrifuged at 3000×g for 10 min at 4 °C, and the plasma was collected, aliquoted, and stored at -80 °C until used.

Proteins known to play key roles in neuroinflammation pathways were selected. For this purpose, Bio-Plex

Pro™ Rat Cytokine 24-plex Assay (Bio-Rad; Milano, Italy) was used. The kit included EPO, G-CSF (CSF3), GM-CSF (CSF2), GRO/KC, IFN-γ, IL-1α, IL-1β, IL-2, IL-4, IL-5, IL-6, IL-7, IL-10, IL-12p70, IL-13, IL-17A, IL-18, M-CSF (CSF1), MCP-1 (CCL2), MIP-1α (CCL3), MIP-3α (CCL20), RANTES (CCL5), TNF-α, and VEGF.

The simultaneous quantification of the different proteins in CSF and plasma was performed using xMAP technology and a MAGPIX Luminex platform. This technology makes use of different populations of color-coded beads of monoclonal antibodies specific to a particular protein, thus allowing simultaneous capture and detection of specific analytes from a sample. All the beads from each set are read off, which further validates the results. Using this process, xMAP Technology allows multiplexing of up to 50 unique bioassays within a single sample, both rapidly and precisely [30, 31]. In brief, after the incubation of a specific monoclonal antibody conjugated bead population with 50 µl of CSF/plasma samples for 1 h at RT, washed beads were incubated with detection antibody solution at RT for 30 min, then with the streptavidin-phycoerythrin conjugated solution (RT, 10 min). After washing, beads were resuspended in the assay buffer, shaken for 1 min and then a reading performed on the MAGPIX instrument. The results were analyzed with xPONENT 4.2 * software and expressed as pg/ml.

Statistical analysis

Student's *t* test to compare means of two experimental groups, one-way ANOVA followed by Dunnett's multiple comparison tests, and two-way ANOVA followed by Bonferroni post-test were used. Data are presented as mean ± standard error of the mean, and significance was set at $P \leq 0.05$. All statistical analyses were performed using GraphPad Prism 6.0 (GraphPad Software).

For the normalization of gene expression on the RT² PCR Profiler Array, five housekeeping genes, ribosomal protein, large, P1, hypoxanthine phosphoribosyltransferase 1, ribosomal protein L13A, lactate dehydrogenase A, and actin beta were used. The CT was determined for each sample and normalized to the average CT of the five housekeeping genes. A comparative CT method was used to calculate relative gene expression. Data are represented as Log2 fold change relative to control. The *P* values were calculated on the basis of a Student's *t* test of the replicate $2^{-(\Delta\Delta C_T)}$ values for each gene in the control group and treatment groups, and *P* values less than 0.05 was considered significant.

Results

Clinical profile and histopathology

The clinical profile of EAE is reported in Fig. 1a, b in which the clinical score (a) and body weight graphs (b)

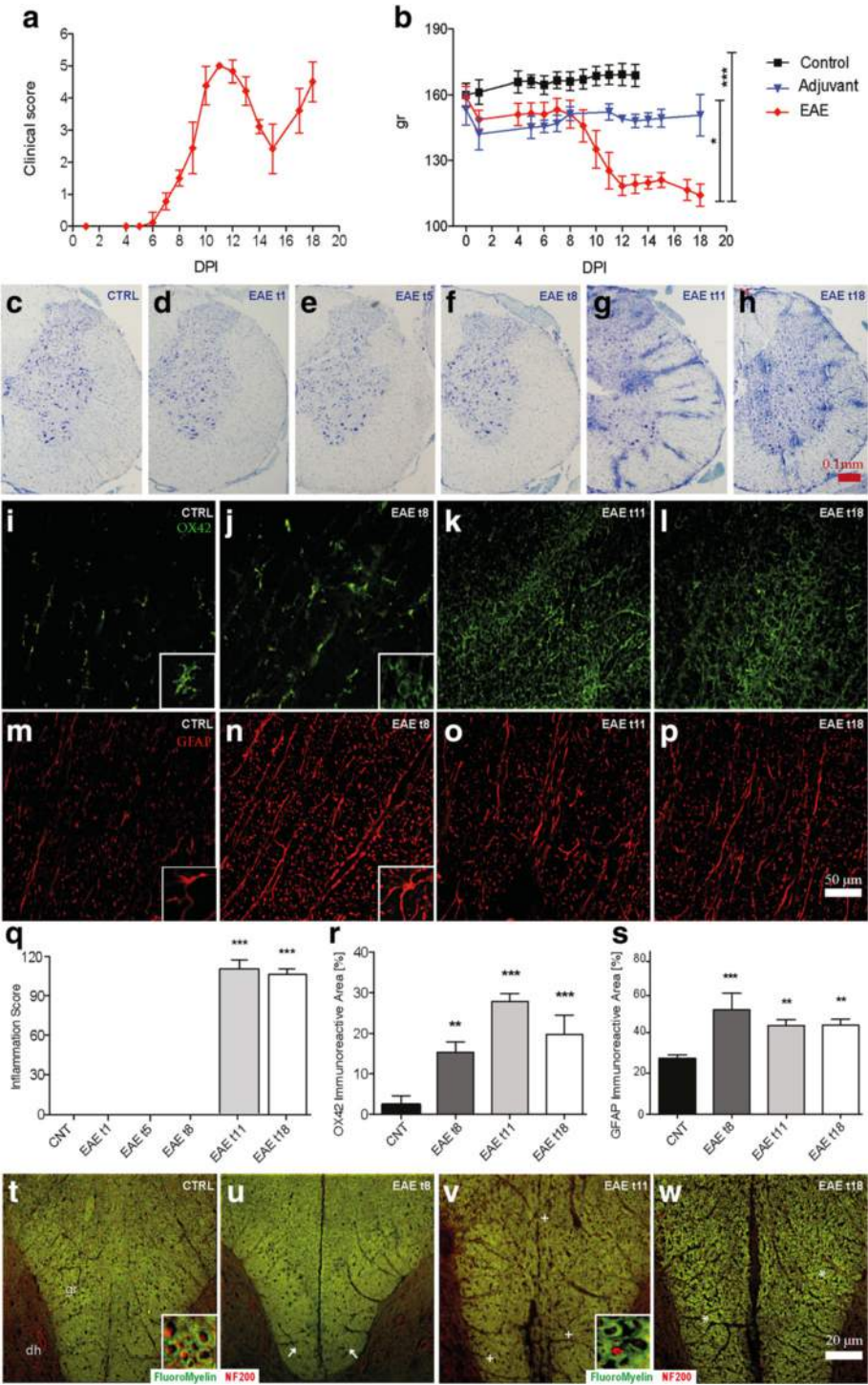


Fig. 1 (See legend on next page.)

(See figure on previous page.)

Fig. 1 EAE clinical profile and histopathology. **a** The time-course of the neurological disability score of EAE animals is reported in the graph (mean \pm SD), showing the peak at day 11 (acute phase), the remission phase at day 16, and relapse at day 18. **b** The body weight gain in experimental animals is reported in the graph (mean \pm SD), revealing a significant difference between the control and EAE group. Statistical analysis: one-way ANOVA, **** $P < 0.0001$. Toluidine blue staining of the lumbar spinal cord (**c-h**) massive cellular infiltrate starting from 11 DPI (EAE t11) OX42-IR microglia staining (**i-l**). GFAP-immunostaining (**m-p**). **q** The semiquantitative evaluation of the inflammation score in the LSC. **r** Immunoreactivity indicates that microglia activation starts at 8 DPI. **s** Astrocyte immunoreactivity starts at 8 DPI. Fluoromyelin staining (**t-w**) in control (**t**); EAE t8 (**u**); EAE t11, the acute phase (**v**); and EAE t18, the remission-relapsing phase (**w**). Arrow in **u** indicate a partial demyelination at 8 DPI; plus in **v** indicates severe demyelination during the acute phase; asterisks in **w** indicate a partial recovery at 18 DPI. Statistical analysis: one-way ANOVA and Dunnett's multiple comparison test (* $P < 0.05$, ** $P < 0.01$, *** $P < 0.001$). *t* time

are shown. Clinical signs of neurological disabilities in EAE started at 7–8 DPI and reached the higher score at 11 DPI (acute phase). A remission phase is then observed, from 12 to 15 DPI, followed by a rapid increase in the clinical score (relapsing phase). Figure 1b shows the body weight gain, which decreases in EAE groups from 2 DPI compared to the control group ($P < 0.001$). A difference between EAE and adjuvant groups is also observed from 7 to 12 DPI ($P = 0.0139$), in close correspondence with the evolution of the symptoms of the disorder, which is followed by a partial recovery.

Histopathology was performed in the LSC at each time point investigated, focusing on inflammation and demyelination. Representative images of toluidine blue staining (C-H) and immunofluorescence visualization of OX42-IR microglia cells (I-L), GFAP-IR astrocytes (M-P), and myelin (T-W) are reported in Fig. 1. Toluidine staining illustrates the massive cellular infiltrate starting from 11 DPI. The semiquantitative evaluation reveals a severe and diffuse cellular infiltrate ($P < 0.0001$) in the LSC at the acute and the remission phases (11, 18 DPI) (Fig. 1q). Significantly, microglial reaction starts at 8 DPI ($P = 0.0001$) (Fig. 1r), when OX42-IR cells take on a rounder morphology (see high-magnification inserts in Fig. 1i, j, EAE t8, compared to the control) and converge around blood vessels, reaching a peak at 11 DPI ($P < 0.0001$). The astroglial reaction was also analyzed by GFAP-immunostaining and a higher immunoreactivity was observed at 8 DPI ($P = 0.0005$) (Fig. 1m, n, control, compared to EAE t8). Demyelination signs appear at 8 DPI as revealed by the slight decrease in FluoroMyelin staining intensity in the gracile fasciculus (gr) of the LSC, (Fig. 1t, u, control, compared to EAE t8; see arrows), which is very extensive at 11 DPI (Fig. 1t, v, EAE t11, compared to the control; see plus) and has partially recovered at 18 DPI (Fig. 1t, w, control, compared to EAE t18; see asterisks).

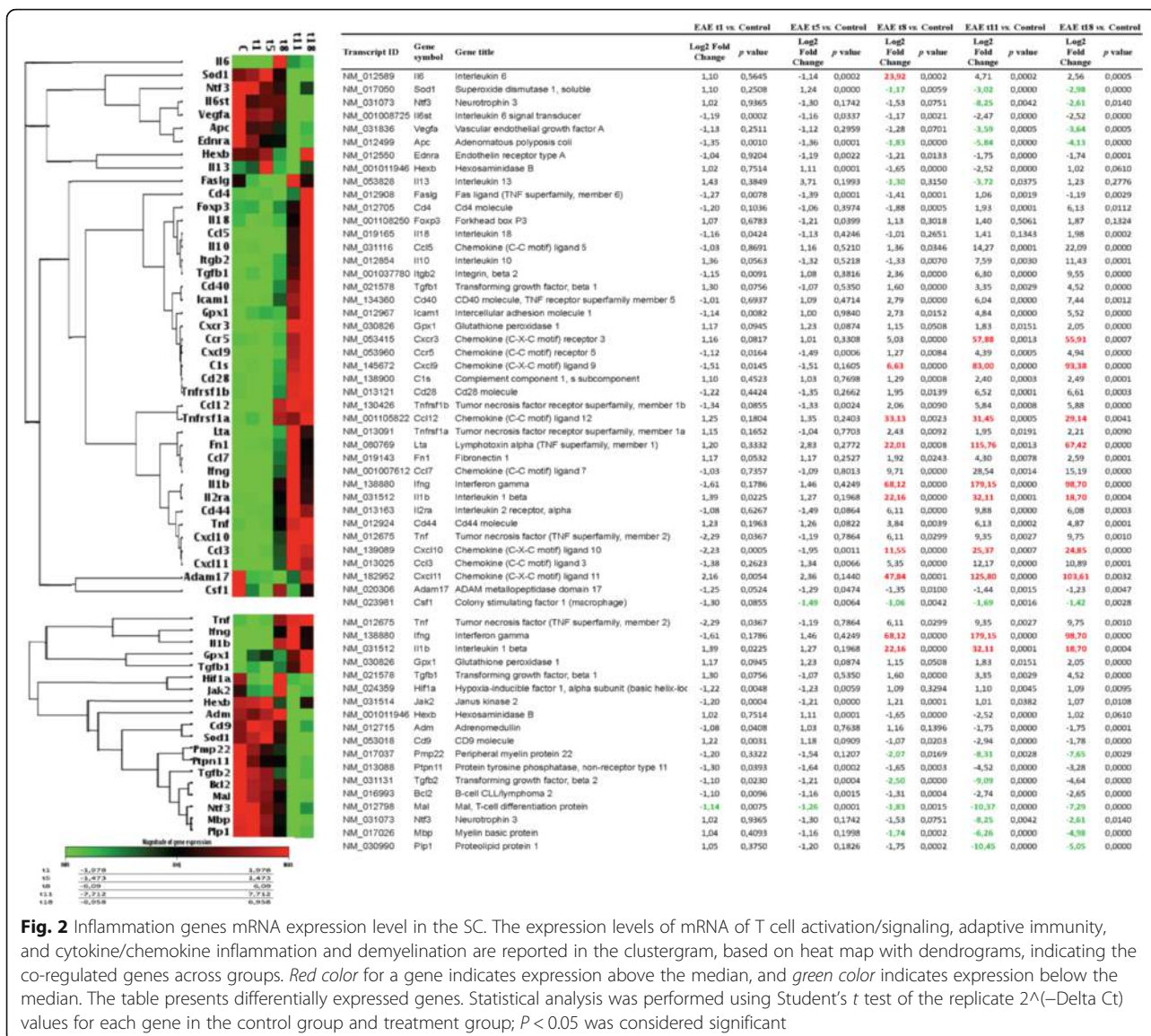
Regulation of inflammatory mediators in SC during early asymptomatic EAE

The mRNA expression of genes that encode for T cell activation/signaling, adaptive immunity, cytokines/chemokines, and cellular stress involved in neuroinflammation and demyelination processes were studied in the SC

by real-time PCR. The complete list of investigated genes is presented in Fig. 2. For biological averaging and variance reduction, samples from each group were pooled for microarray experiments, in fact, for very small designs, pooling dramatically improves accuracy [32–34]. The results from the different groups are presented in a clustergram that performs non-supervised hierarchical clustering to display a heat map with dendrograms indicating co-regulated genes across groups, criteria for significance are reported in the table of magnitude gene expression (Fig. 2). Several pro-inflammatory cytokines and chemokines such as IL-1 β and CCL12 were highly up-regulated in the SC at 8 DPI and reached a peak at 11 DPI. IFN- γ , CXCL11, and LTA were the most up-regulated genes, showing more than 22 Log2 fold change compared to the controls at 8 DPI, around 115 at 11 DPI, and more than 67 Log2 fold change at 18 DPI. The highest up-regulation was observed for IFN- γ , 68.12 Log2 fold change at 8 DPI, 179.15 at 11 DPI, and 98.7 at 18 DPI (Fig. 2). Notably, ADAM17 and CSF1 mRNAs are strongly down-regulated at 1 DPI. Most of the anti-inflammatory cytokines and chemokines were down-regulated with a profile opposite to that observed for the pro-inflammatory ones (starting to decrease from 8 DPI), including VEGF, SOD1, NTF3, APC, HEXB, while an up-regulation was observed for some anti-inflammatory mediators such as GPX1 and IL-10. With regard to genes involved in myelination, a down-regulation starting from 8 DPI was observed, including MAL, MBP and PMP22. To note, the overexpression of IFN- γ mRNA in EAE in acute phase (11 DPI) is the highest EAE-induced up-regulation observed compared to the other inflammatory mediators investigated (Fig. 2).

Inflammation biomarkers at plasma and CSF level are regulated during early asymptomatic EAE

In order to evaluate the kinetics of inflammation biomarkers during EAE, 24 cytokines and chemokines, EPO, G-CSF (CSF3), GM-CSF (CSF2), GRO/KC, IFN- γ , IL-1 α , IL-1 β , IL-2, IL-4, IL-5, IL-6, IL-7, IL-10, IL-12p70, IL-13, IL-17A, IL-18, M-CSF (CSF1), MCP-1 (CCL2), MIP-1 α (CCL3), MIP-3 α (CCL20), RANTES (CCL5), TNF- α , and VEGF, were simultaneously quantified in CSF samples at the different time points investigated

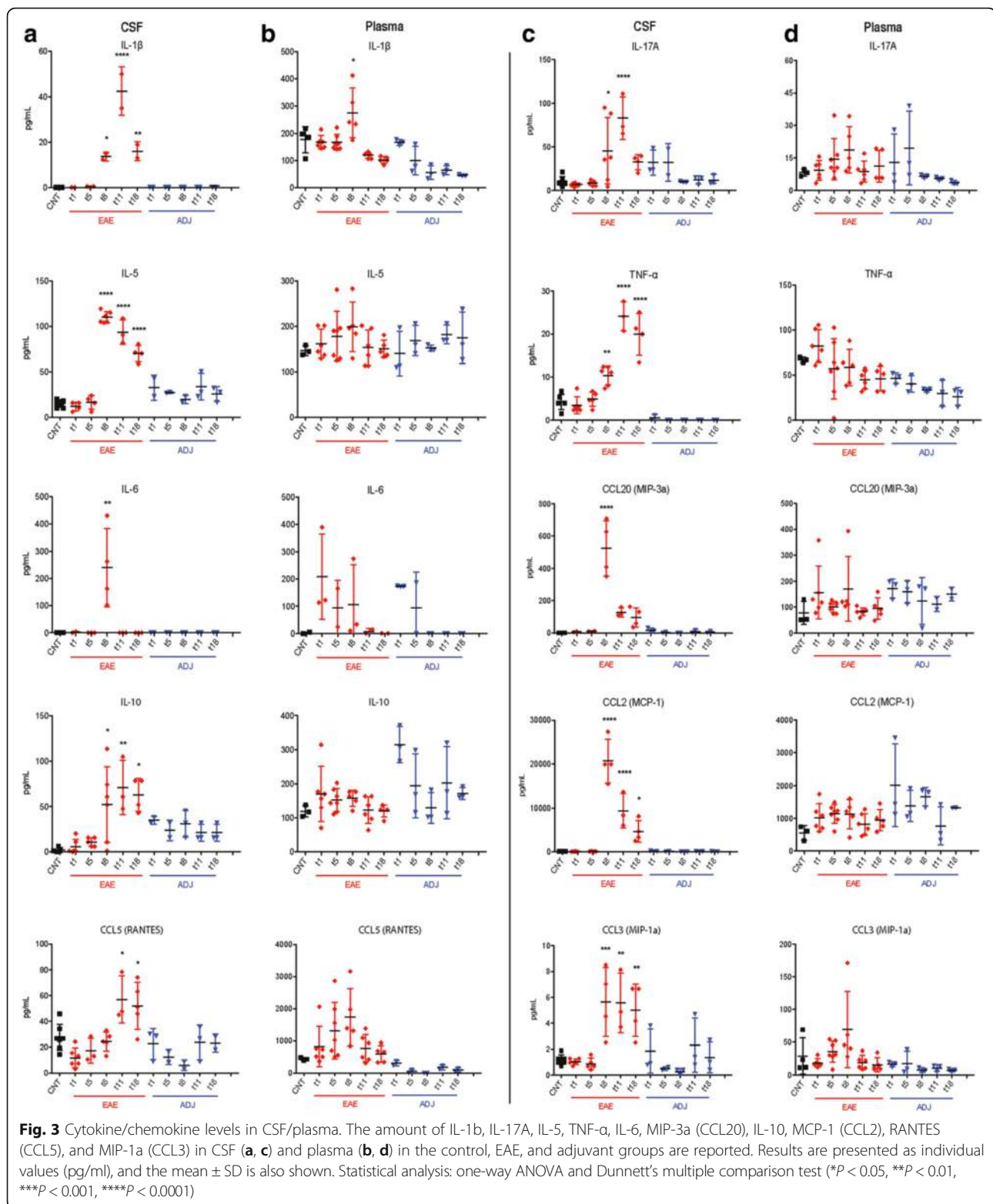


(1, 5, 8, 11, and 18 DPI, Fig. 3a, c). IL-17A, IL-1 β , TNF- α , and IL-10 were significantly increased at 8 DPI in EAE group compared to the control animals ($P = 0.0412$; $P = 0.0127$; $P = 0.0039$; $P = 0.0412$, respectively), reaching a peak at 11 DPI ($P < 0.0001$; $P < 0.0001$; $P < 0.0001$; $P = 0.0074$, respectively) and decreasing again at 18 DPI (ns; $P = 0.0035$; $P < 0.0001$; $P = 0.0128$, respectively). For both pro-inflammatory chemokines CCL2 and CCL3 and for the anti-inflammatory cytokines IL-5, the same significant profile was observed, reaching a peak at 8 DPI ($P < 0.0001$; $P = 0.001$; $P < 0.0001$, respectively) then starting to decrease starting from 11 DPI ($P < 0.0001$; $P = 0.0046$; $P < 0.0001$, respectively). The levels of CCL20 and IL-6 were significantly increased in EAE animals only at 8 DPI ($P < 0.0001$; $P = 0.004$, respectively) (Fig. 3). Unpredictably, IFN- γ , IL-13, IL-2, IL-1 α , IL-

12p70, and GM-CSF were not detected at any of the time points analyzed in the CSF in our experimental conditions.

The different cytokines/chemokines quantified in CSF were also simultaneously measured in plasma samples (Fig. 3b, d) in order to both correlate with CSF changes and to evaluate the peripheral effect of adjuvant. IL-1 β increased in EAE compared to control group of animals at 8 DPI ($P = 0.0231$). GM-CSF was the only cytokine not detectable at any of the time points analyzed, and no significant changes was observed for the rest of the panel compared to the control.

No significant variations between adjuvant and control groups were observed in CSF or plasma at the investigated times.



Immunohistochemical analysis

In order to elucidate the cell type producing the most regulated biomarkers, double-labeling experiments were performed in the LSC of the control and EAE animals.

Representative images from the control and EAE animals at 8, 11, and 18 DPI are shown in Fig. 4. The following markers were investigated: OX42 as marker for microglia; CD86, as marker for M1 macrophages

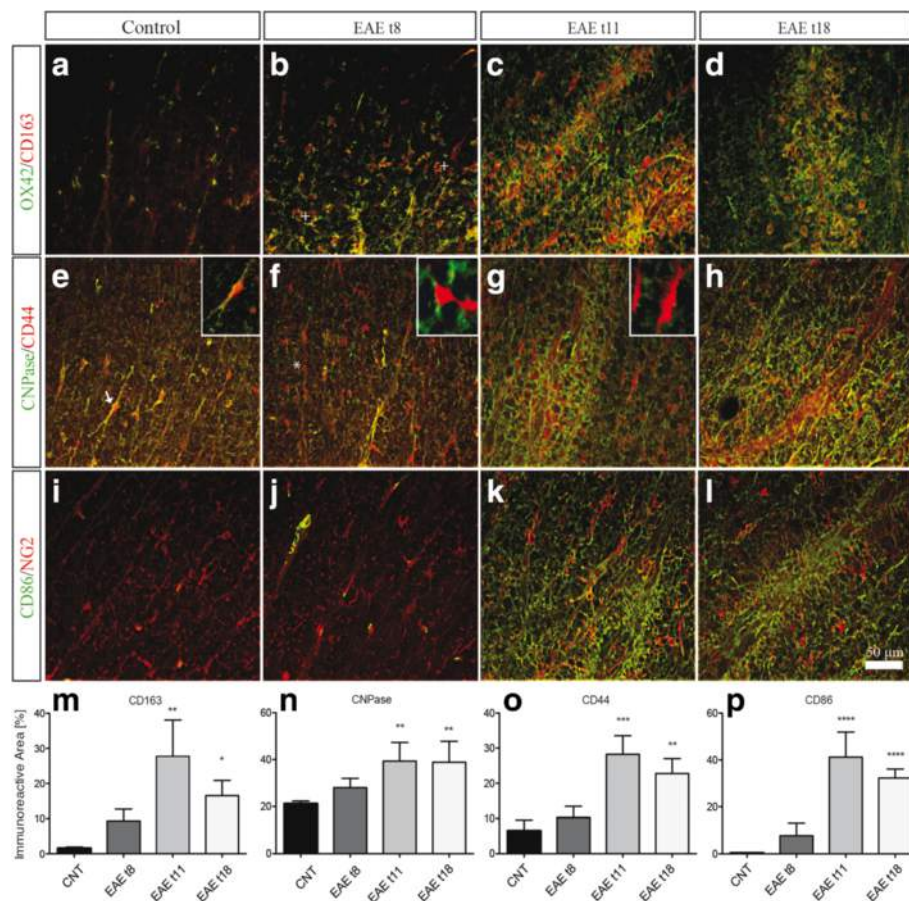


Fig. 4 Immunohistochemistry analysis. Double immunostaining of OX42/CD163, CNPase/CD44 and CD86/NG2 in the lumbar spinal cord of control and EAE rats. **a–d** Double labeling for microglial cells marker (OX42) and M2 macrophages marker (CD163) in the white matter of control (**a**) and EAE experimental groups: 8, 11, and 18 DPI (**b–d**). *Plus* in **b** indicates the activated microglia expressing CD163. **e–h** Double labeling for oligodendrocyte marker (CNPase) and T lymphocyte marker (CD44) (see also the included high-power magnifications). CD44 is expressed by oligodendrocytes in control. *Arrows* in **e** indicate co-localization, although this expression changed at 8 DPI in **f**. **i–l** Double labeling for oligodendrocyte precursor cells (NG2) and M1 macrophages marker (CD86). The immunoreactive area of CD163 (**m**), CNPase (**n**), CD44 (**o**), and CD86 (**p**) in EAE rats compared to controls. Statistical analysis: one-way ANOVA and Dunnett's multiple comparison test (* $P < 0.05$, ** $P < 0.01$, *** $P < 0.001$, **** $P < 0.0001$)

phenotype; CD163, as marker for M2 macrophages phenotype; CD44, as marker for T lymphocytes; NG2, as marker for oligodendrocyte precursor cells (OPCs); and CNPase, as marker for oligodendrocytes. Immunostaining was quantified by a computerized procedure to evaluate the immunoreactive area. As expected, the increase in OX42-IR observed at 8 DPI corresponds to increased expression of the M2 cytokine CD163 (Fig. 4a–d, see plus in B, M), while the M1 macrophage marker CD86 showed the highest immunoreactive area at 11 DPI (Fig. 4i–l, p). This activation was accompanied by an increase in the CNPase immunoreactive (IR) area starting from 8 DPI (Fig. 4e–h, n), which partially contrasts with the FluoroMyelin staining results (Fig. 1t–w). In the control group, CD44 was expressed by oligodendrocytes (Fig. 4e; see arrows), while this co-localization was no longer present in the EAE animals at 8, 11, and 18 DPI (Fig. 4f; see asterisk). The highest up-regulation of the

different markers verified in the white matter was detected in the acute phase of EAE (Fig. 4c, g, and k), where also a significant up-regulation of CD163 ($P = 0.0016$), CNPase ($P = 0.0197$), CD44 ($P = 0.0005$), and CD86-IR ($P < 0.0001$) areas were observed at 11 DPI (Fig. 4m, n, o, and p, respectively).

No significant results were observed in EAE t1, EAE t5, and adjuvant experimental groups (results not shown).

CSF1 regulation in early presymptomatic EAE

Going one step deeper into biomarker regulation at the early phase of EAE, it was found that the pro-inflammatory mediator CSF1 (The CSF-1R is a member of the platelet-derived growth factor receptor (PDGFR) family of class III receptor tyrosine kinases that includes PDGFR α/β , stem cell factor receptor (c-Kit), and Flt3/Flk2) [35] was regulated starting from 1 DPI in EAE

group compared to the control in all the biological samples analyzed (Fig. 5a). In plasma, CSF1 was significantly up-regulated only at 1 DPI ($P = 0.0006$), then continuously decreased till the last time point studied, 18 DPI (Fig. 6b), while in CSF, CSF1 level started to decrease at 1 DPI, becoming significant at 11 and 18 DPI ($P < 0.0001$, $P < 0.0001$) (Fig. 5c). Notably, CSF1-IR in the tissue also increased starting from 1 DPI ($P = 0.0003$) (Fig. 5e, k), then decreased at 5 and 8 DPI (Fig. 5g, h) ultimately reaching the highest immunoreactivity at 11 DPI ($P < 0.0001$) (Fig. 5i, k). The mRNA expression of CSF1 gene in SC was also analyzed (Fig. 2), and a down-regulation at 1 and 11 DPI was observed (Fig. 5d). In the attempt to identify the CSF1-producing cells at 1 and 11 DPI, double-labeling immunostaining of CSF1 with CNPase and GFAP was performed in the LSC (Fig. 5l–o). Figure 6n, o shows that CSF1 is constitutively expressed by astrocytes not only in the EAE animals but also in the control (results not shown). Interestingly, CSF1 was expressed by oligodendrocytes at 1 DPI in EAE (Fig. 5l), while this expression is no longer present as from 11 DPI (Fig. 5m).

Functional pathway and network analysis

In an exploratory study, a pathway analysis approach of the different proteins derived from the most early regulated genes at 8 DPI was implemented. This time point corresponds to the beginning of the regulation of genes in the CNS, while cellular infiltrates are not yet present and clinical signs start to appear. We proceed through the web-software STRING 10.0 (<http://string-db.org/>) and Gene Ontology databases. The protein–protein interaction analysis (both physical and functional interactions) was performed using default parameters (high confidence, 0.7) and *R.norvegicus* as the organism of interest. The software allows the net of interactions including other proteins closely linked to the one analyzed to be extended, in order to obtain a better understanding of the possible pathways affected by EAE in DA rats at early onset. The analysis showed that almost all the proteins deriving from genes of interest (except for the CXC family) did not directly interact with each other (Fig. 6a). The extended network (indirect protein–protein interactions) showed that those proteins were connected in four clusters according to their involvement in the biological process (autoimmune disease), situating STAT1 (signal transducers and activators of transcription), FLT1 (vascular endothelial growth factor receptor 1), and TRAF6 (TNF receptor associated factor) as nodes of the extended net linking the different groups (Fig. 6b). To gain further insight into the biological significance of those clusters in MS, an enrichment analysis using Gene Ontology was performed. It was found that these four clusters consist of a Wnt signaling pathway (the green cluster), a cytokine-mediated signaling

pathway (the yellow cluster), T cell chemotaxis (the blue cluster), and positive regulation of mitogen-activated protein tyrosine kinase (MAPK) (the red cluster). Notably, CSF1 takes part of MAPK cluster.

Effects of selective inhibition of CSF1R activity on the clinical score of EAE animals

Since the peculiar temporal expression pattern of CSF1 in particular in the very early phase of the disease, the tyrosine kinase activity of CSF1R was inhibited by the oral administration of GW2580. GW2580 is a highly selective inhibitor of the c-FMS kinase, and through this pathway, this small molecule blocks CSF1 signaling. Treatment started 1 day before the immunization and till 11 DPI. The clinical profiles of the disease in EAE, EAE + GW2580, control + GW2580, and vehicle groups of animals are reported in Fig. 7, in which the clinical score (a) and body weight graphs (b) are shown. Clinical signs of the neurological disabilities in EAE were the same as reported in the first group of animals included in our study (Fig. 1a), which prove the reproducibility of the model. While the clinical signs started at 6–7 DPI in the EAE group, a delay in the appearance of the neurological disability was observed in the EAE + GW2580 group. The acute phase was at 11–12 DPI with a maximum score of 5, while a significant reduction of the severity of the disease was observed in the EAE + GW2580 group ($P < 0.001$) with a maximum score of 2.8. Interestingly, the EAE + GW2580 animals did not show any relapse phase ($P < 0.001$) and after the acute phase, they were recovering till the 18 DPI, last day of the experiment ($P < 0.001$). Figure 7b shows the body weight gain. A decrease was observed in the EAE + GW2580 groups from 2 DPI compared to the GW2580 animals ($P < 0.001$), which is the same profile of the body weight loss observed in the EAE group but less severe, in close correspondence with the evolution of the symptoms of the disorder, which is followed by a recovery. We also calculated the cumulative disability index, reported in Fig. 7c, observed in EAE compared to the EAE + GW2580 groups ($P < 0.001$).

Discussion

The aim of this study was to investigate the expression profile of molecules involved in inflammation and demyelination in the very early presymptomatic phase of EAE induced by active immunization in female DA rats by comparing the tissue (spinal cord), CSF, and plasma. It was previously demonstrated that in the acute phase of this model, a massive infiltration of inflammatory cells and extensive demyelination were observed in the spinal cord [36–38]. Samples collected at symptom-free times (1 and 5 DPI) and at the symptom onset (8 DPI), peak (11 DPI), and relapse (18 DPI) were then examined

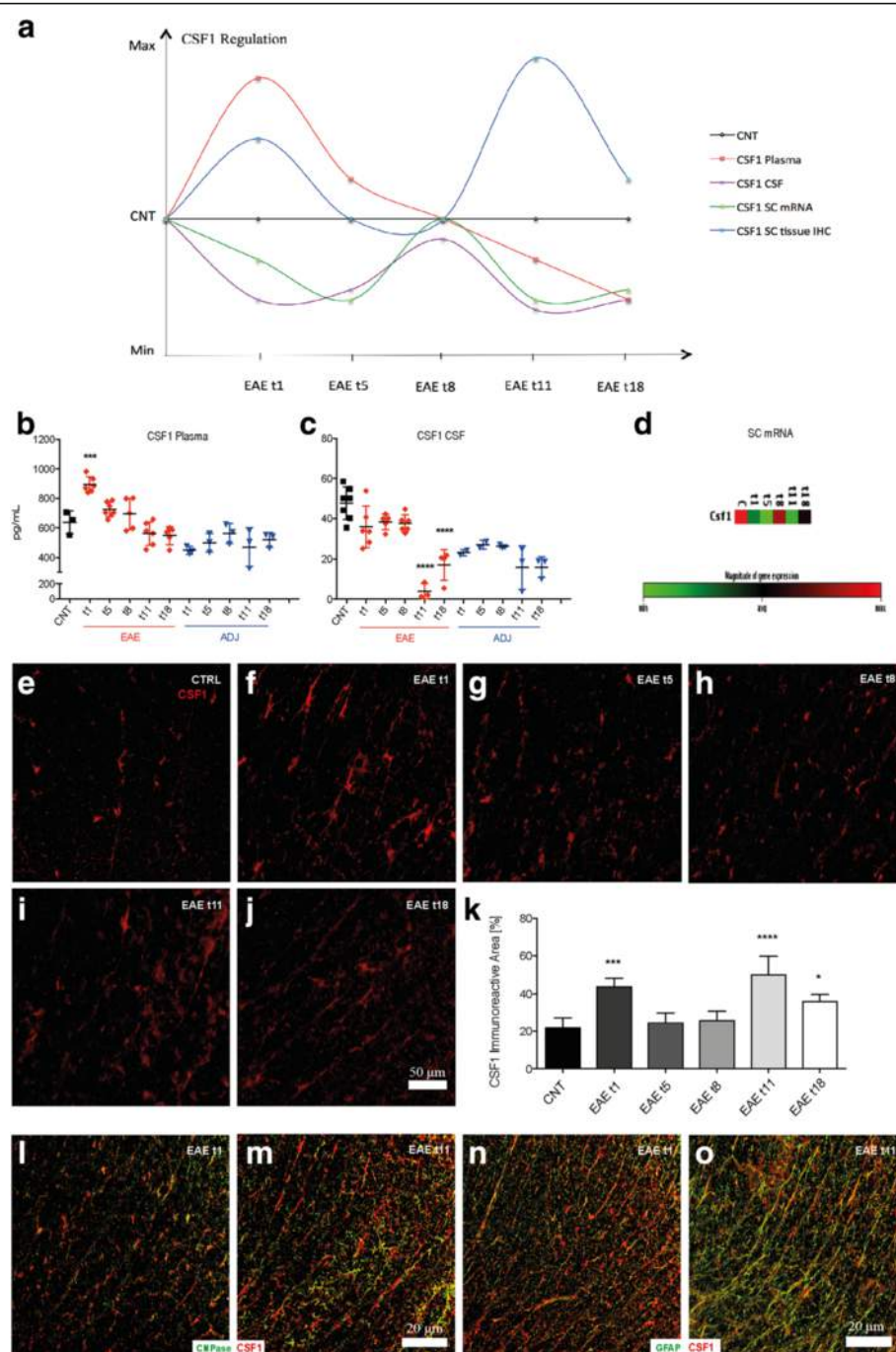
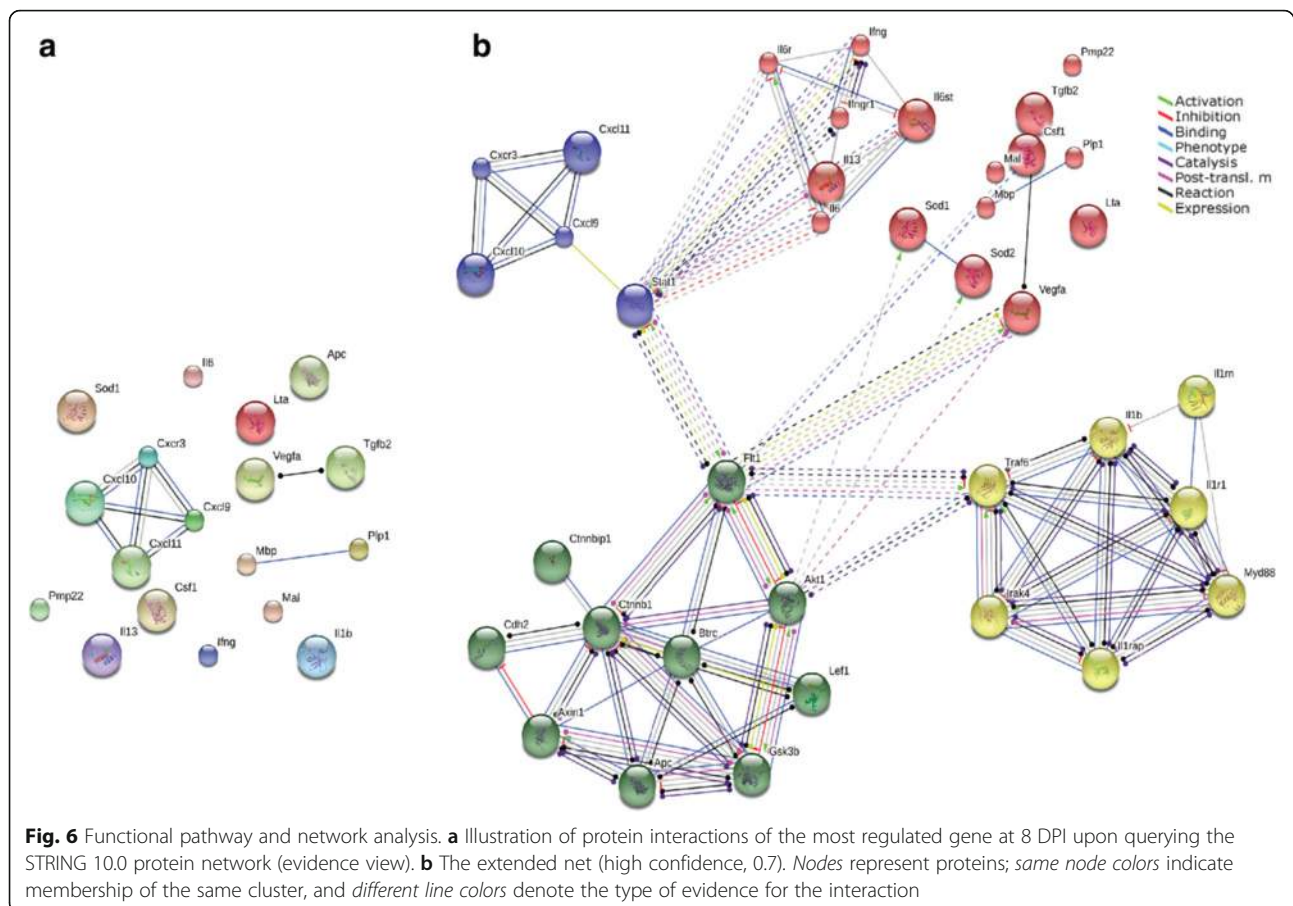


Fig. 5 Early regulation of CSF1 in EAE. **a** Schematic illustration of CSF1 regulation in all the biological samples analyzed on Excel: the XY scatter option is chosen and under the chart subtypes, the option connecting the points with *smooth lines* with markers is selected. The amount of CSF1 in plasma (**b**) and CSF (**c**) in the control, EAE, and adjuvant groups are reported. Results are presented as individual values (pg/ml), and the mean \pm SD is also shown. **d** The expression level of mRNA of CSF1 is reported in the clustergram, based on heat map with dendrograms, indicating the co-regulation across the different groups (**e-j**) **k** CSF1-immunostaining in the white matter of control and EAE experimental groups: 1, 5, 8, 11, and 18 DPI. The immunoreactive area of CSF1 in EAE rats compared to controls. Double labeling for CSF1 and oligodendrocytes marker (CNPase) and GFAP in the EAE group 1 and 11 DPI (**l, m** and **n, o**, consecutively). Statistical analysis: one-way ANOVA and Dunnett's multiple comparison test (* $P < 0.05$, *** $P < 0.001$, **** $P < 0.0001$)

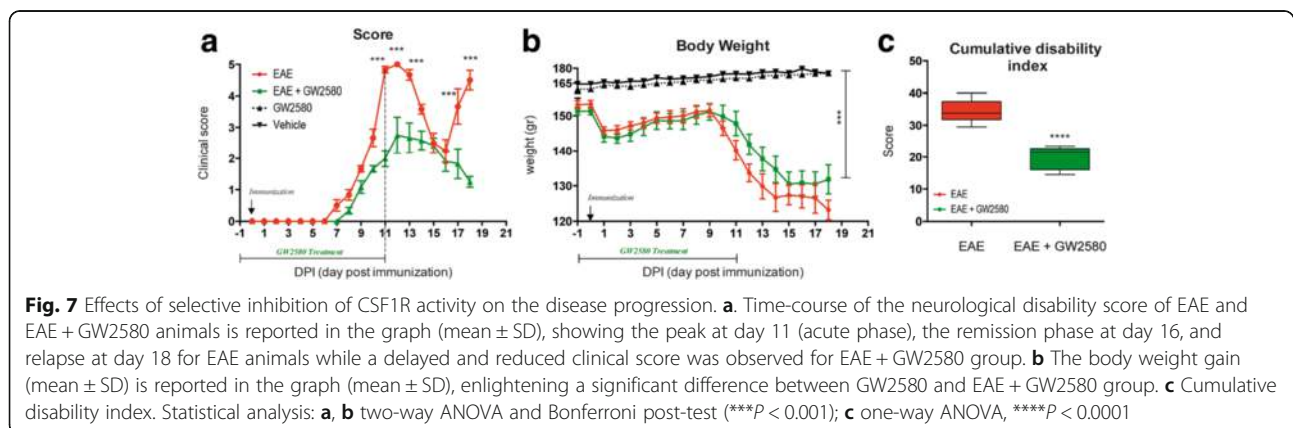


using high-throughput technologies together with bio-informatic analysis for molecule and pathway identification in CNS tissue and biological fluids.

At mRNA level (spinal cord tissue), T cell activation/signaling, adaptive immunity, cytokine/chemokine inflammation, demyelination, and cellular stress were analyzed, thereby including astroglial and microglial markers. Microglia markers refer to the “resting state” (M0); to inflammatory microglia (M1 polarization)

producing numerous pro-inflammatory cytokines/chemokines; and to anti-inflammatory microglia (M2 polarization), which triggers them to endorse regeneration and eliminate debris [39–41]. The most significant results were verified by means of double-labeling immunohistochemistry. At protein level in CSF and plasma, 24 cytokines were analyzed.

Our first important result is that an early regulation of most of the inflammatory and demyelinating biomarkers was observed as soon as symptoms appear (8 DPI) but



before the disease peak (11 DPI). Molecular markers of microglial activation toward a phagocytic phenotype are found (8 DPI), when also astrocyte hypertrophy is observed. The highest regulation of these markers is observed when symptoms peak (11 DPI, acute phase) and then partially recover at relapse (18 DPI). Significantly, microglia and astrocytes were activated early in the EAE animals by 8 DPI. Indeed, almost all the cytokines/chemokines shift their expression at 8 DPI in plasma, CSF, and even in the SC. In particular, a higher regulation of CCL2, TNF- α , and IL-1 β was found, possibly indicating the initiation of BBB breakdown. Indeed, it has been demonstrated that the CCL2-CNS level can be induced by the pro-inflammatory cytokine IFN- γ , TNF- α , and IL-1 β and does affect the BBB integrity and attract monocytes to the CNS [42, 43]. Interestingly, we found that the anti-inflammatory biomarkers, IL-5 and IL10, have the same profile of expression as the pro-inflammatory mediators, revealing that both “M1” and “M2” polarization is present at the same time during EAE. Actually, very recent studies have shown that microglia/macrophages simultaneously express both “M1” and “M2” phenotypic markers in brain trauma, suggesting that these cells display a mixed phenotype due to the fact they cannot adequately switch to a polarized “M1-only” or “M2-only” phenotype [44, 45].

Using a functional pathway analysis tool, Gene Ontology and Enrichment Analysis, four possible pathways were indicated as affording suggestive evidence of being associated with the early phase of MS: the Wnt signaling pathway, the cytokine-mediated signaling pathway, the T cell chemotaxis pathway, and MAPK. Significantly, Wnt signaling has been recognized as the central tenet in the development and regeneration of myelin in the CNS [46]. Chronic activation of canonical Wnt signaling in oligodendrocyte precursors results in delayed developmental and regenerative myelination [47, 48]. Interestingly, IL-6, which belongs to the MAPK pathway, was detected only at 8 DPI. Besides, IL-17A, which is secreted by T helper-17 which contributes to pathogenesis in MS and EAE [49], started to be regulated at 8 DPI, confirming that IL-6 promotes T cell development at 8 DPI. Indeed, it has been shown that IL-6-deficient mice were resistant to EAE because they fail to induce CNS-T helper-17 cells [50].

Our second major result is that the colony-stimulating factor CSF1, part also of MAPK pathway, was regulated at 1 DPI in EAE groups compared to the control, not only in the plasma but also in CSF and SC. CSF1, is an integral tyrosine kinase transmembrane receptor and signals through its receptor CSF1R (also known as c-FMS) to regulate the differentiation, proliferation, and recruitment of microglia [51, 52]. Thus, our data indicate that the first sign of immunological response in

EAE occurs in the CNS already 24 h after immunization and plasma biomarker could reflect microglia activation in the tissue. It was then attempted to identify the cell type producing CSF1. It was found that CSF1 at 1 DPI is expressed by oligodendrocytes and astrocytes in the EAE animals, while in the acute phase (11 DPI), only astrocytes express CSF1. However, it was also seen that CSF1 is expressed by GFAP-positive cells in control, adjuvant-injected, and intact animal. Moreover, we found that the treatment with GW2580, a selective inhibitor of CSF1R, delayed the onset of the disease, significantly reduced the clinical severity and surprisingly prevented the relapse phase even though the treatment was performed till the 11 DPI, thus suggesting the CSF1 is a major molecular regulator in the very early phases of EAE. To our knowledge, our results provide the first evidence of the very early regulation of CSF1 in EAE and on a major role of CSF1-mediated events in EAE onset and progression.

A major question arising from this result is the cell type responsible for this very early effect. The CSF1 receptor (CSF1R), encoded by the proto-oncogene *c-fms* [53, 54] and having CSF1 and IL-34 as natural ligands [55], is expressed by several cell types, including macrophages and microglia [56]. In the brain, it has been confirmed that under normal conditions, microglia are the only cell type that expresses the CSF1R [57, 58]. Several lines of evidence suggest that microglial activation is mediated by the binding of CSF1 to CSF1R, which triggers the release of inflammatory cytokines [59, 60]. A role of CSF1 in microglial activation and disease progression has been described in several models of injury and neurodegenerative diseases, but in few of them, the responsible cell type has been identified. In neuropathic pain induced by peripheral nerve injury, CSF1 is produced and retrograde transported to the spinal cord by sensory neurons [61]. In the mouse model of amyotrophic lateral sclerosis, the positive effects of GW2580 has been attributed to the attenuation of macrophages infiltration of the peripheral nerve [62]. In an Alzheimer's mouse model, prolonged treatment with GW2580 directly target microglia regulating cytokines production and also improving the functional outcome [25]. When used in EAE starting from 10 DPI, GW2580 reduces the proportion of peripheral macrophages, also decreasing the number of inflammatory foci in the CNS [63]. This effect has at least partially attributed to the repression of the autocrine signaling of inflammatory macrophages and microglia, leading to the reduction of neuroinflammatory cytokines and chemokines [57, 64, 65], suggesting that targeting tyrosine kinase receptors such as c-Fms and PDGFR could prevent the development of the disease by enhancing BBB integrity [66].

According to our results, it could thus be speculated that CSF1-CSF1R signaling plays an important role in

not only the early phase of EAE but also all along the disease progression. CSF1 could be so a good trigger for microglial activation and subsequent induction of neuroinflammation, and its increase could be detected in biological fluids including plasma. Further studies will elucidate the mechanism of this early microglial activation, also in view of possible therapeutic implications. In fact, the therapeutic potential of the CSF1R kinase inhibitor has been explored in many pathologies such as cancer, bone disease, inflammatory diseases, and other autoimmune disorders, and so several CSF1R tyrosine kinase inhibitors are under development for clinical applications [67–70].

Conclusions

In the attempt to elucidate still elusive aspects of multiple sclerosis (MS) pathogenesis, we performed a time-course study in experimental allergic encephalomyelitis (EAE), the most widely used MS rodent model, focusing on the presymptomatic phase. By investigating neuroinflammation and demyelination biomarkers in the tissue, CSF, and plasma using high-throughput technology and bioinformatics analysis, we discovered the very early regulation of the chemokine colony-stimulating factor 1 (CSF1), which indicates the occurrence of microglia activation already 1 day after immunization. The selective inhibition of CSF1R decreased EAE clinical severity and prevents the relapse phase suggesting the importance of CSF1-CSF1R signaling in microgliosis and inflammation in MS.

Abbreviations

BBB: Blood–brain barrier; CCL: C–C–L motif chemokine; CNS: Central nervous system; CSF: Cerebrospinal fluid; CSF1: Colony-stimulating factor 1; CXCL: C–X–C motif chemokine; DPI: Day post-immunization; DA: Dark agouti; EAE: Experimental allergic encephalomyelitis; GFAP: Glial fibrillary acidic protein; IC: Inhibitory concentration; IFN- γ : Interferon- γ ; IL: Interleukin; IR: Immunoreactivity; LSC: Lumbar spinal cord; MAPK: Mitogen-activated protein tyrosine kinase; MS: Multiple sclerosis; SC: Spinal cord; TNF: Tumor necrosis factor

Acknowledgements

The research and the researcher leading to these results (NB) received funding from the European Union's Seventh Framework Program FP7 under Grant agreement 607962 (nEUROinflammation).

Funding

This work was supported by the European Union's Seventh Framework Program FP7 under Grant agreement 607962 (nEUROinflammation).

Availability of data and materials

Please contact author for data requests.

Authors' contributions

NB designed the research, performed all the experiments, collected and analyzed data, and wrote the manuscript. MF performed and analyzed some experiments and edited the manuscript. LG designed the research and edited the manuscript. LC designed the research and wrote the manuscript. All authors read and approved the final manuscript.

Competing interests

The authors declare that they have no competing interests.

Consent for publication

Not applicable.

Ethics approval

All animal protocols described herein were carried out in accordance with the European Community Council Directives (86/609/EEC), approved by the intramural ethical committee for animal experimentation of Bologna University and the Ministry of Health no. 158/2013-B and no. 607/2016-PR and comply with the ARRIVE guidelines and guidelines published in the *NIH Guide for the Care and Use of Laboratory Animals*.

Author details

¹Research and Development, Chiesi Farmaceutici S.p.A, Via Palermo 26/A, Parma 43100, Italy. ²Health Science and Technologies Interdepartmental Center for Industrial Research (HST-ICIR), University of Bologna, Via Tolara di Sopra 41/E, Bologna, Ozzano Emilia I 40064, Italy. ³IRET Foundation, Via Tolara di Sopra 41/E, Bologna, Ozzano Emilia 40064, Italy. ⁴Department of Veterinary Medical Sciences, University of Bologna, Via Tolara di Sopra 50, Ozzano Emilia, BO 40064, Italy. ⁵Department of Pharmacy and Biotechnology, University of Bologna, Via Tolara di Sopra 41/E, Bologna, Ozzano Emilia 40064, Italy.

Received: 6 April 2016 Accepted: 2 November 2016

Published online: 15 November 2016

References

- Lassmann H. Neuropathology in multiple sclerosis: new concepts. *Mult Scler*. 1998;4(3):93–8.
- Hauser SL, Oksenberg JR. The neurobiology of multiple sclerosis: genes, inflammation, and neurodegeneration. *Neuron*. 2006;52(1):61–76.
- Hemmer B, Cepok S, Nessler S, Sommer N. Pathogenesis of multiple sclerosis: an update on immunology. *Curr Opin Neurol*. 2002;15(3):227–31.
- Zigmond MJ, Coyle JT, Rowland LP. *Neurobiology of brain disorders: biological basis of neurological and psychiatric disorders*. London: Academic; 2015. p. 497–520.
- Lassmann H, van Horssen J, Mahad D. Progressive multiple sclerosis: pathology and pathogenesis. *Nat Rev Neurol*. 2012;8(11):647–56.
- Dendrou CA, Fugger L, Friese MA. Immunopathology of multiple sclerosis. *Nat Rev Immunol*. 2015;15(9):545–58.
- Aharoni R. New findings and old controversies in the research of multiple sclerosis and its model experimental autoimmune encephalomyelitis. *Expert Rev Clin Immunol*. 2013;9(5):423–40.
- Guerreiro-Cacais AO, Laaksonen H, Flytzani S, N'diaye M, Olsson T, Jagodic M. Translational utility of experimental autoimmune encephalomyelitis: recent developments. *J Inflamm Res*. 2015;8:211–25.
- Robinson AP, Harp CT, Noronha A, Miller SD. The experimental autoimmune encephalomyelitis (EAE) model of MS: utility for understanding disease pathophysiology and treatment. *Handb Clin Neurol*. 2014;122:173–89.
- Constantinescu CS, Farooqi N, O'Brien K, Gran B. Experimental autoimmune encephalomyelitis (EAE) as a model for multiple sclerosis (MS). *Br J Pharmacol*. 2011;164(4):1079–106.
- Hart BA, van Kooyk Y, Geurts JJ, Gran B. The primate autoimmune encephalomyelitis model; a bridge between mouse and man. *Ann Clin Transl Neurol*. 2015;2(5):581–93.
- Ben-Nun A, et al. From classic to spontaneous and humanized models of multiple sclerosis: impact on understanding pathogenesis and drug development. *J Autoimmun*. 2014;54:33–50.
- Piras G, Rattazzi L, McDermott A, Deacon R, D'Acquisto F. Emotional change-associated T cell mobilization at the early stage of a mouse model of multiple sclerosis. *Front Immunol*. 2013;4:400.
- Barkauskas DS, et al. Focal transient CNS vessel leak provides a tissue niche for sequential immune cell accumulation during the asymptomatic phase of EAE induction. *Exp Neurol*. 2015;266:74–85.
- Olechowski CJ, Truong JJ, Kerr BJ. Neuropathic pain behaviours in a chronic-relapsing model of experimental autoimmune encephalomyelitis (EAE). *Pain*. 2009;141(1–2):156–64.
- Benson C, Paylor JW, Tenorio G, Winship I, Baker G, Kerr BJ. Voluntary wheel running delays disease onset and reduces pain hypersensitivity in early experimental autoimmune encephalomyelitis (EAE). *Exp Neurol*. 2015;271:279–90.

17. 't Hart BA, Gran B, Weissert R. EAE: imperfect but useful models of multiple sclerosis. *Trends Mol Med*. 2011;17(3):119–25.
18. Ringheim GE, et al. Teriflunomide attenuates immunopathological changes in the dark agouti rat model of experimental autoimmune encephalomyelitis. *Front Neurol*. 2013;4.
19. Skundric DS. Experimental models of relapsing-remitting multiple sclerosis: current concepts and perspective. *Curr Neurovasc Res*. 2005;2(4):349–62.
20. Stadelmann C. Multiple sclerosis as a neurodegenerative disease: pathology, mechanisms and therapeutic implications. *Curr Opin Neurol*. 2011;24(3):224–9.
21. Bjartmar C, Wujek JR, Trapp BD. Axonal loss in the pathology of MS: consequences for understanding the progressive phase of the disease. *J Neurol Sci*. 2003;206(2):165–71.
22. Calza L, Fernandez M, Giuliani A, Aloe L, Giardino L. Thyroid hormone activates oligodendrocyte precursors and increases a myelin-forming protein and NGF content in the spinal cord during experimental allergic encephalomyelitis. *Proc Natl Acad Sci U S A*. 2002;99(5):3258–63.
23. Louhimies S, Louhimies S. Directive 86/609/EEC on the protection of animals used for experimental and other scientific purposes. *Altern Lab Anim ATLA*. 2002;30 Suppl 2:217–9.
24. Gómez-Nicola D, Fransen NL, Suzzi S, Perry VH. Regulation of microglial proliferation during chronic neurodegeneration. *J Neurosci Off J Soc Neurosci*. 2013;33(6):2481–93.
25. Olmos-Alonso A, et al. Pharmacological targeting of CSF1R inhibits microglial proliferation and prevents the progression of Alzheimer's-like pathology. *Brain*. 2016;139(3):891–907.
26. Leblond A-L, et al. Systemic and cardiac depletion of M2 macrophage through CSF-1R signaling inhibition alters cardiac function post myocardial infarction. *PLoS One*. 2015;10(9):e0137515.
27. Conway JG, et al. Inhibition of colony-stimulating-factor-1 signaling in vivo with the orally bioavailable cFMS kinase inhibitor GW2580. *Proc Natl Acad Sci U S A*. 2005;102(44):16078–83.
28. Hickey WF, Cohen JA, Burns JB. A quantitative immunohistochemical comparison of actively versus adoptively induced experimental allergic encephalomyelitis in the Lewis rat. *Cell Immunol*. 1987;109(2):272–81.
29. Liu L, Duff K. A technique for serial collection of cerebrospinal fluid from the cisterna magna in mouse. *J Vis Exp*. 2008;21:e960. (<http://www.jove.com/details.php?id=960>).
30. Houser B. Bio-Rad's Bio-Plex® suspension array system, xMAP technology overview. *Arch Physiol Biochem*. 2012;118(4):192–6.
31. Blankesteijn M, Altara R. Inflammation in heart failure. 1st ed. New York: Academic; 2014.
32. Kendzioriski C, Irizarry RA, Chen K-S, Haag JD, Gould MN. On the utility of pooling biological samples in microarray experiments. *Proc Natl Acad Sci U S A*. 2005;102(12):4252–7.
33. Kendzioriski CM, Zhang Y, Lan H, Attie AD. The efficiency of pooling mRNA in microarray experiments. *Biostat Oxf Engl*. 2003;4(3):465–77.
34. Chabas D, et al. The influence of the proinflammatory cytokine, osteopontin, on autoimmune demyelinating disease. *Science*. 2001; 294(5547):1731–5.
35. Yu W, Chen J, Xiong Y, Pixley FJ, Yeung Y-G, Stanley ER. Macrophage proliferation is regulated through CSF-1 receptor tyrosines 544, 559, and 807. *J Biol Chem*. 2012;287(17):13694–704.
36. Calza L, Giardino L, Pozza M, Micera A, Aloe L. Time-course changes of nerve growth factor, corticotropin-releasing hormone, and nitric oxide synthase isoforms and their possible role in the development of inflammatory response in experimental allergic encephalomyelitis. *Proc Natl Acad Sci U S A*. 1997;94(7):3368–73.
37. Dell'Acqua ML, et al. Functional and molecular evidence of myelin- and neuroprotection by thyroid hormone administration in experimental allergic encephalomyelitis. *Neuropathol Appl Neurobiol*. 2012;38(5):454–70.
38. Massella A, et al. Gender effect on neurodegeneration and myelin markers in an animal model for multiple sclerosis. *BMC Neurosci*. 2012;13:12.
39. Mildner A, et al. Distinct and non-redundant roles of microglia and myeloid subsets in mouse models of Alzheimer's disease. *J Neurosci Off J Soc Neurosci*. 2011;31(31):11159–71.
40. Goldmann T, Prinz M. Role of microglia in CNS autoimmunity. *Clin Dev Immunol*. 2013;2013:208093.
41. Wynn TA, Chawla A, Pollard JW. Macrophage biology in development, homeostasis and disease. *Nature*. 2013;496(7446):445–55.
42. Semple BD, Kossmann T, Morganti-Kossmann MC. Role of chemokines in CNS health and pathology: a focus on the CCL2/CCR2 and CXCL8/CXCR2 networks. *J Cereb Blood Flow Metab Off J Int Soc Cereb Blood Flow Metab*. 2010;30(3):459–73.
43. Guo Y-Q, et al. Expression of CCL2 and CCR2 in the hippocampus and the interventional roles of propofol in rat cerebral ischemia/reperfusion. *Exp Ther Med*. 2014;8(2):657–61.
44. Kumar A, Stoica BA, Sabirzhanov B, Burns MP, Faden AI, Loane DJ. Traumatic brain injury in aged animals increases lesion size and chronically alters microglial/macrophage classical and alternative activation states. *Neurobiol Aging*. 2013;34(5):1397–411.
45. Morganti JM, Riparip L-K, Rosi S. Call off the Dog(ma): M1/M2 polarization is concurrent following traumatic brain injury. *PLoS One*. 2016;11(1):e0148001.
46. Lee HK, et al. Daam2-PIP5K is a regulatory pathway for Wnt signaling and therapeutic target for remyelination in the CNS. *Neuron*. 2015;85(6):1227–43.
47. Emery B. Regulation of oligodendrocyte differentiation and myelination. *Science*. 2010;330(6005):779–82.
48. Fancy SPJ, et al. Parallel states of pathological Wnt signaling in neonatal brain injury and colon cancer. *Nat Neurosci*. 2014;17(4):506–12.
49. Serada S, et al. IL-6 blockade inhibits the induction of myelin antigen-specific Th17 cells and Th1 cells in experimental autoimmune encephalomyelitis. *Proc Natl Acad Sci U S A*. 2008;105(26):9041–6.
50. Eugster H-P, Frei K, Kopf M, Lassmann H, Fontana A. IL-6-deficient mice resist myelin oligodendrocyte glycoprotein-induced autoimmune encephalomyelitis. *Eur J Immunol*. 1998;28(7):2178–87.
51. Pixley FJ, Stanley ER. CSF-1 regulation of the wandering macrophage: complexity in action. *Trends Cell Biol*. 2004;14(11):628–38.
52. Kierdorf K, Prinz M. Factors regulating microglia activation. *Front Cell Neurosci*. 2013;7:44.
53. Clark SC, Kamen R. The human hematopoietic colony-stimulating factors. *Science*. 1987;236(4806):1229–37.
54. Roth P, Stanley ER. The biology of CSF-1 and its receptor. *Curr Top Microbiol Immunol*. 1992;181:141–67.
55. Lin H, et al. Discovery of a cytokine and its receptor by functional screening of the extracellular proteome. *Science*. 2008;320(5877):807–11.
56. Prinz M, Priller J. Microglia and brain macrophages in the molecular age: from origin to neuropsychiatric disease. *Nat Rev Neurosci*. 2014;15(5):300–12.
57. Erblich B, Zhu L, Etgen AM, Dobrenis K, Pollard JW. Absence of colony stimulation factor-1 receptor results in loss of microglia, disrupted brain development and olfactory deficits. *PLoS One*. 2011;6(10):e26317.
58. Nandi S, et al. The CSF-1 receptor ligands IL-34 and CSF-1 exhibit distinct developmental brain expression patterns and regulate neural progenitor cell maintenance and maturation. *Dev Biol*. 2012;367(2):100–13.
59. Hao A-J, Dheen ST, Ling E-A. Expression of macrophage colony-stimulating factor and its receptor in microglia activation is linked to teratogen-induced neuronal damage. *Neuroscience*. 2002;112(4):889–900.
60. Waisman A, Ginhoux F, Greter M, Bruttger J. Homeostasis of microglia in the adult brain: review of novel microglia depletion systems. *Trends Immunol*. 2015;10:625–36.
61. Guan Z, et al. Injured sensory neuron-derived CSF1 induces microglial proliferation and DAP12-dependent pain. *Nat Neurosci*. 2016;19(1):94–101.
62. Martínez-Muriana A, et al. CSF1R Blockade Slows the Progression of Amyotrophic Lateral Sclerosis by Reducing Microgliosis and Invasion of Macrophages into Peripheral Nerves. *Sci Rep*. 2016;13(6):25663.
63. Crespo O, et al. Tyrosine kinase inhibitors ameliorate autoimmune encephalomyelitis in a mouse model of multiple sclerosis. *J Clin Immunol*. 2011;31(6):1010–20.
64. Irvine KM, Burns CJ, Wilks AF, Su S, Hume DA, Sweet MJ. A CSF-1 receptor kinase inhibitor targets effector functions and inhibits pro-inflammatory cytokine production from murine macrophage populations. *FASEB J Off Publ Fed Am Soc Exp Biol*. 2006;20(11):1921–3.
65. Ginhoux F, et al. Fate mapping analysis reveals that adult microglia derive from primitive macrophages. *Science*. 2010;330(6005):841–5.
66. Adzemovic MV, Adzemovic MZ, Zeitelhofer M, Eriksson U, Olsson T, Nilsson I. Imatinib ameliorates neuroinflammation in a rat model of multiple sclerosis by enhancing blood-brain barrier integrity and by modulating the peripheral immune response. *PLoS One*. 2013;8(2):e56586.
67. Hume DA, MacDonald KPA. Therapeutic applications of macrophage colony-stimulating factor-1 (CSF-1) and antagonists of CSF-1 receptor (CSF-1R) signaling. *Blood*. 2012;119(8):1810–20.
68. Burns CJ, Wilks AF. c-FMS inhibitors: a patent review. *Expert Opin Ther Pat*. 2011;21(2):147–65.

- 69 Rahat MA, Hemmerlein B, Iragavarapu-Charyulu V. The regulation of angiogenesis by tissue cell-macrophage interactions. *Mediators of Inflammation*; 2016. (eBook).
- 70 Hambardzumyan D, Gutmann DH, Kettenmann H. The role of microglia and macrophages in glioma maintenance and progression. *Nat Neurosci*. 2016;19(1):20–7.

Submit your next manuscript to BioMed Central and we will help you at every step:

- We accept pre-submission inquiries
- Our selector tool helps you to find the most relevant journal
- We provide round the clock customer support
- Convenient online submission
- Thorough peer review
- Inclusion in PubMed and all major indexing services
- Maximum visibility for your research

Submit your manuscript at
www.biomedcentral.com/submit



CHAPTER II

Effect of CSF1R inhibition on Blood-Brain Barrier Disruption and temporal evolution of experimental allergic encephalomyelitis in rats.

Effect of CSF1R inhibition on Blood-Brain Barrier Disruption with the temporal evolution of experimental allergic encephalomyelitis in rats

Nozha Borjini^{1, 2, 3}, Mercedes Fernandez^{3, 4}, Luciana Giardino^{3, 4, 5}, Lydia Sorokin^{6, 7} and Laura Calzà^{2, 3, 4}.

¹Research & Development, Chiesi Farmaceutici S.p.A, Via Palermo 26/A, Parma 43100, Italy.

²Health Science and Technologies Interdepartmental Center for Industrial Research (HST-ICIR), University of Bologna, Via Tolara di Sopra 41/E, Bologna, Ozzano Emilia I-40064, Italy.

³IRET Foundation, Via Tolara di Sopra 41/E, Bologna, Ozzano Emilia 40064, Italy.

⁴Department of Pharmacy and Biotechnology, University of Bologna, Via Tolara di Sopra 41/E, Bologna, Ozzano Emilia 40064, Italy.

⁵Department of Veterinary Medical Sciences, University of Bologna, Via Tolara di Sopra 50, Ozzano Emilia (BO) 40064, Italy.

⁶Institute of Physiological Chemistry and Pathobiochemistry, University of Muenster, 48149 Muenster, Germany

⁷Cells-in-Motion Cluster of Excellence, University of Muenster, 48149 Muenster, Germany

Abstract:

Dysfunction of the blood-brain barrier (BBB) is a primary characteristic of experimental allergic encephalomyelitis (EAE), an experimental model of multiple sclerosis (MS). We have previously demonstrated that, GW2580, a selective inhibitor of CSF1R, slow the disease progression, reduce the severity and prevent the relapse phase. However, whether this effect of GW2580 is through protecting the integrity and function of the BBB is not known. In the present study, we show that GW2580 treatment had a therapeutic effect in EAE rats, with reduction of microglia activation, IgG extravasation, and T-cell infiltration. Our findings demonstrate that GW2580 down regulating microglia activation reduces BBB leakage by inhibiting activities of MMP-2 and -9. Taken together, our results identify a novel mechanism underlying the effect of GW2580 that could be a novel therapy for MS.

To whom correspondence should be addressed:

Nozha Borjini
Research & Development, Chiesi Farmaceutici S.p.A,
Via Palermo 26/A, Parma 43100, Italy
E-mail: n.borjini@chiesi.com

Introduction

Although multiple sclerosis (MS) pathology is not fully understood, blood-brain barrier (BBB) dysfunction plays a crucial role in the pathogenesis of this disease. In both MS and experimental allergic encephalomyelitis (EAE), the most widely used animal model for MS, proinflammatory cells and toxic mediators migrate into the brain via the damaged BBB, resulting in cerebral edema, demyelination, and neural cell death (Varatharaj and Galea, 2017; Varatharaj et al., 2017).

It has been shown that BBB breakdown is accompanied by excessive expression of matrix metalloproteinases (MMPs) (Lakhan et al., 2013; Zhang et al., 2013). MMPs, including MMP-9 and MMP-2, belong to a class of zinc-bound proteases, whose functions include induction of inflammation, cleavage of myelin proteins, activation or degradation of inflammatory mediators, and direct damage to CNS cells (Lu et al., 2011; Song et al., 2015). Abnormal increases in MMP-9 and MMP-2 in endothelial cells may collectively impair endothelial barrier function by degrading the vascular basement membrane and tight junctions (TJs) (Abbott et al., 2006; Alvarez et al., 2011; Ransohoff et al., 2003; Stamatovic et al., 2008; Tietz and Engelhardt, 2015). Inflammatory mediators derived from infiltrating leukocytes regulate MMP-2/9 activity at the parenchymal border, which in turn promotes astrocyte secretion of chemokines and differentially modulates the activity of different cytokines/chemokines at the CNS border, thereby promoting leukocyte migration out of the cuff (Malemud, 2006; Song et al., 2015; Turner and Sharp, 2016). Hence, cytokines, chemokines, and cytokine-induced MMP-2/9 activity specifically at the inflammatory border collectively act to accelerate leukocyte chemotaxis across the parenchymal border.

Data suggest that penetration of the endothelial and parenchymal barriers are independent steps involving distinct molecular mechanisms. While several factors have been identified that play important roles in penetration of the endothelial cell monolayer (Engelhardt and Liebner, 2014) and its basement membrane (Sixt et al., 2001; Sorokin, 2010) comparatively little is known about the subsequent penetration of the parenchymal border. Chemokines such as CXCL12 have been shown to be required for holding T cells in the perivascular cuff, and its proteolytic degradation by MMPs releases leukocytes to migrate into the CNS parenchyma (Laoui et al., 2014; McCandless et al., 2006).

Our previous data suggest that the treatment with GW2580, a selective inhibitor of CSF1R, decreased EAE clinical severity and prevented the relapse phase, thus suggesting the importance of CSF1-CSF1R signaling in microgliosis and inflammation in EAE (Borjini et al., 2016). However, whether this effect of GW2580 is through protecting the integrity and function of the BBB is not known. In the present study, we show that GW2580 treatment had a therapeutic effect in EAE rats, with reduction of microglia activation, IgG extravasation, and T-cell infiltration. Furthermore, GW2580 treatment reduced BBB leakage by inhibiting activities of MMP-2/9, and down regulating microglia activation. Our results suggest that inhibition of early microglia activation by inhibiting CSF1R during the presymptomatic EAE partially restores functional BBB integrity and limits immune cell infiltration into the CNS.

Materials and methods

Animals

Female Dark-Agouti rats (DA) (Harlan, Italy), 151-167 g body weight, were used in this study, placed on *ad libitum* food and water, and housed three per cage on a 12 h light/dark cycle. All animal protocols described herein were carried out in accordance with European Community Council Directives (86/609/EEC), approved by the intramural ethical committee for animal experimentation of Bologna University and the Ministry of Health (n° 158/2013-B, n° 607/2016-PR) and comply with the guidelines published in the NIH Guide for the Care and Use of Laboratory Animals (Louhimies, 2002).

EAE induction and GW2580 treatment

Rats were sensitized by a medium containing 0.15mg/ml guinea pig spinal cord tissue in complete Freund's adjuvant (CFA, Sigma, Saint Louse, USA), 50% v/v, to which 5 mg/ml of heat-inactivated Mycobacterium tuberculosis (Difco H37Ra, DB, Milan, Italy) was added. Sensitization was performed by injecting 100 µl in both hind pads. EAE (n=48) and adjuvant-injected rats (CFA, 50% v/v, heat-inactivated Mycobacterium tuberculosis, 5 mg/ml) (n=15) were sacrificed at 1, 5, 8, 11 and 18-day post immunization (DPI). GW2580 (LC Laboratories, Boston, USA) was dissolved in 0.5% hydroxypropylmethylcellulose and 0.1% Tween 80 (Conway et al., 2005; Leblond et al., 2015). Rats (control+GW2580 and EAE+GW2580 groups) were under GW2580 treatment at 40 mg/Kg once daily by oral gavage using flexible plastic feeding tubes FTP-15-78-50 (Instech Laboratories, Netherlands) for one-day prior and eleven consecutive

days following the immunization. Control rats (n=8), vehicle (0.5% hydroxypropylmethylcellulose / 0.1% Tween 80) (n=6); control+GW2580 (n=6); EAE+GW2580 (n=6) were sacrificed at 18 DPI (last day of the experiment).

Rats were weighed daily and examined for clinical signs of EAE, according to the following semi quantitative score for neurological disability: 0 = no signs, 1 = loss of tail tone, 2 = mono or bilateral weakness of hind legs or middle ataxia, 3 = ataxia or paralysis, 4 = severe hind legs paralysis, 5 = severe hind leg paralysis and urinary incontinence (Calza et al., 2002). In view of the animals' disability, wet food was included inside the cages to facilitate feeding. At 1, 5, 8, 11 and 18 DPI, eight EAE rats were randomly sacrificed. From each experimental group, five animals were used for proteomic and molecular biology experiments and three for morphology and immunohistochemistry.

Spinal cord mRNA analysis

Total RNA was prepared from spinal cord using QIAzol Reagent, cleaned with RNeasy Mini kit (Qiagen; Milano- Italy) and eluted in RNase Free Water and purity and concentration were evaluated by spectrophotometry using NanoDrop ND-2000 (ThermoScientific, Milano, Italy). cDNA synthesis was performed using RT² First Strand kit following the manufacturer's instructions. In brief, after incubation for 5 min at 42°C with Genomic DNA elimination mix in order to avoid any DNA contamination, a reverse-transcription mix of BC3, P2, RE2 and H₂O was used and the transcription performed in a final volume of 20 µl by heating first at 42°C for 15 min, then at 95°C for 5 min. Real-time PCR amplification was performed using the Stratagene Mx3005P multiplex quantitative PCR system (Agilent Technologies). The expression of genes involved in cell adhesion and inflammatory cells infiltration was carried out using RT² SYBR Green qPCR Mastermix (Qiagen). The raw data obtained was uploaded into GeneGlobe Data Analysis software (SABiosciences, Qiagen) for analysis. Relative quantification of mRNA expression was calculated using the comparative cycle threshold (CT) method and is expressed as Log 2 Fold Change of expression. The Fold Change ($2^{(-\Delta\Delta Ct)}$) is the normalized gene expression ($2^{(-\Delta Ct)}$) in the test sample divided by the normalized gene expression ($2^{(-\Delta Ct)}$) in the control sample.

Histochemical staining

To analyze the cerebellum's perivascular cuffs, tissues were cut into 10 µm thickness sections on the cryostat (Leica CM1950, Walldorf, Germany), and stained with hematoxylin and eosin (H&E) according to standard procedures.

Immunohistochemistry

Cerebellum tissues were fixed in 1.5% paraformaldehyde saturated aqueous solution in 0.1 M Sörensen buffer pH 7 for 4 h then embedded in Tissue-Tek® O.C.T.™ Compound (Sakura Finetek Europe, Alphen aan den Rijn, Netherlands). Tissues were frozen and kept at -80°C until processed. Sections (10µm thickness) cut on the cryostat (Leica CM1950, Walldorf, Germany) were incubated for 1 h with PBS-0.5% Triton X-100, 1% BSA, followed by incubation with the primary antibodies diluted in the pre-absorption solution overnight at 4°C. The primary antibodies and dilutions used were: rabbit anti-human CD3 (1: 400), Alexa Fluor 488 mouse anti-glial fibrillary acidic protein (GFAP) (1: 1000), mouse anti-mouse neuronal nuclei (NeuN), rabbit anti-mouse Ionized calcium binding adaptor molecule 1 (Iba 1) (1: 100), rabbit anti-human SDF-1 (Cxcl-12a) (1: 400), donkey anti-rat IgG Alexa Fluor 594 (1: 1000).

After rinsing in PBS, the sections were incubated at 37°C for 2 h with the secondary antibodies diluted in the pre-absorption solution. Sections were then rinsed in PBS and mounted in Evanol solution. Control slices were incubated with the secondary antibodies only and processed in parallel. Sections were examined using a Zeiss Axio Imager equipped with epifluorescent optics or a Zeiss LSM 700 confocal microscope and documented using a Hamamatsu ORCA-ER camera. Images were captured and analyzed using Volocity 5.1 software (Improvision).

Gelatin gel zymography

Gelatin gel zymography was performed as described previously (Song et al., 2015). 6 mg of the cerebellum lysates was used for MMP prepurification, and the resulting 20 ml eluted from the columns was loaded onto the gelatin gels. This permitted comparison of the relative proportions of pro-MMP-2/9 and activated MMP-2/9 in control versus EAE at different time point (8, 11 and 18) and EAE rats treated with GW2580.

Results

GW2580 decreased EAE clinical severity and prevents the relapse phase

By the oral administration of GW2580, the tyrosine kinase activity of CSF1R was inhibited. GW2580 is a highly selective inhibitor of the cFMS kinase and through this pathway it blocks CSF1 signaling. Animals were treated one day before the immunization and till 11 days after immunization. The clinical profiles of the disease in EAE, EAE+GW2580, control+GW2580 and vehicle groups of animals are reported in Figure 1, in which clinical score (A) and body weight graphs (B) are shown. While clinical signs of the neurological disabilities started at 6-7 DPI in the EAE group, a delay in the appearance of the neurological disability observed in EAE+GW2580 group. A maximum score 5 was reached by 11-12 DPI which witness the acute phase, while a significant reduction of the severity of the disease was observed in EAE+GW2580 group ($P<0.001$) with a maximum score of 2.8. Remarkably, EAE+GW2580 animals didn't show any relapse phase ($P<0.001$), they were recovering ($P<0.001$) till the last day of the experiment (18 DPI). A decrease the body weight (Figure 1B) was observed in EAE+GW2580 group from 2 DPI compared to the GW2580 animals ($P<0.001$), which is the same profile of the body weight loss observed in EAE group but less severe, in close correspondence with the evolution of the symptoms of the disorder, which is followed by a recovery.

Reduction of BBB damage and IgG extravasation under GW2580

A straightforward method of assessing BBB disruption is measurement of extravasated blood proteins. We investigated by immunofluorescence the extravasation of endogenous anti-rat immunoglobulin G (IgG) in the cerebellum parenchyma (Figure 2). At 8 DPI, circulating IgG was accumulated inside the blood vessels, which witness an intact BBB at this time point. At 11 DPI, the acute phase (Figure 2B), and 18 DPI, the relapse phase (Figure 2C), a disruption of the BBB was observed, evidenced through leakage of IgG into the cerebellum parenchyma and hemorrhage around capillaries (Figure 2B-C). With the inhibition of CSF1R in EAE by using GW2580 (EAE+GW2580 18 DPI) (Figure 2D), in some part of the cerebellum we noticed few IgG extravasation into the CNS tissue, while the major part of IgG staining was within the blood vessels (Figure 2D).

Altered expression of BBB genes in SC during early presymptomatic EAE

We then quantified the expression of 24 genes coding for proteins and enzymes forming

and modifying the BBB in the SC of control and EAE rats. The complete list of investigated genes is presented in figure 3. The results are presented in a clustergram that performs non-supervised hierarchical clustering to display a heat map with dendrograms indicating co-regulated genes across groups, criteria for significance are reported in the table of magnitude gene expression (Figure 3). Of the 24 BBB genes tested, an early regulation of most of the genes was observed as soon as symptoms appear (8 DPI) but before the disease peak (11 DPI). Several adhesion genes such as VCAM, ICAM, were up-regulated in the SC at 8 DPI. Most of the chemokines such as CXCL-10, CCL-12, CXCR-3 were also up-regulated starting from 8 DPI. With regard to MMP-9, an up-regulation starting from 8 DPI was observed with 5,46 Log 2 Fold Change. Notably, ADAM-17 (metallopeptidase domain 17) mRNAs is strongly down regulated at 1 DPI. The highest upregulation was observed for IFN- γ ; 68.12 Log 2 Fold Change at 8 DPI, 179.15 at 11 DPI and 98.7 at 18 DPI (Figure 3). To note, the overexpression of IFN- γ mRNA in EAE-acute phase (11 DPI) is the highest EAE-induced up-regulation observed compared with the other genes investigated (Figure 3).

Effect of GW2580 on cerebellum's perivascular cuffs

Representative images of hematoxylin and eosin (H&E) staining show absence of pathology in healthy controls (data not shown). In the cerebellum white matter at 8 DPI (Figure 4A), intact perivascular cuffs (Figure 4E) could be observed where the immune cells were accumulated in the perivascular space, in contrast to robust inflammatory lesions in the cerebellum white matter at the peak of the disease (11 DPI) (Figure 4B) and at the relapse phase (18 DPI) (Figure 4C), where all perivascular cuffs are destroyed (Figure 4F), the immune cells quit the perivascular space and infiltrated to the CNS tissue. With the selective inhibition of CSF1R in EAE with GW2580 (EAE+GW2580 18 DPI) (Figure 4D), we could observe much more intact perivascular cuffs as seen at 8 DPI, but also some destroyed ones where the immune cells started to infiltrate to the cerebellum parenchyma (Figure 4G).

Cerebellum's glial activation under GW2580

In order to evaluate the cerebellum's glial activation, immunohistochemistry analysis were performed in the cerebellum of control (data not shown), EAE animals (8, 11 and 18 DPI) and EAE + GW2580 at 18 DPI. Representative images are shown in Figure 5. A slight activation of microglia and astrocyte was noticed at 8 DPI (Figure 5A-C) whereas

intact perivascular cuffs were observed where perivascular astrocytic endfeet perfectly surrounding the blood vessel. Iba-1 immunofluorescence revealed a strong activation and amoeboid form of resident microglia and perivascular macrophages at 11 DPI and 18 DPI (Figure 5E-F and H-I). A decrease of GFAP- immunofluorescence surrounding vessels was observed, at the acute and relapse phase (Figure 5D and G). With the inhibition of CSF1R using the oral administration of GW2580, less glial activation was observed (Figure 6J-L) comparing to EAE 18 DPI.

GW2580 attenuate T-cells infiltration in EAE

Immune cell infiltration into the cerebellum parenchyma was assessed per CD3- immunofluorescence analyses. Intact perivascular cuffs were observed at 8 DPI (Figure 6A), few CD3⁺ cells (Figure 6B) were found within the perivascular spaces (Figure 6C). At 18 DPI destroyed cuffs were observed, evidenced through gaps occur between astrocytes' endfeet, supposing to cover microvessels in the CNS and form the glia limits (Figure 6D), and a plethora of T-cells infiltrate to the cerebellum parenchyma (Figure 6E-F). Comparing with EAE 18 DPI, the treatment with GW2580 (Figure 6G-I) seems to maintain the perivascular astrocytic endfeet and attenuate T-cells infiltration.

MMP-2 and MMP-9 in the course of EAE

MMP-2 and MMP-9 activity have been previously shown to occur at sites of leukocyte penetration of the CNS parenchyma (Agrawal et al., 2013; Song et al., 2015) but have not been analyzed during the course of presymptomatic EAE. We therefore performed gelatin gel zymography for MMP-2 and MMP-9 on cerebellum extracts from naïve DA rats, at 8 DPI, peak EAE (11 DPI) and EAE relapse phases (18 DPI), revealing that pro- and activated-MMP-9 were up-regulated upon appearance of EAE symptoms (8 DPI) and declined during recovery phases (Figure 7); while in all samples pro and activated MMP-2 were constitutively expressed (Figure 7). With the inhibition of CSF1R using the small molecule GW2580, activated MMP-9 was down-regulated comparing with the EAE 18 DPI.

Effect of CSF1R inhibition on CXCL-12 chemokine

Since CXCL12 is inactivated by MMP-2 and MMP-9 (McQuibban et al., 2001), and as the cleaved form is localized only within CNS parenchyma (Song et al., 2015), we used an antibody that recognizes both full-length and cleaved CXCL12. At 18 DPI, few full-length form of CXCL12 was observed within cuffs with high signal for the cleaved form

within the cerebellum parenchyma (Figure 8A-C). Comparing to 18 DPI, the major CXCL12 in EAE rats under GW2580 treatment at 18 DPI (Figure 8D-F) seems to be full-length form with little signal for the cleaved one and localized at the parenchymal border.

Discussion

Multiple sclerosis lesions have been classified into several patterns on the basis of demyelination, and the nature and persistence of an inflammatory response leading to severe neuronal degeneration (Compston and Coles, 2002; Frohman et al., 2006; Lassmann et al., 2012; Trapp and Nave, 2008). Despite the heterogeneity of these lesions, alterations in BBB permeability have long been thought to be a key initiating factor in MS and EAE (Zigmond et al., 2014). Previously, we have demonstrated that the oral administration of GW2580, a selective inhibitor of CSF1R, an integral tyrosine kinase transmembrane receptor expressed by microglia cells under normal conditions, decreased EAE clinical severity and prevents the relapse phase, thus suggesting the importance of CSF1-CSF1R signaling in microgliosis and inflammation in MS (Borjini et al., 2016). The current study therefore extended our previous finding to investigate whether this effect of GW2580 is through protecting the integrity and function of the BBB.

At mRNA level (spinal cord tissue), genes coding for proteins and enzymes forming and modifying the BBB were regulated as soon as symptoms appear (8 DPI) in EAE rats compared to control, while no BBB disruption was seen by that time point. A straightforward method of assessing BBB disruption is the measurement of extravasation blood proteins in the brain parenchyma, using immunofluorescence or immunohistochemistry. An advantage of this method is that no exogenous tracer is introduced into the circulation, eliminating potential confounding factors (Kassner and Merali, 2015). Remarkably, the presence of IgG-immunofluorescence within the blood vessels and few IgG leakages into the CNS parenchyma indicates that a reduction of BBB damage was observed in EAE treated rats with GW2580. The integrity of the BBB is maintained by multiple components, including the tight junction (TJ)-sealed capillary ECs, pericytes and the extracellular matrix (ECM) and astrocyte endfeet (Neuwelt et al., 2011; Shi et al., 2016). Under GW2580, we observed intact perivascular cuffs, where perivascular astrocytic endfeet perfectly surround the blood vessel, and no gaps occur between astrocytes' endfeet.

Inflammatory perivascular cuffs are comprised of leucocytes that accumulate in the

perivascular space around post-capillary venules before their penetration into the parenchyma of the CNS. Inflammatory perivascular cuffs are commonly found in the CNS of patients with MS and animals with EAE (Song et al., 2015). Interestingly, GW2580, the selective inhibitor of CSF1R in EAE, attenuated T-cells infiltration within the CNS parenchyma. In fact, it has been shown that when GW2580 used in EAE starting from 10 days after immunization, it reduces the amount of peripheral macrophages and decreases the number of inflammatory foci in the CNS (Crespo et al., 2011a). This effect has at least partially accredited to the conquest of the autocrine signaling of inflammatory microglia and macrophages, inducing the decrease of neuroinflammatory mediators (Erblich et al., 2011; Ginhoux et al., 2010; Irvine et al., 2006), suggesting that targeting tyrosine kinase receptors could avoid the development of the disease by boosting BBB integrity (Adzemovic et al., 2013; Crespo et al., 2011b).

The process of leucocyte transmigration across a post-capillary venule into the CNS includes several important steps (Engelhardt and Ransohoff, 2005; Larochelle et al., 2011). The first step is a slowing of leucocytes within the blood through the interaction and binding of integrin alpha 4 beta 1 receptors present on leucocytes with several cell adhesion molecules on the endothelium including VCAM1 and ICAM1 (Engelhardt and Ransohoff, 2005; Sixt et al., 2001; Tietz and Engelhardt, 2015). This is followed by leucocyte arrest to endothelial cells possibly due to a response to chemokines secreted by endothelial cells (Alt et al., 2002; Dorovini-Zis, 2015). Once leucocytes adhere, they cross the endothelial cell barrier and endothelial basement membrane to accumulate in the perivascular space and form the inflammatory perivascular cuff (Agrawal et al., 2013).

With the inhibition of CSF1R using the small molecule GW2580, on gel zymography we observed that activated MMP-9 was down regulated comparing with the EAE 18 DPI which could explain the reduction of CD3⁺ cells transminating the perivascular space to the CNS tissue. Indeed, the family of matrix metalloproteinases helps leucocytes transit into the CNS. MMPs do not seem to be required in leucocyte migration across the endothelial basement membrane (Wu et al., 2009), but they are necessary when leucocytes transigrate the parenchymal border (Clark et al., 2011; Toft-Hansen et al., 2004; Yamamura and Gran, 2013). Specifically, MMP2 and MMP9 have been shown to cleave β -dystroglycan, a receptor on astrocyte end feet that abuts the parenchymal basement membrane, allowing cells to enter the CNS parenchyma (Agrawal et al., 2006;

Kim and Joh, 2012).

Under GW2580 treatment, we also observed that the majority of the chemokine CXCL12 (stromal cell-derived factor 1 alpha), seems to be at the full-length form with little signal for the cleaved form, and localized at the parenchymal border, which could explain the reduction of T-cells' infiltration within the CNS tissue and the down-regulation of MMP-9 on EAE + GW2580 rats. It has been demonstrated that CXCL12 is required for holding T-cells in the perivascular cuff, and its proteolytic degradation by MMP-2/-9 releases leukocytes to migrate into the CNS parenchyma (Chu et al., 2017; McCandless et al., 2006; Meiron et al., 2008). The initial recruitment of T cells to the CNS is likely to be controlled by CXCL12, which has been shown by others to hold immune cells in the perivascular cuff in its intact form only within the perivascular cuff (McCandless et al., 2006; Song et al., 2015).

Collectively, our study demonstrates that improving BBB integrity is one of the mechanisms of GW2580 action in EAE therapy. This effect is at least partially through inhibiting activities of MMP-2/-9 and protecting the BBB integrity. As a result, inflammatory infiltration into the CNS is largely reduced. While the process of immune cell extravasation is partially an endothelial cell-mediated process, whether GW2580 reduces this pathway of immune cell infiltration is not yet known. Nevertheless, results from the present study, together with the reduction effect of GW2580 on microglia cells activation that we have previously shown (Borjini et al., 2016) and its safety (Conway et al., 2005, 2008), suggest that GW2580 could qualify as an effective, alternative remedy in MS therapy and that further investigation to test this possibility is justified.

References

- Abbott, N.J., Rönnebeck, L., and Hansson, E. (2006). Astrocyte-endothelial interactions at the blood-brain barrier. *Nat. Rev. Neurosci.* 7, 41–53.
- Adzemovic, M.V., Adzemovic, M.Z., Zeitelhofer, M., Eriksson, U., Olsson, T., and Nilsson, I. (2013). Imatinib ameliorates neuroinflammation in a rat model of multiple sclerosis by enhancing blood-brain barrier integrity and by modulating the peripheral immune response. *PloS One* 8, e56586.
- Agrawal, S., Anderson, P., Durbeek, M., van Rooijen, N., Ivars, F., Opdenakker, G., and Sorokin, L.M. (2006). Dystroglycan is selectively cleaved at the parenchymal basement membrane at sites of leukocyte extravasation in experimental autoimmune encephalomyelitis. *J. Exp. Med.* 203, 1007–1019.
- Agrawal, S.M., Williamson, J., Sharma, R., Kebir, H., Patel, K., Prat, A., and Yong, V.W. (2013). Extracellular matrix metalloproteinase inducer shows active perivascular cuffs in multiple sclerosis. *Brain* 136, 1760–1777.
- Alt, C., Laschinger, M., and Engelhardt, B. (2002). Functional expression of the lymphoid chemokines CCL19 (ELC) and CCL 21 (SLC) at the blood-brain barrier suggests their involvement in G-protein-dependent lymphocyte recruitment into the central nervous system during experimental autoimmune encephalomyelitis. *Eur. J. Immunol.* 32, 2133–2144.
- Alvarez, J.I., Cayrol, R., and Prat, A. (2011). Disruption of central nervous system barriers in multiple sclerosis. *Biochim. Biophys. Acta BBA - Mol. Basis Dis.* 1812, 252–264.
- Borjini, N., Fernández, M., Giardino, L., and Calzà, L. (2016). Cytokine and chemokine alterations in tissue, CSF, and plasma in early presymptomatic phase of experimental allergic encephalomyelitis (EAE), in a rat model of multiple sclerosis. *J. Neuroinflammation* 13, 291.
- Calza, L., Fernandez, M., Giuliani, A., Aloe, L., and Giardino, L. (2002). Thyroid hormone activates oligodendrocyte precursors and increases a myelin-forming protein and NGF content in the spinal cord during experimental allergic encephalomyelitis. *Proc. Natl. Acad. Sci. U. S. A.* 99, 3258–3263.
- Chu, T., Shields, L.B.E., Zhang, Y.P., Feng, S.-Q., Shields, C.B., and Cai, J. (2017). CXCL12/CXCR4/CXCR7 Chemokine Axis in the Central Nervous System: Therapeutic Targets for Remyelination in Demyelinating Diseases. *The Neuroscientist* 1073858416685690.
- Clark, R.T., Philip Nance, J., Noor, S., and Wilson, E.H. (2011). T-cell production of matrix metalloproteinases and inhibition of parasite clearance by TIMP-1 during chronic Toxoplasma infection in the brain. *ASN NEURO* 3.
- Compston, A., and Coles, A. (2002). Multiple sclerosis. *Lancet Lond. Engl.* 359, 1221–1231.

- Conway, J.G., McDonald, B., Parham, J., Keith, B., Rusnak, D.W., Shaw, E., Jansen, M., Lin, P., Payne, A., Crosby, R.M., et al. (2005). Inhibition of colony-stimulating-factor-1 signaling in vivo with the orally bioavailable cFMS kinase inhibitor GW2580. *Proc. Natl. Acad. Sci. U. S. A.* *102*, 16078–16083.
- Conway, J.G., Pink, H., Bergquist, M.L., Han, B., Depee, S., Tadepalli, S., Lin, P., Crumrine, R.C., Binz, J., Clark, R.L., et al. (2008). Effects of the cFMS Kinase Inhibitor 5-(3-Methoxy-4-((4-methoxybenzyl)oxy)benzyl)pyrimidine-2,4-diamine (GW2580) in Normal and Arthritic Rats. *J. Pharmacol. Exp. Ther.* *326*, 41–50.
- Crespo, O., Kang, S.C., Daneman, R., Lindstrom, T.M., Ho, P.P., Sobel, R.A., Steinman, L., and Robinson, W.H. (2011a). Tyrosine Kinase Inhibitors Ameliorate Autoimmune Encephalomyelitis in a Mouse Model of Multiple Sclerosis. *J. Clin. Immunol.* *31*, 1010–1020.
- Crespo, O., Kang, S.C., Daneman, R., Lindstrom, T.M., Ho, P.P., Sobel, R.A., Steinman, L., and Robinson, W.H. (2011b). Tyrosine Kinase Inhibitors Ameliorate Autoimmune Encephalomyelitis in a Mouse Model of Multiple Sclerosis. *J. Clin. Immunol.* *31*, 1010–1020.
- Dorovini-Zis, K. (2015). *The Blood-Brain Barrier in Health and Disease, Volume One: Morphology, Biology and Immune Function* (CRC Press).
- Engelhardt, B., and Liebner, S. (2014). Novel insights into the development and maintenance of the blood–brain barrier. *Cell Tissue Res.* *355*, 687–699.
- Engelhardt, B., and Ransohoff, R.M. (2005). The ins and outs of T-lymphocyte trafficking to the CNS: anatomical sites and molecular mechanisms. *Trends Immunol.* *26*, 485–495.
- Erblich, B., Zhu, L., Etgen, A.M., Dobrenis, K., and Pollard, J.W. (2011). Absence of colony stimulation factor-1 receptor results in loss of microglia, disrupted brain development and olfactory deficits. *PloS One* *6*, e26317.
- Frohman, E.M., Racke, M.K., and Raine, C.S. (2006). Multiple sclerosis--the plaque and its pathogenesis. *N. Engl. J. Med.* *354*, 942–955.
- Ginhoux, F., Greter, M., Leboeuf, M., Nandi, S., See, P., Gokhan, S., Mehler, M.F., Conway, S.J., Ng, L.G., Stanley, E.R., et al. (2010). Fate Mapping Analysis Reveals That Adult Microglia Derive from Primitive Macrophages. *Science* *330*, 841–845.
- Irvine, K.M., Burns, C.J., Wilks, A.F., Su, S., Hume, D.A., and Sweet, M.J. (2006). A CSF-1 receptor kinase inhibitor targets effector functions and inhibits pro-inflammatory cytokine production from murine macrophage populations. *FASEB J. Off. Publ. Fed. Am. Soc. Exp. Biol.* *20*, 1921–1923.
- Kassner, A., and Merali, Z. (2015). Assessment of Blood–Brain Barrier Disruption in Stroke. *Stroke* *46*, 3310–3315.

- Kim, Y.-S., and Joh, T.H. (2012). Matrix Metalloproteinases, New Insights into the Understanding of Neurodegenerative Disorders. *Biomol. Ther.* 20, 133–143.
- Lakhan, S.E., Kirchgessner, A., Tepper, D., and Leonard, A. (2013). Matrix Metalloproteinases and Blood-Brain Barrier Disruption in Acute Ischemic Stroke. *Front. Neurol.* 4.
- Laoui, D., Van Overmeire, E., De Baetselier, P., Van Ginderachter, J.A., and Raes, G. (2014). Functional Relationship between Tumor-Associated Macrophages and Macrophage Colony-Stimulating Factor as Contributors to Cancer Progression. *Front. Immunol.* 5, 489.
- Larochelle, C., Alvarez, J.I., and Prat, A. (2011). How do immune cells overcome the blood–brain barrier in multiple sclerosis? *FEBS Lett.* 585, 3770–3780.
- Lassmann, H., van Horssen, J., and Mahad, D. (2012). Progressive multiple sclerosis: pathology and pathogenesis. *Nat. Rev. Neurol.* 8, 647–656.
- Leblond, A.-L., Klinkert, K., Martin, K., Turner, E.C., Kumar, A.H., Browne, T., and Caplice, N.M. (2015). Systemic and Cardiac Depletion of M2 Macrophage through CSF-1R Signaling Inhibition Alters Cardiac Function Post Myocardial Infarction. *PloS One* 10, e0137515.
- Louhimies, S. (2002). Directive 86/609/EEC on the protection of animals used for experimental and other scientific purposes. *Altern. Lab. Anim. ATLA* 30 *Suppl* 2, 217–219.
- Lu, P., Takai, K., Weaver, V.M., and Werb, Z. (2011). Extracellular Matrix Degradation and Remodeling in Development and Disease. *Cold Spring Harb. Perspect. Biol.* 3.
- Malemud, C.J. (2006). Matrix metalloproteinases (MMPs) in health and disease: an overview. *Front. Biosci. J. Virtual Libr.* 11, 1696–1701.
- McCandless, E.E., Wang, Q., Woerner, B.M., Harper, J.M., and Klein, R.S. (2006). CXCL12 limits inflammation by localizing mononuclear infiltrates to the perivascular space during experimental autoimmune encephalomyelitis. *J. Immunol. Baltim. Md* 1950 177, 8053–8064.
- McQuibban, G.A., Butler, G.S., Gong, J.H., Bendall, L., Power, C., Clark-Lewis, I., and Overall, C.M. (2001). Matrix metalloproteinase activity inactivates the CXC chemokine stromal cell-derived factor-1. *J. Biol. Chem.* 276, 43503–43508.
- Meiron, M., Zohar, Y., Anunu, R., Wildbaum, G., and Karin, N. (2008). CXCL12 (SDF-1 α) suppresses ongoing experimental autoimmune encephalomyelitis by selecting antigen-specific regulatory T cells. *J. Exp. Med.* 205, 2643–2655.
- Neuwelt, E.A., Bauer, B., Fahlke, C., Fricker, G., Iadecola, C., Janigro, D., Leybaert, L., Molnár, Z., O'Donnell, M.E., Povlishock, J.T., et al. (2011). Engaging neuroscience to advance translational research in brain barrier biology. *Nat. Rev. Neurosci.* 12, 169–182.

Ransohoff, R.M., Kivisäkk, P., and Kidd, G. (2003). Three or more routes for leukocyte migration into the central nervous system. *Nat. Rev. Immunol.* 3, 569–581.

Shi, Y., Zhang, L., Pu, H., Mao, L., Hu, X., Jiang, X., Xu, N., Stetler, R.A., Zhang, F., Liu, X., et al. (2016). Rapid endothelial cytoskeletal reorganization enables early blood–brain barrier disruption and long-term ischaemic reperfusion brain injury. *Nat. Commun.* 7, 10523.

Sixt, M., Engelhardt, B., Pausch, F., Hallmann, R., Wendler, O., and Sorokin, L.M. (2001). Endothelial cell laminin isoforms, laminins 8 and 10, play decisive roles in T cell recruitment across the blood-brain barrier in experimental autoimmune encephalomyelitis. *J. Cell Biol.* 153, 933–946.

Song, J., Wu, C., Korpos, E., Zhang, X., Agrawal, S.M., Wang, Y., Faber, C., Schäfers, M., Körner, H., Opdenakker, G., et al. (2015). Focal MMP-2 and MMP-9 activity at the blood-brain barrier promotes chemokine-induced leukocyte migration. *Cell Rep.* 10, 1040–1054.

Sorokin, L. (2010). The impact of the extracellular matrix on inflammation. *Nat. Rev. Immunol.* 10, 712–723.

Stamatovic, S.M., Keep, R.F., and Andjelkovic, A.V. (2008). Brain Endothelial Cell-Cell Junctions: How to “Open” the Blood Brain Barrier. *Curr. Neuropharmacol.* 6, 179–192.

Tietz, S., and Engelhardt, B. (2015). Brain barriers: Crosstalk between complex tight junctions and adherens junctions. *J Cell Biol* 209, 493–506.

Toft-Hansen, H., Nuttall, R.K., Edwards, D.R., and Owens, T. (2004). Key metalloproteinases are expressed by specific cell types in experimental autoimmune encephalomyelitis. *J. Immunol. Baltim. Md 1950* 173, 5209–5218.

Trapp, B.D., and Nave, K.-A. (2008). Multiple sclerosis: an immune or neurodegenerative disorder? *Annu. Rev. Neurosci.* 31, 247–269.

Turner, R.J., and Sharp, F.R. (2016). Implications of MMP9 for Blood Brain Barrier Disruption and Hemorrhagic Transformation Following Ischemic Stroke. *Front. Cell. Neurosci.* 10.

Varatharaj, A., and Galea, I. (2017). The blood-brain barrier in systemic inflammation. *Brain. Behav. Immun.* 60, 1–12.

Varatharaj, A., Liljeroth, M., Cramer, S., Stuart, C., Zotova, E., Darekar, A., Larsson, H., and Galea, I. (2017). Systemic inflammation and blood–brain barrier abnormality in relapsing–remitting multiple sclerosis. *The Lancet* 389, *Supplement 1*, S96.

Wu, C., Ivars, F., Anderson, P., Hallmann, R., Vestweber, D., Nilsson, P., Robenek, H., Tryggvason, K., Song, J., Korpos, E., et al. (2009). Endothelial basement membrane laminin alpha5 selectively inhibits T lymphocyte extravasation into the brain. *Nat. Med.* 15, 519–527.

Yamamura, T., and Gran, B. (2013). Multiple Sclerosis Immunology: A Foundation for Current and Future Treatments (Springer Science & Business Media).

Zhang, S., Kan, Q.-C., Xu, Y., Zhang, G.-X., and Zhu, L. (2013). Inhibitory Effect of Matrine on Blood-Brain Barrier Disruption for the Treatment of Experimental Autoimmune Encephalomyelitis. *Mediators Inflamm.* 2013.

Zigmond, M.J., Coyle, J.T., and Rowland, L.P. (2014). Neurobiology of Brain Disorders: Biological Basis of Neurological and Psychiatric Disorders (Elsevier).

Legend to the figures

Figure 1. Effects of selective inhibition of CSF1R activity on the disease progression.

(A) Time-course of the neurological disability score of EAE and EAE+GW2580 animals is reported in the graph (mean \pm SD), showing the peak at day 11 (acute phase), the remission phase at day 16 and relapse at day 18 for EAE animals while a delayed and reduced clinical score was observed for EAE+GW2580 group. (B) The body weight gain (mean \pm SD) is reported in the graph (mean \pm SD), enlightening a significant difference between GW2580 and EAE + GW2580 group. Statistical analysis: (A) two-way ANOVA and Bonferroni post-test ($***P<0.001$), (B) one-way ANOVA, $***P<0.0001$.

Figure 2. Cerebellum's IgG extravasation in; (A) EAE rats at 8 DPI (EAE t8) (B) the acute phase at 11 DPI (EAE t11) (C) during the relapse phase 18 DPI (EAE t18) and (D) under the treatment of CSF1R inhibitor, GW2580 at 18 DPI (EAE t18 + GW2580).

Figure 3. BBB genes mRNA expression level in the SC. The expression levels of mRNA of genes coding for proteins and enzymes forming and modifying the BBB in control and EAE rats are reported in the clustergram, based on heat map with dendrograms, indicating the co-regulated genes across groups. Red color for a gene indicates expression above the median and green color indicates expression below the median. The table presents differentially expressed genes. Statistical analysis was performed using Student's *t*-test of the replicate $2^{(-\Delta\Delta Ct)}$ values for each gene in the control group and treatment group; $P<0.05$ was considered significant.

Figure 4. Cerebellum's perivascular cuffs. Hematoxylin and eosin staining (H&E) of the cerebellum at (A) 8 DPI EAE (EAE t8), (B) the acute phase 11 DPI (EAE t11), (C) during the relapse phase 18 DPI (EAE t18), and (D) under the treatment of CSF1R inhibitor, GW2580 at 18 DPI (EAE t18 + GW2580). High-magnification of perivascular cuff at EAE 8 DPI (E), EAE 11 DPI (F) and under the treatment GW2580 at 18 DPI (G).

Figure 5. Cerebellum's glial activation. Immunofluorescence staining of thin (10 μ m) cerebellum sections of EAE rats at 8 DPI (A-C), 11 DPI (D-F), 18 DPI (G-I), with the treatment GW2580 at 18 DPI (J-L). The sections were stained with anti-Iba1 antibody to visualize microglia/macrophages (red), with anti-GFAP antibody to mark astrocytes (green). DAPI stains all nuclei (blue).

Figure 6. T-cells infiltration in EAE. Immunofluorescence staining of 10 μ m cerebellum sections with anti-CD3 antibody to mark CD3⁺ infiltrating T-cells (red) and anti-GFAP antibody to mark astrocytes (green). DAPI stains all nuclei (blue). Pictures are representatives from similar data from 6 rats each.

Figure 7. Effects of CSF1R inhibition on MMP2/9 activation. Gelatin gel zymography of cerebellum lysates of control rats, EAE rats at 8 DPI EAE, the acute phase (EAE t11), during the relapse phase 18 DPI (EAE t18) and under the treatment of CSF1R inhibitor, GW2580 at 18 DPI (EAE t18 + GW2580).

Figure 8. Effects of CSF1R inhibition on CXCL-12 chemokine. Immunofluorescence staining of inflammatory perivascular cuffs in the white matter of cerebellum of EAE rat at relapse phase 18 DPI (A-C) and treated EAE rats with GW2580 (D-F), The sections were stained with anti-Pan LM antibody to visualize BMs of blood vessels (green), and with anti-CXCL-12 antibody (red). DAPI stains all nuclei (blue).

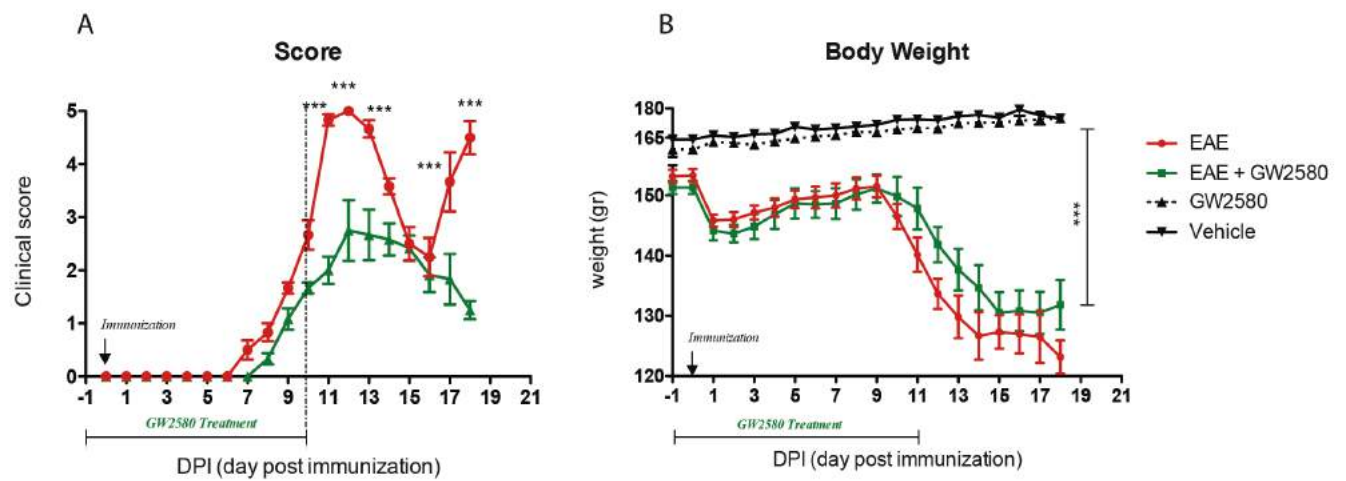


Figure.1

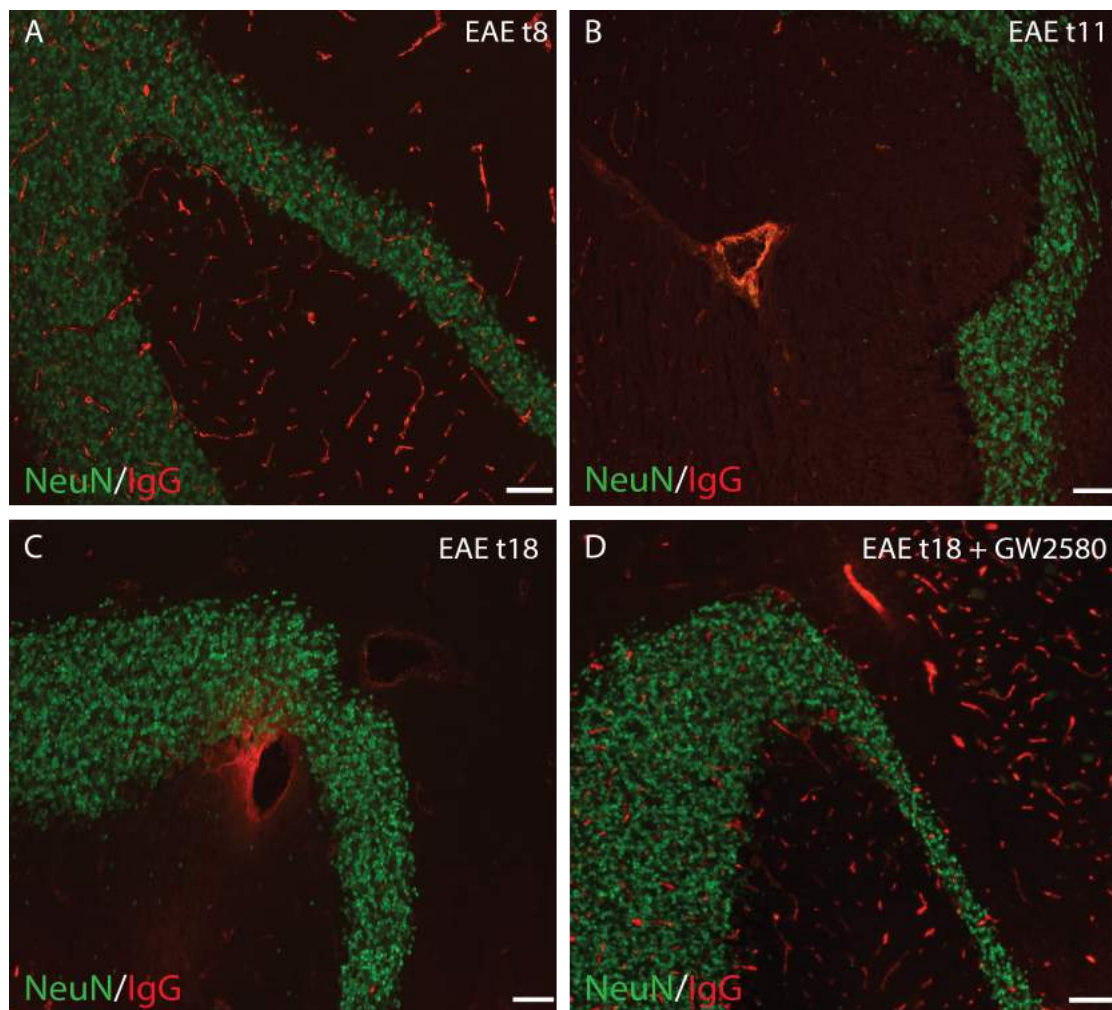
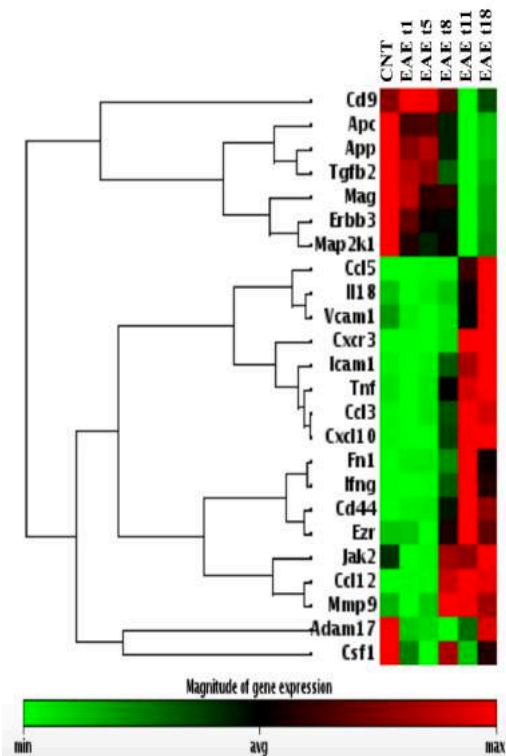


Figure. 2



Transcript ID	Gene symbol	Gene title	EAE t1 vs. Control		EAE t5 vs. Control		EAE t8 vs. Control		EAE t11 vs. Control		EAE t18 vs. Control	
			Log2 Fold Change	p value	Fold Change	p value	Fold Change	p value	Fold Change	p value	Fold Change	p value
NM_053018	Cd9	CD9 molecule	1,225	0,0031	1,181	0,0909	-1,072	0,0203	-2,938	0,0000	-1,784	0,0000
NM_012499	Apc	Adenomatous polyposis coli	-1,354	0,0010	-1,357	0,0001	-1,828	0,0000	-5,836	0,0000	-4,127	0,0000
NM_019288	App	Amyloid beta (A4) precursor protein	-1,123	0,0001	-1,079	0,0300	-1,526	0,0000	-3,084	0,0000	-2,704	0,0000
NM_031131	Tgfb2	Transforming growth factor, beta 2	-1,100	0,0230	-1,214	0,0004	-2,497	0,0000	-9,095	0,0000	-4,643	0,0000
NM_017190	Mag	Myelin-associated glycoprotein	-1,063	0,5654	-1,464	0,0039	-1,464	0,0001	-5,796	0,0000	-3,422	0,0000
NM_017218	ErbB3	V-erb-b2 erythroblastic leukemia viral oncogene	-1,229	0,1260	-1,464	0,0389	-1,569	0,0162	-3,877	0,0014	-2,761	0,0019
NM_031643	Map2k1	Mitogen activated protein kinase kinase 1	-1,317	0,0064	-1,516	0,0015	-1,414	0,0033	-3,084	0,0000	-2,338	0,0003
NM_031116	Ccl5	Chemokine (C-C motif) ligand 5	-1,034	0,8691	1,165	0,5210	1,357	0,0346	14,271	0,0001	22,085	0,0000
NM_019165	Il18	Interleukin 18	-1,163	0,0424	-1,125	0,4246	-1,007	0,2651	1,409	0,1343	1,979	0,0002
NM_012889	Vcam1	Vascular cell adhesion molecule 1	-1,272	0,0001	-1,376	0,0111	-1,257	0,0048	1,235	0,0475	1,821	0,0001
NM_053415	Cxcr3	Chemokine (C-X-C motif) receptor 3	1,159	0,0817	1,014	0,3308	5,028	0,0000	57,880	0,0013	55,909	0,0007
NM_012967	Icam1	Intercellular adhesion molecule 1	-1,139	0,0082	1,000	0,9840	2,732	0,0152	4,840	0,0000	5,521	0,0000
NM_012675	Tnf	Tumor necrosis factor (TNF superfamily, member 2)	-2,293	0,0367	-1,189	0,7864	6,105	0,0299	9,350	0,0027	9,747	0,0010
NM_013025	Ccl3	Chemokine (C-C motif) ligand 3	-1,383	0,2623	1,338	0,0066	5,352	0,0000	12,168	0,0000	10,891	0,0001
NM_139089	Cxcl10	Chemokine (C-X-C motif) ligand 10	-2,231	0,0005	-1,945	0,0011	11,551	0,0000	25,369	0,0007	24,847	0,0000
NM_019143	Fn1	Fibronectin 1	1,175	0,0532	1,173	0,2527	1,919	0,0243	4,302	0,0078	2,594	0,0001
NM_138880	Ifng	Interferon gamma	-1,611	0,1786	1,464	0,4249	68,120	0,0000	179,147	0,0000	98,702	0,0000
NM_012924	Cd44	Cd44 molecule	1,233	0,1963	1,257	0,0822	3,837	0,0039	6,126	0,0002	4,874	0,0001
NM_019357	Ezr	Ezrin	1,030	0,7152	-1,125	0,0948	1,516	0,0207	1,723	0,1172	1,380	0,5413
NM_031514	Jak2	Janus kinase 2	-1,204	0,0004	-1,214	0,0000	1,206	0,0001	1,011	0,0382	1,068	0,0108
NM_001105822	Ccl12	Chemokine (C-C motif) ligand 12	1,251	0,1804	1,347	0,2403	33,129	0,0023	31,450	0,0005	29,141	0,0041
NM_031055	Mmp9	Matrix metalloproteinase 9	-3,804	0,0437	-1,320	0,2762	5,464	0,0000	4,579	0,0003	3,745	0,0011
NM_023981	Csf1	Colony stimulating factor 1 (macrophage)	-1,299	0,0855	-1,495	0,0064	-1,057	0,0043	-1,688	0,0016	-1,419	0,0028
NM_020306	Adam17	ADAM metalloproteinase domain 17	-1,255	0,0524	-1,292	0,0474	-1,347	0,0100	-1,439	0,0015	-1,227	0,0047

Figure. 3

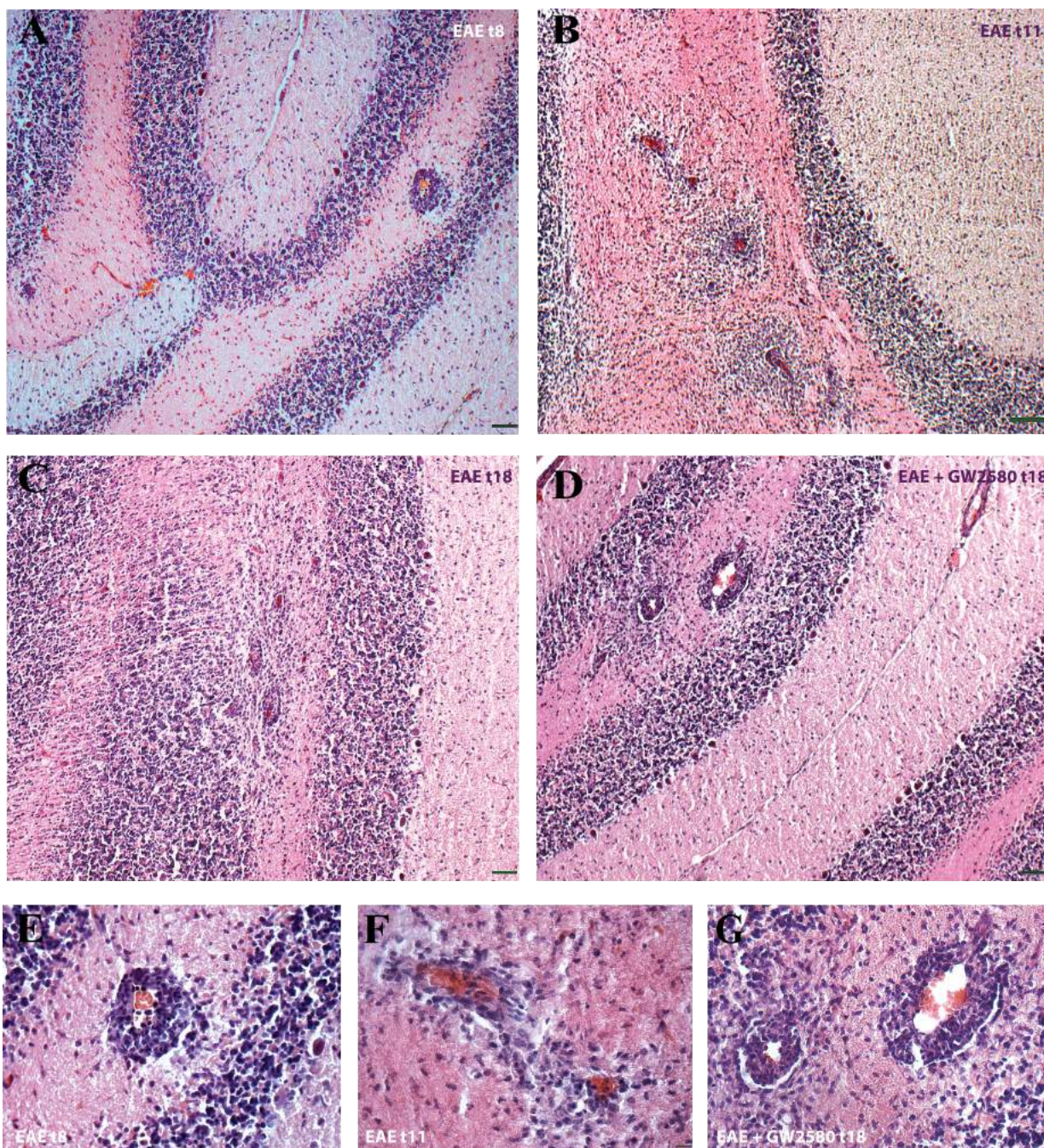


Figure. 4

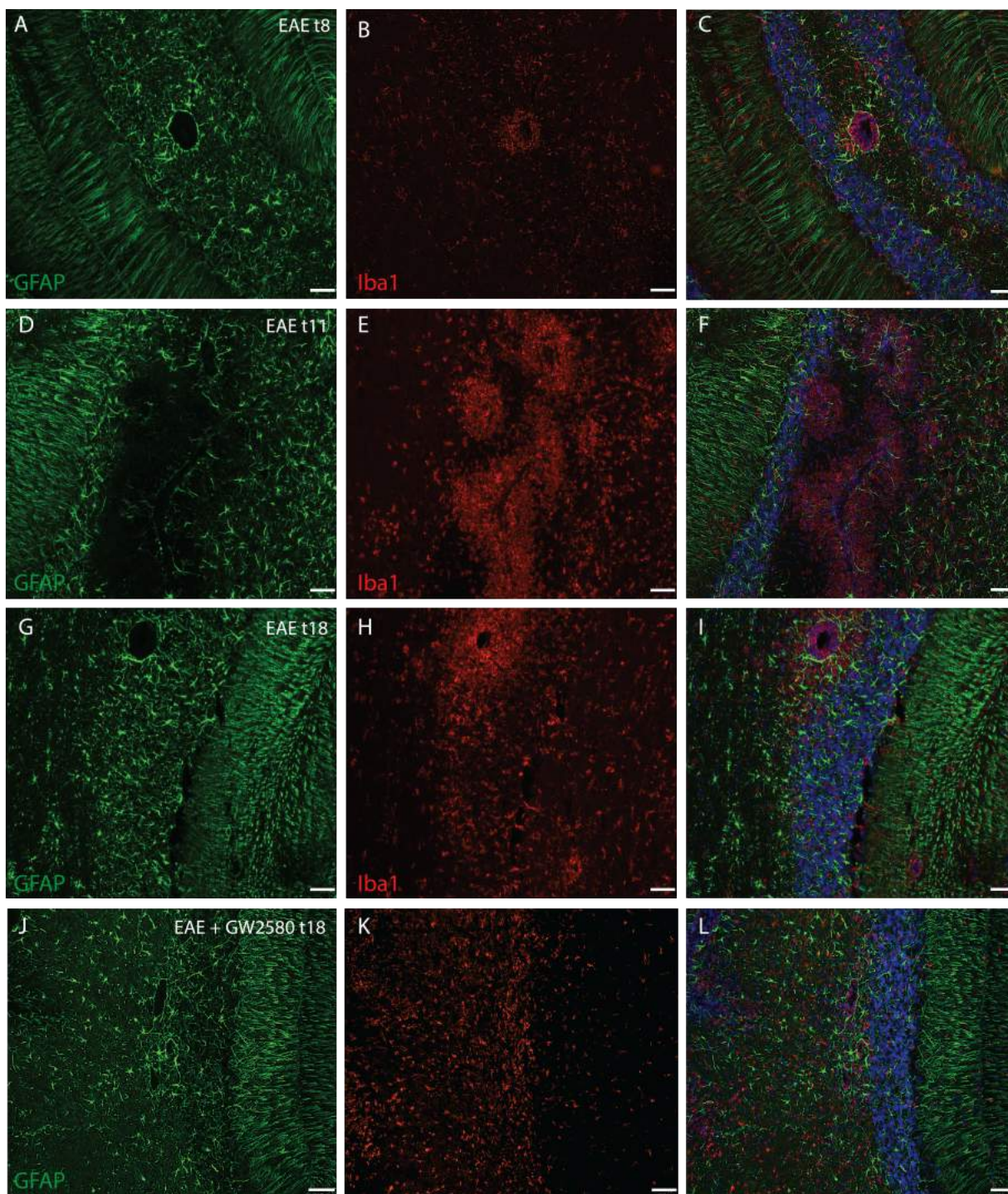


Figure. 5

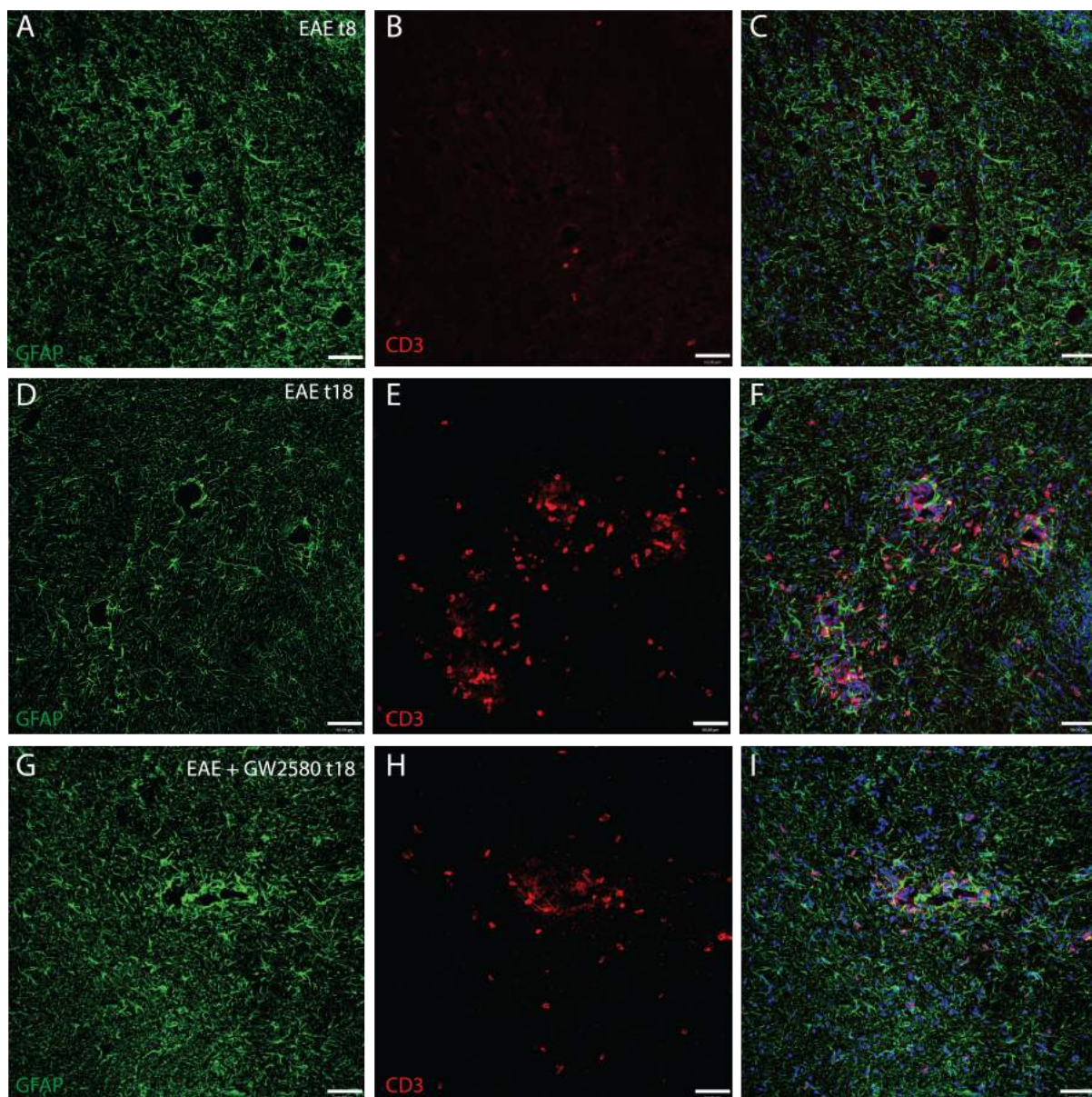


Figure. 6

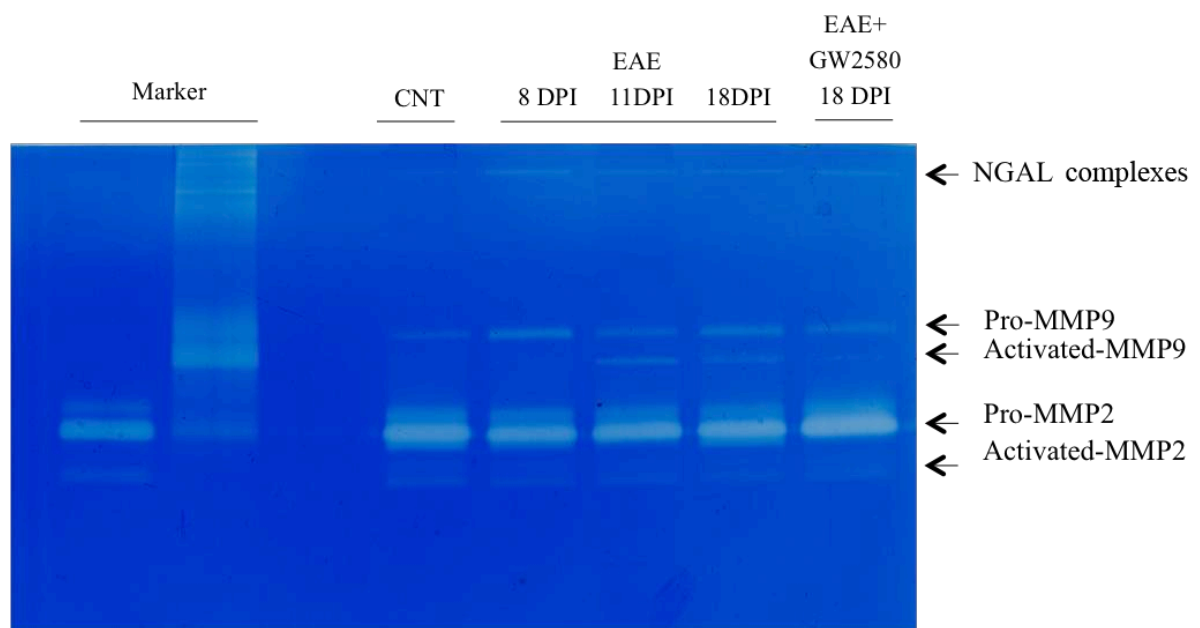


Figure. 7

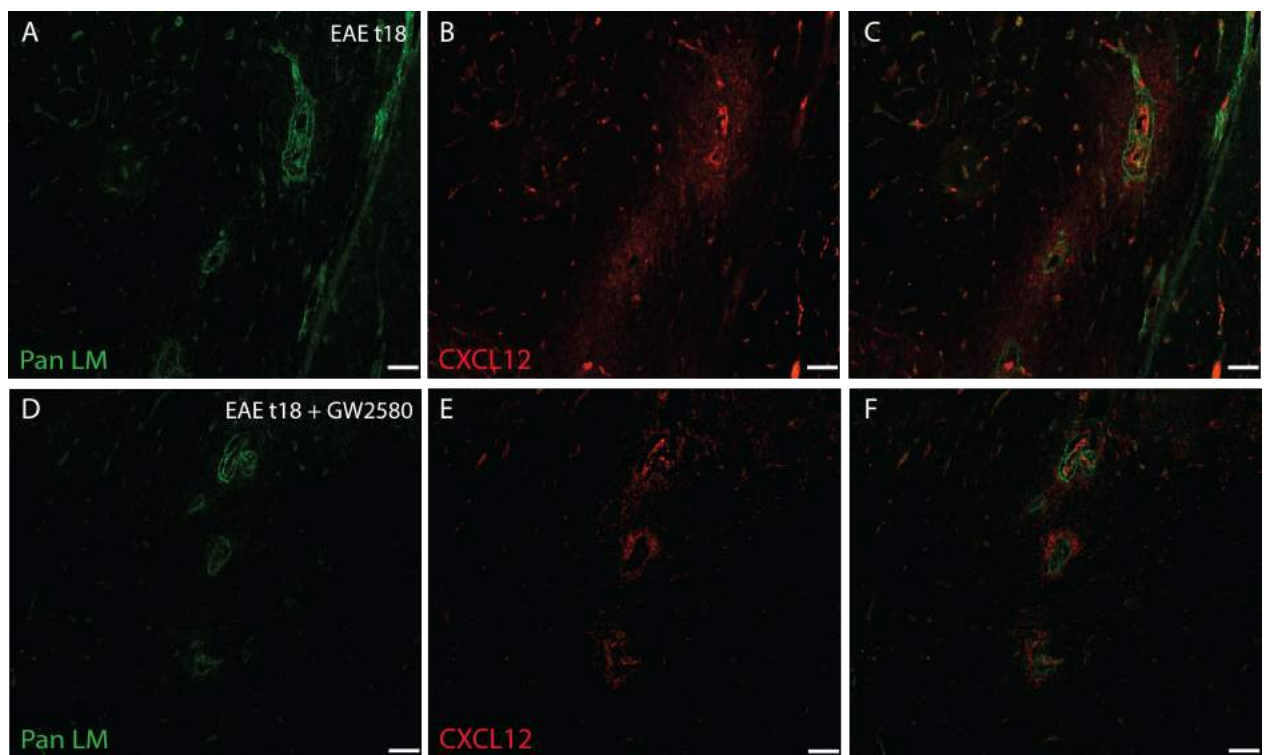


Figure. 8

CHAPTER III

Biomarkers of inflammation during neonatal hypoxia/ischemia and their correlation with the neurological symptoms.

Biomarkers of inflammation during neonatal hypoxia/ischemia and their correlation with the neurological symptoms.

Nozha Borjini^{1,2,3}, Sandra Sivilia³, Alessandro Giuliani^{3,4}, Luciana Giardino^{2,3,4}, Fabrizio Facchinetti¹ and Laura Calzà^{2,3,5}.

¹Research & Development, Chiesi Farmaceutici S.p.A, Via Palermo 26/A, Parma 43100, Italy.

²Health Science and Technologies Interdepartmental Center for Industrial Research (HST-ICIR), University of Bologna, Via Tolara di Sopra 41/E, Bologna, Ozzano Emilia I-40064, Italy.

³IRET Foundation, Via Tolara di Sopra 41/E, Bologna, Ozzano Emilia 40064, Italy.

⁴Department of Veterinary Medical Sciences, University of Bologna, Via Tolara di Sopra 50, Ozzano Emilia (BO) 40064, Italy.

⁵Department of Pharmacy and Biotechnology, University of Bologna, Via Tolara di Sopra 41/E, Bologna, Ozzano Emilia 40064, Italy.

Abstract:

Hypoxia/ischemia causes serious injury to newborns. Clinical imaging is the basic assessment method for neonatal severe injury but it has several limitations. Therefore, searching for reliable biomarkers has become a research hot spot. In this study, both male and female Wistar rats were used; the right carotid artery was permanently doubly occluded and animals were exposed to 8% oxygen for 90 min; control rats received sham surgery. Sensory and cognitive parameters were assessed by the use of open field, rotarod, CatWalk and Morris water maze test. After behavioral testing, plasma and CSF were used to investigate proinflammatory and immunoregulatory biomarkers on the acute (24h and 72h) and chronic phase (4 weeks). Our data suggest that HI induced an early activation of the inflammatory cascade leads to increased production of a large number of proinflammatory mediators that could be the cause of tissue loss of hypoxic hemisphere, which in his turn might leads to short-term- as well as long-lasting behavioral- deficits.

To whom correspondence should be addressed:

Nozha Borjini
Research & Development, Chiesi Farmaceutici S.p.A,
Via Palermo 26/A, Parma 43100, Italy
E-mail: n.borjini@chiesi.com

Introduction

Perinatal brain injury remains an important clinical problem due to resulting neurological disabilities and increased risk of adult-onset neurological disorders (Vannucci and Hagberg, 2004). Neonatal hypoxia-ischemia (HI) is the most frequent cause of neurological morbidity and mortality in infants, often leading to mental retardation, seizures, and cerebral palsy (Bhalala et al., 2015; Hagberg et al., 2015). Several studies have shown that neonatal HI triggers extensive inflammatory reactions in the brain, which includes activation of the innate immune system (Hedtjärn et al., 2004) and experimental studies in neonatal animals have demonstrate that inhibition of pro-inflammatory biomediators is neuroprotective (Doverhag et al., 2010; Hedtjärn et al., 2002; Svedin et al., 2007). Cytokines and chemokines are important inflammatory and immunoregulatory mediators, and cerebral ischemic injury can trigger a cascade of inflammatory mediators induction that acts to orchestrate an in situ inflammatory response (Alsulaimani et al., 2015; Saliba and Henrot, 2001a) and maintains CNS tissue homeostasis (Hopkins, 2003). Overall, the role of cytokines and chemokines are pleiotropic, and whether the general effects are pro- or anti-inflammatory in the context of hypoxic ischemic insults remains controversial even in adult models, for which there are more data than for HI in neonates (Albertsson et al., 2014; Bona et al., 1999; Saliba and Henrot, 2001b).

The susceptibility of the immature central nervous system (CNS) to HI and related inflammation is largely dependent on the temporal and regional course of developmental processes, as well as on the regulation of cerebral blood flow and metabolism (Vexler and Ferriero, 2001). Intrapartum asphyxia is associated with inflammation in the brain and there are increased levels of cytokines and chemokines in the cerebral spinal fluid (CSF) in term infants that have suffered birth asphyxia (Dammann and O'Shea, 2008; Fatemi et al., 2009; Sävman et al., 1998). The course of inflammatory process with respect to neuropathological alterations in HI has been investigated only partly in the neonatal setting (McRae et al., 1995; Sawada et al., 1990).

After neonatal HI onset, there is a time difference in the range of 24 h between metabolism changes, tissue morphological changes and pathological changes in the brain. Possible intervention strategies need to be tailored on the precise stage of the lesion. The clinical diagnosis and severity assessment of neonatal HI mainly rely on the Sarnat score (Robertson and Perlman, 2006), brain CT (computed tomography) scans (Acharya et al.,

2017), MRI (magnetic resonance imaging), ultrasound diagnosis and EEG (electroencephalogram) detection methods (Jan et al., 2017; Lv et al., 2015). Because of the influence of the progressive disease process and other factors, the Sarnat score is subjective, and other tests have certain limitations and effectiveness. Neuroimaging studies have demonstrated that the appearance of CNS damage is delayed compared to the underlying pathology mechanism, taking up to 72 h (Thoresen et al., 2010; Thornton et al., 2012). Therefore, the early monitoring of biomarkers in serum or CSF of neonatal HI is particularly important. Thus, the early clinical detection of blood or CSF biomarkers might allow an earlier diagnosis compared with MRI or CT results. The identification of early noninvasive biomarkers of disease is a vital question, especially during the first period of lifetime, since it could provide valuable, beneficial and advanced diagnostic evidence when clinical and radiological signs are still silent.

An accepted rodent model of neonatal asphyxia is a modification of the Levine model (Levine, 1960) done by Rice et al. (Rice et al., 1981), consisting in the combination of ischemia, achieved by unilateral occlusion of carotid artery, followed by exposure to hypoxia in 7-day-old rats. Indeed in rats, hypoxic seizures could be induced during the critical developmental window, P6–12, which is a period of synaptic maturation and myelination, is thought to match with a human nearby 32–36 weeks of gestation, and corresponds to the age of clinical hypoxia producing neonatal seizure (Jensen et al., 1991; Leonard et al., 2013; Owens et al., 1997; Rakhade et al., 2011). Thus, the most widely used animal model is the unilateral common carotid artery ligation followed by exposure to hypoxia in rats at 7 days old (P7).

Therefore, this study aimed to investigate the mechanisms underlying hypoxic ischemic injury and the following immune response through detection of the levels of inflammatory mediators in plasma and CSF in a rat model of HI, and their correlate with the neurological symptoms. Here we demonstrate that HI in rats leads to short-term as well as long-lasting neurological and behavioral deficits up to four weeks after the injury and extensive brain hemisphere atrophy which could be the consequence of an early activation of the inflammatory cascade leading to increased production of a large number of proinflammatory cytokines and chemokines.

Materials and methods

Animals and experimental groups

A total of 65 Wistar rat pups of both sexes were used in this study. Animals were maintained in an animal room on a 12-h light/12-h dark cycle and at constant temperature ($22 \pm 2^\circ\text{C}$), food and water *ad libitum*. All animal protocols described herein were carried out in accordance with the European Community Council Directives (86/609/EEC), approved by the intramural ethical committee for animal experimentation of Bologna University and comply with the guidelines published in the *NIH Guide for the Care and Use of Laboratory*.

The animals were divided into three experimental groups: A) 24h HI (n=7), 24h sham (n=6); B) 72h HI (n=9), 72h sham (n=6) (both male and female rats were pooled at these time points); C) P44 HI male (n=13), P44 sham male (n=8), P44 HI female (n=6), P44 sham female (n=7).

Inclusion and exclusion criteria

Rat pups from the same litter were served for both HI group and sham and pups with weight less than 12g and higher than 14g were excluded from the experiment.

Neonatal hypoxia-ischemia injury model

The surgery was performed on Wistar rats at postnatal day 7 (P7) under surgical microscope as described previously (Rice et al., 1981) with introduction of some modifications. In brief, the pup was first weighed and then anesthetized with 3% isoflurane. The surgery lasted less than 5 min. After placing the rat on surgical heating pad at 37°C , the skin was cleaned with 10% povidone iodide and a less than 1 cm longitudinal midline incision of the neck was performed to expose the right common carotid artery (CCA). The fibrous sheath that wraps together both the carotid and the vagus nerve was broken and separated in order to avoid an overextension of the nerve. The CCA was permanently doubly ligated with a 5/0 silk suture. After the ligation few drops of surgical glue was used for the suture of the skin. Pups were placed above a heat mat at 37°C until awakening and recovering then were returned to their dam and were allowed to recuperate for 1.5 hours. Pups were then placed in a hypoxic chamber that contains 8% O_2 and 92% N_2 with a constant flow of 3L/min for 90 min, submerged in a water bath maintained at 32°C , which is the usual temperature to which rat pups are exposed when huddling with their mother (Hosono et al., 2010; Mortola and Dotta, 1992).

After hypoxia, all pups were returned again to their dam for recovery. Sham animals underwent the HI surgical procedures (i.e. exposure of the CCA) without artery ligation and without exposure to hypoxic conditions.

Short-term neurofunctional outcome following cerebral HI

The examination of neurobehavioral development were performed for all rat pups from P8 to the P21 after the hypoxic ischemia insult, and were carried out daily between 10 and 12 a.m. Body weights of rat pups were recorded daily. Pups were tested for the following neurological reflexes, (1) *Righting reflex*: this test is believed to be a reflection of subcortical maturation estimate, the generation of these movements from circuits in the spine connected to the supplementary motor area, the basal ganglia, and the reticular formation. the time (sec) used by the animal to go from a supine to a prone position by placing all four paws on the surface was recorded. (2) *Negative geotaxis*: this test examines the sensorimotor function of neonatal rats (Rumajogee et al., 2016). Rat pups were placed upside down in the middle of a slope (45°) of 30 cm. The latency to turned 180 degree to an upward direction was recorded. From the day when the animal turns to go up, the time (sec) it took to reach the upper side of the plane was recorded. The maximum duration of recording was 30 seconds otherwise the test was considered negative. (3) *Sensory reflex*: the ear and the eyelid of the pup were touched with a cotton swab and the first day of the ear twitch reflex and the contraction of the eyelid was recorded. (4) *Auditory startle*: the first day of the startle response to a clapping sound was observed. (5) *Crossed extensor reflex*: the left hind paw was pinched and the possible extension of the right paw was recorded. (6) *Limb placing*: the back of the forepaw and hindpaw was touched with the edge of the bench while the animal suspended, and the first day of lifting and placing the paws on the table was noted. (7) *Limb grasp*: the forelimbs were touched with a thin rod, and the first day of grasping onto the rod was recorded. (8) *Gait*: the animals are placed at the center of a white plexiglass circle ($\varnothing = 13\text{cm}$). Register the day when they start to move out of the circle with both front paws, estimate the time (sec) that the animal uses to exit out of the circle. In the case in which the animal does not leave the circle within 30 seconds, the test is considered negative. In order to assess the developpement of neurological reflex, rats are given a score the to the corresponding time (sec). The higher score indicates greater capacity for development of neurological reflexes.

Long-term neurofunctional outcome after HI insult

The assessment of long-term neurofunctional handicap was performed in sham and HI groups three weeks after the insult (P28). These tasks consisted of the open field, Rota-rod, Catwalk and Morris water maze.

Open field

Animals were observed for locomotor behavior in an open-field. Pups were placed in an open-field consisting of a 46x46 cm wooden chamber with 21 cm high walls around, with a dark gray floor divided into 16 fields. Rats were placed individually in the center, always facing the same direction, in the center of the chamber and the latency to leave this first square will be recorded. The following parameters were measured using EthoVision tracking software (Noldus Information Technology, Inc.): distance travelled, rearing, grooming and ambulation frequency. Speed was calculated from the ambulatory time and the total travelled distance. Animals were video-recorded for 10 min (Balduini et al., 2000a).

Rota-rod

The rotarod test (LE 8500 RotaRod : 2Biological Instruments, Varese, Italy) consist on two days test. Animals were exposed to one habituation session during 3 min in the apparatus on slow velocity (20 rpm). In the test session, 24 h later, animal's motor ability was evaluated. The rotarod test was performed by placing rats on rotating drums and measuring the time each animal was to maintain its balance on the rod. The speed of the rotarod accelerated from 16 to 40 rpm over a 6 min period. Variables recorded were: latency of the first downfall, number of falls (maximum 3) and time of permanence in the apparatus (Rojas et al., 2013; Takao et al., 2010).

Catwalk

Cerebellar function was analysed by CatWalk (Noldus Information Technology, Wageningen, The Netherlands), a quantitative gait analysis system. Each rat ran across a glass walkway transversely and three complete runs were recorded using a camera positioned below, and the average will be calculated. If an animal failed to complete a run within 5 s, walked backwards or reared during the run, the process was repeated. The experiment was performed in the dark; the glass walkway was illuminated with beams of

light, thereby allowing the animals' paws to reflect light as they touched the glass floor. Each paw was labeled on the recorded video in order to calculate paw-related parameters. The gait-related parameters measured using the CatWalk system was the following: *maximum contact area*: the maximum area of a paw that comes into contact with the glass plate, *stand*: stance phase is the duration in seconds of contact of a paw with the glass plate and swing speed: is the speed (Distance Unit/second) of the paw during Swing. The formula of *Swing Speed* is: $\text{Swing Speed} = \frac{\text{Distance Unit}}{\text{Swing (s) Phase}}$ which is the duration in seconds of no contact of a paw with the glass plate. The Stride Length which is the distance (in Distance Units) between successive placements of the same paw, the calculation of Stride Length is based on the X-coordinates of the center of the paw print of two consecutive placements of the same paw during Max contact and taking into account Pythagoras' theorem (Hattori et al., 2015).

Morris Water Maze

Three weeks after HI lesion, the spatial memory performance was evaluated using an MWM (180 cm diameter, 45 cm high) conceptually divided in four equal imaginary quadrants. The water of the pool was made opaque by using non-toxic grey tempera paint. Training on spatial version of the MWM was carried out over 4 consecutive days. Each day, rats received four training trials in which a randomly starting point was used, such that 2 successive trials never began from the same position. The training consisted of a swim followed by a 30 seconds platform sit. The escape latency to find the platform was measured for individual animals on each day. The experimenter guided rats that did not find the platform within 120 seconds to it. To assess long-term memory, 24 hours after the final trial, the platform was removed from the maze and a 2-minute free swim will be conducted, and time (seconds) spend during the first 20 seconds and the entire swim in the quadrant formerly occupied by the platform will be recorded (Chou et al., 2001).

CSF and plasma biomarker analysis

The method of CSF sampling was adapted from the method of Liu, L. and Duff, K and Rodríguez-Fanjul (Liu and Duff, 2008; Rodríguez-Fanjul et al., 2015). Briefly, the rat pup was anesthetized by isoflurane inhalation (isoflurane 4%) (Gas Anesthesia System-21100, Ugo Basile, Varese, Italy) and fixed by one investigator with the head positioned at 90° angle. A sagittal incision of the skin was made below the occiput, and the subcutaneous tissue and neck muscles through the midline were separated and held apart

using a microretractor. The dura mater of the cisterna magna was then penetrated by an 8-cm long glass capillary, which had a narrowed tip with an inner diameter of about 0.3 mm so that the CSF flowed into the capillary. After collection, each sample was centrifuged at 2000×g for 10 min at 4 °C, and the supernatant aliquoted and stored at –80 °C for biochemical assays.

Blood was collected from the abdominal aorta in EDTA-K2 Vacutainer tubes and centrifuged at 3000×g for 10 min at 4 °C, and the plasma was collected, aliquoted, and stored at –80 °C until used.

Proteins known to play key roles in neuroinflammation pathways were selected. For this purpose, Bio-Plex Pro™ Rat Cytokine 24-plex Assay (Bio-Rad; Milano, Italy) was used. The kit included EPO, G-CSF (CSF3), GM-CSF (CSF2), GRO/KC, IFN- γ , IL-1 α , IL-1 β , IL-2, IL-4, IL-5, IL-6, IL-7, IL-10, IL-12p70, IL-13, IL-17A, IL-18, M-CSF (CSF1), MCP-1 (CCL2), MIP-1 α (CCL3), MIP-3 α (CCL20), RANTES (CCL5), TNF- α , and VEGF.

The simultaneous quantification of the different proteins in CSF and plasma was performed using xMAP technology and a MAGPIX Luminex platform. This technology makes use of different populations of color-coded beads of monoclonal antibodies specific to a particular protein, thus allowing simultaneous capture and detection of specific analytes from a sample. All the beads from each set are read off, which further validates the results. Using this process, xMAP Technology allows multiplexing of up to 50 unique bioassays within a single sample, both rapidly and precisely (Blankestijn and Altara, 2014; Houser, 2012). In brief, after the incubation of a specific monoclonal antibody conjugated bead population with 50 μ l of CSF/plasma samples for 1 h at RT, washed beads were incubated with detection antibody solution at RT for 30 min, then with the streptavidin–phycoerythrin conjugated solution (RT, 10 min). After washing, beads were resuspended in the assay buffer, shaken for 1 min and then a reading performed on the MAGPIX instrument. The results were analyzed with xPONENT 4.2 ® software and expressed as pg/ml.

Statistics

Results in appearance of physical and neurological reflexes as well as body weights were compared with Student's *t*-test. Statistical differences between groups for each outcome

measured were analyzed using one-way ANOVA or Two-way ANOVA followed by Tukey post-hoc. All the data were expressed as mean \pm SD and significance was set at $P \leq 0.05$. All statistical analyses were performed using GraphPad Prism 7.0 (GraphPad Software).

Results

Three rats died during different steps of the experiment (4.6%). Animals were weighed every day of life, and all along the experiment there were no significant differences in body weight neither between sham and HI groups nor between HI males and females (Figure 1A). HI induced brain edema in the acute phase 24 and 72h after unilateral ligation of the right carotid artery and hypoxia for 90 min in neonatal rat and tissue loss in the chronic phase, i.e. after 4 weeks (Figure 1B). At the end of the experiment, when sacrificed, we found different degrees of brain damage in adult HI animals, an extensive damage to the cerebral cortex, hippocampus and striatum ipsilateral to the ligated carotid.

Neurological reflexes

As it is shown in Table 1, right eye opening was delayed in hypoxic–ischemic animals ($P < 0.0001$). In addition, several neurological reflexes, such as negative geotaxis, ear twitch reflex, auditory startle, hindlimb grasp and gait reflex ($P = 0.0042$; $P = 0.0025$, $P = 0.0032$; $P = 0.0127$; $P = 0.0008$ respectively) appeared significantly later compared to normal pups. Hypoxic–ischemic injury caused not only delay in the appearance of some reflexes but animals performed certain tasks in significantly longer times.

Open-field activity

The Open Field test was performed as a measure of exploratory locomotion in a novel environment. There was no significant difference between HI and sham rats concerning the number of crossing, general activity and movement pattern (Figure 2A). HI males more than females rats spent more time in the center ($P = 0.0005$; $P = 0.0007$ respectively) of the open field and less time at walls and in corners than sham rats (Figure 2B,C). There was no significant difference in the time spent with grooming activity or in the number of fecal boluses at any time-point between the different groups (data not shown) while a significant difference was observed in HI male and female rats in the number of rearing all along the test duration comparing to sham animals ($P < 0.0001$; $P < 0.0001$

respectively) as it is shown in Figure 2D. Among HI rats, there was a significant difference between genders ($P=0.0052$).

Rota-Rod performance

Rota-Rod test was performed for sensory-motor coordination. During the habituation session HI (Figure 3A), rats were not able to stay on the rod comparing to sham when the rod was rotated at a steady-rate of 20 rotations per minute ($P<0.0001$; $P<0.0001$ HI female vs sham female and HI male vs sham male respectively). During the test session (Figure 3B), 24h later, HI female and male rats held on the Rota-rod for a significantly shorter time comparing to sham ($P<0.0001$, $P<0.0001$). Among HI rats, there were no significant differences between genders.

MWM performance

In order to determine the effect of HI injury on cognitive capacities, 30 days old rats were trained in the spatial version of the MWM. Two-way ANOVA test revealed significant differences in the escape latency of the second between the experimental groups ($P<0.0001$, $P<0.0001$ HI female vs sham female and HI male vs sham male respectively) during the training period (Figure 4A). As shown in Figure 4B, the cumulative distance to platform to forth days and even on the test day, was shorter in sham-operated rats when compared with the HI groups, indicating that HI impaired memory performance in the injured animals and among HI rats, no significant differences between genders was detected.

CatWalk performance

The CatWalk assessment of gait analysis post HI in rat demonstrate long-term deficit in behavioral parameters related to the hindpaw. Parameters detected by CatWalk (maximum contact area, stand and swing speed of the 4 limbs) in ischemic rats subjected to 90 minutes of hypoxia are presented in Figure 5. Additional post Tukey analysis showed that HI animals have significant impairment in the maximum contact area of their right fore (RF), right hind (RH), left fore (LF) and especially the left hind (LH) paws in comparing to sham rats (Figure 5A), ($P<0.05$ or $P<0.01$ or $P<0.001$ or $P<0.0001$). Figure 5B indicate that the duration in seconds of contact of a paw with the glass plate of HI rats comparing with sham, showed an increase in stand duration ($P<0.05$ or $P<0.01$ or $P<0.001$). In HI animals the swing speed (Figure 5C) of their 4 limbs were all decreased

compared to those of the rats in the sham group ($P<0.05$ or $P<0.01$). Overall, HI induced sensorimotor function deficits in HI rats and HI males were worse than HI females.

Inflammation biomarkers at plasma and CSF levels

Twenty-four cytokines and chemokines were simultaneously quantified in plasma and CSF samples at the different time points investigated, in the acute phase 24 and 72h and in the chronic phase 4 weeks. Those cytokines and chemokines are EPO, G-CSF (CSF3), GM-CSF (CSF2), GRO/KC, IFN- γ , IL-1 α , IL-1 β , IL-2, IL-4, IL-5, IL-6, IL-7, IL-10, IL-12p70, IL-13, IL-17A, IL-18, M-CSF (CSF1), MCP-1 (CCL2), MIP-1 α (CCL3), MIP-3 α (CCL20), RANTES (CCL5), TNF- α and VEGF.

Several pro-inflammatory biomarkers such as CCL3, CCL2 and IL-6 ($P=0.0412$; $P=0.0127$; $P=0.004$, respectively) in plasma (Figure 6A, C, F) and TNF- α , CCL2 ($P=0.0412$; $P<0.0001$, respectively) in CSF (Figure 7G, B) were significantly regulated as soon as 24h after HI while the major part of the biomarkers investigated were regulated after 72h after HI such as CSF1, IFN- γ , CCL5 ($P=0.0483$; $P=0.0193$; ns, respectively) in plasma (Figure 6A, C, F) and CCL5, CSF1, VEGF, IL-17A ($P<0.0001$; $P=0.0003$; $P=0.0024$, $P<0.0001$ respectively) in CSF (Figure 7A, C, E, H).

During the chronic phase, 4 weeks after the injury, in plasma only TNF- α and IFN- γ ($P<0.0001$; $P=0.0047$, respectively) were significantly up-regulated at this time point in male HI comparing to sham male (Figure 6D,E) and only TNF- α ($P=0.0009$) was significantly increased on female HI comparing to female sham group (Figure 6D). In CSF only CCL5 and TNF- α ($P=0.0164$; $P=0.0012$, respectively) were significantly up-regulated at this time point in male HI comparing to sham male (Figure 7A,G) and only TNF- α ($P=0.0164$) was significantly increased on female HI comparing to female sham group (Figure 7G). The rest of measurable biomarkers of the panel, at the chronic phase in plasma and CSF HI rats, showed no significant change nor between HI and sham males neither between HI and sham females. Among HI rats, there were no significant differences between genders (Figure 6 and 7).

The biomarkers G-CSF (CSF3), GM-CSF (CSF2), IL-1 α , IL-7, IL-10 and IL-12p70 were not detected at any of the time points analyzed in the CSF in our experimental conditions. No significant changes were observed for rest of the panel compared to sham group.

Discussion

The main goal of the present study was to investigate plasma and CSF biomarkers after acute and chronic HI, performed at P7 on Wistar rats, and their correlation with neurological and behavioral parameters. We have shown that atrophy and tissue loss of hypoxic hemisphere in HI rats leads to short-term, retarded neurobehavioral development as shown by delayed appearance and worse performance of some neurological reflexes, as well as long-lasting behavioral deficits as shown by retarded development of motor coordination, thus confirming and extending previous studies reporting that hypoxic–ischemic animals display short and long-term learning deficits (Arteni et al., 2003; Balduini et al., 2000a; Jansen and Low, 1996; Lubics et al., 2005). We also showed some important differences between male and female rats.

In contrast to what was reported previously that HI animals have significantly lower daily weights and pups needed artificial feeding due to their severe body weight loss (Ten et al., 2003; Wagner et al., 2002), in our HI rat model we didn't observe any significant difference in the somatic development. Our results show that HI animals perform worse in negative geotaxis, ear twitch, auditory startle, hindlimb grasp and gait test as measured by the reflex times, those reflexes were largely independent of gender. Several groups reported that hypoxic–ischemic injury in rodent models affects the short-term outcome of righting, geotaxis reflexes as measured 1 and 24 h after the injury (Lubics et al., 2005; Rakhade et al., 2011; Ten et al., 2003). According to our observations, neurological reflexes are affected also later in age in rats, in the chronic phase after four weeks post injury.

In order to assess the long-term neurofunctional following neonatal HI, several tests have been described such as rotarod, open field, CatWalk and Morris water maze. However, results are contradicted from study to other. One of the most frequently used test is rotarod test, which has been described as a useful tool to measure reduced motor coordination and learning ability after HI insults. Our results show significant differences between sham and hypoxic animals in the rotarod test for motor coordination, while no significant difference between genders was observed. Several studies reported that rotarod test was sensitive to the insult in neonatal HI rats and a significant difference was observed between HI and sham group (Tata et al., 2015). However, some authors do not confirm these results (Lee et al., 2010; Lubics et al., 2005).

Concerning the locomotor behavior in an open-field, both hyper- and hypoactivity have been described following HI insults. In accordance with other reports (Balduini et al., 2000b; Lubics et al., 2005; Patel et al., 2015), we didn't see any significant difference concerning the number of crossing, general activity and movement pattern in the time spent with grooming activity or in the number of fecal boluses at any time-point between the different groups, while a significant difference was observed in HI male and female rats in the number of rearing all along the test duration comparing to sham animals. In contrast, Antier et al. (Antier et al., 1998) found hypoactivity in adult rats who underwent neonatal HI. Our observations show that HI rats spent more time in the center and less time at walls and in corners than sham rats, and this alteration is more pronounced in male than females rats. Notably, this is exactly the opposite of the natural reflex of the pups, who quickly find the wall where they feel more safe. This may be explained by the age of the rats, since the test was performed after 4 weeks after HI insult (adolescent age).

In order to determine the effect of HI insult on cognitive capacities and spatial memory performance, MWM was used, a well-established and widely accepted tool of testing these parameters. The escape latency to reach the platform, a revealing parameter of working memory that is tested during the training phase, was significantly longer in HI group compared to sham in the first four days of MWM task. Moreover, the cumulative distance to platform measured as reference memory components and recorded on the probe phase (5th day) of the task, was significantly reduced in sham-operated rats when compared with the HI groups. Our data clearly indicates that HI injury impaired learning and memory performance in the injured animals. In harmony with our finding, results from De Paula et al. and Goren et al. have shown that the MWM test was sensitive to brain damage in neonatal HI rats (Goren et al., 2017; de Paula et al., 2009), although contrasting data have been also reported (Tian et al., 2013).

The CatWalk assessment of sensorimotor function post HI in our rat model demonstrate long-term deficit in gait parameters related to the hindpaw. Indeed, the CatWalk can show detailed impairment of each individual paw and overall gait pattern. Our results show that HI animals have significant impairment in the maximum contact area of their 4 limbs and especially the left hind paws in comparing to sham rats. In addition, our results show that the duration in seconds of contact of a paw with the glass plate of HI rats comparing with

sham, showed an increase in stand duration and the swing speed of the 4 limbs were all decreased compared to those of the sham group.

Overall, we have demonstrated HI males were worse than HI females and hypoxia ischemia insult do induce sensorimotor function deficits in HI rats in some parameters while in some others we observe a slight recovery and no significant difference between HI and sham group. This could be explained by the fact of the high neuronal plasticity of the neonatal brain, and it is possible that the control of motor coordination has shifted from a brain structure damaged by ischemia to an unharmed structure (Balduini et al., 2000a; Barth and Stanfield, 1990; Goren et al., 2017).

Several studies have shown that neonatal HI triggers widespread inflammatory reactions in the brain including activation of the innate immune system (Alsulaimani et al., 2015; Hedtj rn et al., 2004; Moyer, 2012). Our results demonstrate that an early regulation of most of the inflammatory biomarkers was observed as soon as 24 and 72h, during the acute phase, while at the chronic phase in plasma and CSF HI rats, no significant change nor between HI and sham males neither between HI and sham females was observed. Some pro-inflammatory biomarkers such as CCL3, CCL2 and IL-6 in plasma and CSF regulated as soon as 24h after HI while the major part of the biomarkers investigated were regulated after 72h after HI such as CSF1, IFN- γ , CCL5. It has been shown by other that in term neonates, the magnitude of IL-6 CSF levels after perinatal asphyxia is related to the severity of early neonatal HI and late neurological outcome (Drews et al., 1995; Lusyati et al., 2013; Mart n-Ancel et al., 1997; Moyer, 2012; Saliba and Henrot, 2001b; Shahkar et al., 2011). In our model we do observe an upregulation of IL-6 at 24 and 72h in plasma and CSF and this could explain the short-term as well as long-lasting behavioral deficits observed in HI rats. Both CCL2 and CCL3 are necessary for recruiting monocyte to the injury site, where they play an important role in CNS plasticity and repair (Biber and Boddeke, 2014; Dimitrijevic et al., 2007). It was recently described that CCL2 and its receptor CCR2 regulates macrophage trafficking by induction of leukocyte adhesion to the microvascular endothelium after brain injury (Schilling et al., 2009). In our model, 24h after HI insult, we observed a decrease in the level of CCL2 and CCL3 in plasma after 24h after HI insult and in the meanwhile were both upregulated in CSF. This could be explained by early quick response of the neonate brain to the insult, leading to a cell recruitment to the injury site. Schilling et al. have demonstrated that CCL2-CCR2

axis differentially regulates hematogenous cell recruitment and sequential inhibition of selective CCL2 dependent pathways by CCR2 blockade may be an effective treatment to ameliorate tissue damage (Schilling et al., 2009).

It has been demonstrated previously, that TNF- α is mainly secreted by activated macrophages and its overexpression is toxic to cells (Li et al., 2014). TNF- α plays critical role in HI induced neutrophil infiltration and tissue damage. It can also increase permeability of endotheliocyte and activate matrix metalloproteinases, which damage the blood brain barrier leading to swelling and degeneration of neurons and glial cells (Liu and McCullough, 2013; Szaflarski et al., 1995). Kaur et al. have demonstrated that the unmyelinated axons showed an upregulated expression of TNF-R₁ coupled with the disruption of myelin basic protein immunopositive processes of oligodendrocytes in the periventricular white matter of HI neonatal rats suggesting that overproduction of TNF- α may damage axons and delay their myelination (Deng et al., 2010; Kaur et al., 2013). Our results show that, TNF- α was upregulated in CSF as soon as 24h after HI till the end of the experiment and in plasma it was regulated during the chronic phase, which may explain the tissue loss that was observed at the sacrifice time.

We have previously suggested that the overexpression of CSF1 (macrophage colony stimulating factor) in CSF aggravate the inflammatory process in experimental allergic encephalomyelitis (EAE), a rat model for multiple sclerosis, by propagating the proinflammatory signals to the nearby resting microglia and astrocytes through increased production of proinflammatory cytokines (Borjini et al., 2016). Those finding was also investigated on HI rodent model and recent results suggest that amoeboid microglial cells-derived CSF1 promotes astrocytes to generate proinflammatory cytokines, which may be involved in axonal damage following HI insult (Denes et al., 2007; Deng et al., 2010; Escamilla et al., 2015; Kaur et al., 2013; Sanchez-Niño et al., 2016). In this study we show that CSF1 was significantly regulated on the acute phase after HI insult, at 72h, in plasma and in CSF. According to our results, it could thus be speculated that CSF1 signaling plays an important role in the early phase of HI, by triggering microglial activation, subsequent induction of neuroinflammation and axonal damage and this could leads to short-term as well as long-lasting behavioral deficits after the injury.

While either sex of rats has been used for modeling hypoxia seizures, male rats are preferred in most studies to avoid potential bias due to gender difference. Female rats

show different developmental GABA profile during the critical period (Galanopoulou, 2008) and therefore responses differently to hypoxia-induced neonatal seizures. However, overall in our model we didn't observe that much gender difference that should suggest a discrimination of one gender.

In conclusion, in the HI used in this study we have shown an early activation of the inflammatory cascade leads to increased production of a large number of proinflammatory cytokines and chemokines. This could lead to the tissue loss observed in the hypoxic hemisphere, which in his turn may leads to short-term neurological- as well as long-lasting behavioral- deficits in particular in motor coordination. Their significance as early biomarkers is greater than the one of the chronic phase, since cytokines and chemokines production precedes and induces the brain damage. The different mechanisms appear to be interlinked and culminate in heightened inflammation. An understanding of these mechanisms would let the earlier characterization of the degree of the brain damage, initiation of intervention procedures to improve neonatal survival and reduce the degree of the injury.

References

- Acharya, J., Rajamohan, A.G., Skalski, M.R., Law, M., and Gibbs, W. (2017). CT Angiography of the Head in Extracorporeal Membrane Oxygenation. *Am. J. Neuroradiol.*
- Albertsson, A.-M., Bi, D., Duan, L., Zhang, X., Leavenworth, J.W., Qiao, L., Zhu, C., Cardell, S., Cantor, H., Hagberg, H., et al. (2014). The immune response after hypoxia-ischemia in a mouse model of preterm brain injury. *J. Neuroinflammation* 11.
- Alsulaimani, A.A., Abuelsaad, A.S., and Mohamed, N.M. (2015). Inflammatory Cytokines in Neonatal Hypoxic Ischemic Encephalopathy and their Correlation with Brain Marker S100 Protein: A Case Control Study in Saudi Arabia. *J. Clin. Cell. Immunol.* 6, 1–8.
- Antier, D., Zhang, B.-L., Mailliet, F., Akoka, S., Pourcelot, L., and Sannajust, F. (1998). Effects of neonatal focal cerebral hypoxia-ischemia on sleep-waking pattern, ECoG power spectra and locomotor activity in the adult rat. *Brain Res.* 807, 29–37.
- Arteni, N.S., Salgueiro, J., Torres, I., Achaval, M., and Netto, C.A. (2003). Neonatal cerebral hypoxia-ischemia causes lateralized memory impairments in the adult rat. *Brain Res.* 973, 171–178.
- Balduini, W., De Angelis, V., Mazzoni, E., and Cimino, M. (2000a). Long-lasting behavioral alterations following a hypoxic/ischemic brain injury in neonatal rats. *Brain Res.* 859, 318–325.
- Balduini, W., De Angelis, V., Mazzoni, E., and Cimino, M. (2000b). Long-lasting behavioral alterations following a hypoxic/ischemic brain injury in neonatal rats. *Brain Res.* 859, 318–325.
- Barth, T.M., and Stanfield, B.B. (1990). The recovery of forelimb-placing behavior in rats with neonatal unilateral cortical damage involves the remaining hemisphere. *J. Neurosci.* 10, 3449–3459.
- Bhalala, U.S., Koehler, R.C., and Kannan, S. (2015). Neuroinflammation and Neuroimmune Dysregulation after Acute Hypoxic-Ischemic Injury of Developing Brain. *Front. Pediatr.* 2.
- Biber, K., and Boddeke, E. (2014). Neuronal CC chemokines: the distinct roles of CCL21 and CCL2 in neuropathic pain. *Front. Cell. Neurosci.* 8.
- Blankesteyn, M., and Altara, R. (2014). *Inflammation in Heart Failure* (Academic Press).
- Bona, E., Andersson, A.-L., Blomgren, K., Gilland, E., Puka-Sundvall, M., Gustafson, K., and Hagberg, H. (1999). Chemokine and Inflammatory Cell Response to Hypoxia-Ischemia in Immature Rats. *Pediatr. Res.* 45, 500–509.
- Borjini, N., Fernández, M., Giardino, L., and Calzà, L. (2016). Cytokine and chemokine alterations in tissue, CSF, and plasma in early presymptomatic phase of experimental

allergic encephalomyelitis (EAE), in a rat model of multiple sclerosis. *J. Neuroinflammation* 13, 291.

Chou, I.-C., Trakht, T., Signori, C., Smith, J., Felt, B.T., Vazquez, D.M., and Barks, J.D.E. (2001). Behavioral/Environmental Intervention Improves Learning After Cerebral Hypoxia-Ischemia in Rats. *Stroke* 32, 2192–2197.

Dammann, O., and O'Shea, T.M. (2008). Cytokines and perinatal brain damage. *Clin. Perinatol.* 35, 643–663, v.

Denes, A., Vidyasagar, R., Feng, J., Narvainen, J., McColl, B.W., Kauppinen, R.A., and Allan, S.M. (2007). Proliferating resident microglia after focal cerebral ischaemia in mice. *J. Cereb. Blood Flow Metab. Off. J. Int. Soc. Cereb. Blood Flow Metab.* 27, 1941–1953.

Deng, Y.Y., Lu, J., Ling, E.-A., and Kaur, C. (2010). Microglia-derived macrophage colony stimulating factor promotes generation of proinflammatory cytokines by astrocytes in the periventricular white matter in the hypoxic neonatal brain. *Brain Pathol. Zurich Switz.* 20, 909–925.

Dimitrijevic, O.B., Stamatovic, S.M., Keep, R.F., and Andjelkovic, A.V. (2007). Absence of the Chemokine Receptor CCR2 Protects Against Cerebral Ischemia/Reperfusion Injury in Mice. *Stroke* 38, 1345–1353.

Doverhag, C., Hedtj rn, M., Poirier, F., Mallard, C., Hagberg, H., Karlsson, A., and S vman, K. (2010). Galectin-3 contributes to neonatal hypoxic-ischemic brain injury. *Neurobiol. Dis.* 38, 36–46.

Drews, K., Szczapa, J.,  zak, J., Andrzejewska, R.,  zak, L., and Mackiewicz, A. (1995). Blood Serum Concentration of C-Reactive Protein and Interleukin-6 in Diagnosis of Neonatal Infections. *Ann. N. Y. Acad. Sci.* 762, 398–399.

Escamilla, J., Schokrpur, S., Liu, C., Priceman, S.J., Moughon, D., Jiang, Z., Pouliot, F., Magyar, C., Sung, J.L., Xu, J., et al. (2015). CSF1 receptor targeting in prostate cancer reverses macrophage-mediated resistance to androgen blockade therapy. *Cancer Res.* 75, 950–962.

Fatemi, A., Wilson, M.A., and Johnston, M.V. (2009). Hypoxic-ischemic encephalopathy in the term infant. *Clin. Perinatol.* 36, 835–858, vii.

Galanopoulou, A.S. (2008). Dissociated Gender-Specific Effects of Recurrent Seizures on GABA Signaling in CA1 Pyramidal Neurons: Role of GABAA Receptors. *J. Neurosci.* 28, 1557–1567.

Goren, B., Cakir, A., Ocalan, B., Serter Kocoglu, S., Alkan, T., Cansev, M., and Kahveci, N. (2017). Long-term cognitive effects of uridine treatment in a neonatal rat model of hypoxic-ischemic encephalopathy. *Brain Res.* 1659, 81–87.

- Hagberg, H., Mallard, C., Ferriero, D.M., Vannucci, S.J., Levison, S.W., Vexler, Z.S., and Gressens, P. (2015). The role of inflammation in perinatal brain injury. *Nat. Rev. Neurol.* *11*, 192–208.
- Hattori, T., Sato, Y., Kondo, T., Ichinohashi, Y., Sugiyama, Y., Yamamoto, M., Kotani, T., Hirata, H., Hirakawa, A., Suzuki, S., et al. (2015). Administration of Umbilical Cord Blood Cells Transiently Decreased Hypoxic-Ischemic Brain Injury in Neonatal Rats. *Dev. Neurosci.* *37*, 95–104.
- Hedtj rn, M., Leverin, A.-L., Eriksson, K., Blomgren, K., Mallard, C., and Hagberg, H. (2002). Interleukin-18 involvement in hypoxic-ischemic brain injury. *J. Neurosci. Off. J. Soc. Neurosci.* *22*, 5910–5919.
- Hedtj rn, M., Mallard, C., and Hagberg, H. (2004). Inflammatory gene profiling in the developing mouse brain after hypoxia-ischemia. *J. Cereb. Blood Flow Metab. Off. J. Int. Soc. Cereb. Blood Flow Metab.* *24*, 1333–1351.
- Hopkins, S.J. (2003). The pathophysiological role of cytokines. *Leg. Med. Tokyo Jpn.* *5 Suppl 1*, S45-57.
- Hosono, T., Kamo, A., Hakotani, S., Minato, K., Akeno, H., Taguchi, Y., Miyano, A., and Iseki, T. (2010). Effect of hypothermia on motor function of adult rats after neonatal hyperthermic hypoxic–ischemic brain insult. *Eur. J. Appl. Physiol.* *109*, 35–39.
- Houser, B. (2012). Bio-Rad’s Bio-Plex® suspension array system, xMAP technology overview. *Arch. Physiol. Biochem.* *118*, 192–196.
- Jan, S., Northington, F.J., Parkinson, C.M., and Stafstrom, C.E. (2017). EEG Monitoring Technique Influences the Management of Hypoxic-Ischemic Seizures in Neonates Undergoing Therapeutic Hypothermia. *Dev. Neurosci.*
- Jansen, E.M., and Low, W.C. (1996). Long-term effects of neonatal ischemic-hypoxic brain injury on sensorimotor and locomotor tasks in rats. *Behav. Brain Res.* *78*, 189–194.
- Jensen, F.E., Applegate, C.D., Holtzman, D., Belin, T.R., and Burchfiel, J.L. (1991). Epileptogenic effect of hypoxia in the immature rodent brain. *Ann. Neurol.* *29*, 629–637.
- Kaur, C., Rathnasamy, G., and Ling, E.-A. (2013). Roles of Activated Microglia in Hypoxia Induced Neuroinflammation in the Developing Brain and the Retina. *J. Neuroimmune Pharmacol.* *8*, 66–78.
- Lee, B.S., Woo, C.-W., Kim, S.-T., and Kim, K.-S. (2010). Long-term neuroprotective effect of postischemic hypothermia in a neonatal rat model of severe hypoxic ischemic encephalopathy: a comparative study on the duration and depth of hypothermia. *Pediatr. Res.* *68*, 303–308.
- Leonard, A.S., Hyder, S.N., Kolls, B.J., Arehart, E., W. Ng, K.C., Veerapandiyan, A., and Mikati, M.A. (2013). Seizure predisposition after perinatal hypoxia: Effects of subsequent age and of an epilepsy predisposing gene mutation. *Epilepsia* *54*, 1789–1800.

- Levine, S. (1960). Anoxic-Ischemic Encephalopathy in Rats. *Am. J. Pathol.* 36, 1–17.
- Li, S.-J., Liu, W., Wang, J.-L., Zhang, Y., Zhao, D.-J., Wang, T.-J., and Li, Y.-Y. (2014). The role of TNF- α , IL-6, IL-10, and GDNF in neuronal apoptosis in neonatal rat with hypoxic-ischemic encephalopathy. *Eur. Rev. Med. Pharmacol. Sci.* 18, 905–909.
- Liu, F., and McCullough, L.D. (2013). Inflammatory responses in hypoxic ischemic encephalopathy. *Acta Pharmacol. Sin.* 34, 1121–1130.
- Liu, L., and Duff, K. (2008). A technique for serial collection of cerebrospinal fluid from the cisterna magna in mouse. *J. Vis. Exp. JoVE*.
- Lubics, A., Reglődi, D., Tamás, A., Kiss, P., Szalai, M., Szalontay, L., and Lengvári, I. (2005). Neurological reflexes and early motor behavior in rats subjected to neonatal hypoxic–ischemic injury. *Behav. Brain Res.* 157, 157–165.
- Lusyati, S., Hulzebos, C.V., Zandvoort, J., Sukandar, H., and Sauer, P.J.J. (2013). Cytokines patterns in newborn infants with late onset sepsis. *J. Neonatal-Perinat. Med.* 6, 153–163.
- Lv, H., Wang, Q., Wu, S., Yang, L., Ren, P., Yang, Y., Gao, J., and Li, L. (2015). Neonatal hypoxic ischemic encephalopathy-related biomarkers in serum and cerebrospinal fluid. *Clin. Chim. Acta* 450, 282–297.
- Martín-Ancel, A., García-Alix, A., Pascual-Salcedo, D., Cabañas, F., Valcarce, M., and Quero, J. (1997). Interleukin-6 in the cerebrospinal fluid after perinatal asphyxia is related to early and late neurological manifestations. *Pediatrics* 100, 789–794.
- McRae, A., Gilland, E., Bona, E., and Hagberg, H. (1995). Microglia activation after neonatal hypoxic-ischemia. *Brain Res. Dev. Brain Res.* 84, 245–252.
- Mortola, J.P., and Dotta, A. (1992). Effects of hypoxia and ambient temperature on gaseous metabolism of newborn rats. *Am. J. Physiol.* 263, R267-272.
- Moyer, M.W. (2012). New biomarkers sought for improving sepsis management and care. *Nat. Med.* 18, 999.
- Owens, J., Robbins, C.A., Wenzel, H.J., and Schwartzkroin, P.A. (1997). Acute and chronic effects of hypoxia on the developing hippocampus. *Ann. Neurol.* 41, 187–199.
- Patel, S.D., Pierce, L., Ciardiello, A., Hutton, A., Paskewitz, S., Aronowitz, E., Voss, H.U., Moore, H., and Vannucci, S.J. (2015). Therapeutic hypothermia and hypoxia-ischemia in the term-equivalent neonatal rat: characterization of a translational preclinical model. *Pediatr. Res.* 78, 264–271.
- de Paula, S., Vitola, A.S., Greggio, S., de Paula, D., Mello, P.B., Lubianca, J.M., Xavier, L.L., Fiori, H.H., and Dacosta, J.C. (2009). Hemispheric Brain Injury and Behavioral Deficits Induced by Severe Neonatal Hypoxia-Ischemia in Rats Are Not Attenuated by Intravenous Administration of Human Umbilical Cord Blood Cells. *Pediatr. Res.* 65, 631–635.

- Rakhade, S.N., Klein, P.M., Huynh, T., Hilario-Gomez, C., Kosaras, B., Rotenberg, A., and Jensen, F.E. (2011). Development of later life spontaneous seizures in a rodent model of hypoxia-induced neonatal seizures. *Epilepsia* 52, 753–765.
- Rice, J.E., Vannucci, R.C., and Brierley, J.B. (1981). The influence of immaturity on hypoxic-ischemic brain damage in the rat. *Ann. Neurol.* 9, 131–141.
- Robertson, C.M., and Perlman, M. (2006). Follow-up of the term infant after hypoxic-ischemic encephalopathy. *Paediatr. Child Health* 11, 278–282.
- Rodríguez-Fanjul, J., Fernández-Feijóo, C.D., and Camprubí, M.C. (2015). A New Technique for Collection of Cerebrospinal Fluid in Rat Pups. *J. Exp. Neurosci.* 9, 37–41.
- Rojas, J.J., Deniz, B.F., Miguel, P.M., Diaz, R., Hermel, É. do E.-S., Achaval, M., Netto, C.A., and Pereira, L.O. (2013). Effects of daily environmental enrichment on behavior and dendritic spine density in hippocampus following neonatal hypoxia–ischemia in the rat. *Exp. Neurol.* 241, 25–33.
- Rumajogee, P., Bregman, T., Miller, S.P., Yager, J.Y., and Fehlings, M.G. (2016). Rodent Hypoxia–Ischemia Models for Cerebral Palsy Research: A Systematic Review. *Front. Neurol.* 7.
- Saliba, E., and Henrot, A. (2001a). Inflammatory mediators and neonatal brain damage. *Biol. Neonate* 79, 224–227.
- Saliba, E., and Henrot, A. (2001b). Inflammatory mediators and neonatal brain damage. *Biol. Neonate* 79, 224–227.
- Sanchez-Niño, M.D., Sanz, A.B., and Ortiz, A. (2016). Chronicity following ischaemia-reperfusion injury depends on tubular-macrophage crosstalk involving two tubular cell-derived CSF-1R activators: CSF-1 and IL-34. *Nephrol. Dial. Transplant.* 31, 1409–1416.
- Sävman, K., Blennow, M., Gustafson, K., Tarkowski, E., and Hagberg, H. (1998). Cytokine response in cerebrospinal fluid after birth asphyxia. *Pediatr. Res.* 43, 746–751.
- Sawada, M., Suzumura, A., Yamamoto, H., and Marunouchi, T. (1990). Activation and proliferation of the isolated microglia by colony stimulating factor-1 and possible involvement of protein kinase C. *Brain Res.* 509, 119–124.
- Schilling, M., Strecker, J.-K., Ringelstein, E.B., Schäbitz, W.-R., and Kiefer, R. (2009). The role of CC chemokine receptor 2 on microglia activation and blood-borne cell recruitment after transient focal cerebral ischemia in mice. *Brain Res.* 1289, 79–84.
- Shahkar, L., Keshtkar, A., Mirfazeli, A., Ahani, A., and Roshandel, G. (2011). The Role of IL-6 for Predicting Neonatal Sepsis: A Systematic Review and Meta-Analysis. *Iran. J. Pediatr.* 21, 411–417.
- Svedin, P., Hagberg, H., Sävman, K., Zhu, C., and Mallard, C. (2007). Matrix metalloproteinase-9 gene knock-out protects the immature brain after cerebral hypoxia-ischemia. *J. Neurosci. Off. J. Soc. Neurosci.* 27, 1511–1518.

Szaflarski, J., Burtrum, D., and Silverstein, F.S. (1995). Cerebral hypoxia-ischemia stimulates cytokine gene expression in perinatal rats. *Stroke* 26, 1093–1100.

Takao, K., Tanda, K., Nakamura, K., Kasahara, J., Nakao, K., Katsuki, M., Nakanishi, K., Yamasaki, N., Toyama, K., Adachi, M., et al. (2010). Comprehensive Behavioral Analysis of Calcium/Calmodulin-Dependent Protein Kinase IV Knockout Mice. *PLOS ONE* 5, e9460.

Tata, D.A., Markostamou, I., Ioannidis, A., Gkioka, M., Simeonidou, C., Anogianakis, G., and Spandou, E. (2015). Effects of maternal separation on behavior and brain damage in adult rats exposed to neonatal hypoxia–ischemia. *Behav. Brain Res.* 280, 51–61.

Ten, V.S., Bradley-Moore, M., Gingrich, J.A., Stark, R.I., and Pinsky, D.J. (2003). Brain injury and neurofunctional deficit in neonatal mice with hypoxic-ischemic encephalopathy. *Behav. Brain Res.* 145, 209–219.

Thoresen, M., Hellström-Westas, L., Liu, X., and de Vries, L.S. (2010). Effect of hypothermia on amplitude-integrated electroencephalogram in infants with asphyxia. *Pediatrics* 126, e131-139.

Thornton, C., Rousset, C.I., Kichev, A., Miyakuni, Y., Vontell, R., Baburamani, A.A., Fleiss, B., Gressens, P., and Hagberg, H. (2012). Molecular Mechanisms of Neonatal Brain Injury. *Neurol. Res. Int.* 2012, e506320.

Tian, S.-F., Yang, H.-H., Xiao, D.-P., Huang, Y.-J., He, G.-Y., Ma, H.-R., Xia, F., and Shi, X.-C. (2013). Mechanisms of Neuroprotection from Hypoxia-Ischemia (HI) Brain Injury by Up-regulation of Cytochrome (CYGB) in a Neonatal Rat Model. *J. Biol. Chem.* 288, 15988–16003.

Vannucci, S.J., and Hagberg, H. (2004). Hypoxia-ischemia in the immature brain. *J. Exp. Biol.* 207, 3149–3154.

Vexler, Z.S., and Ferriero, D.M. (2001). Molecular and biochemical mechanisms of perinatal brain injury. *Semin. Neonatol.* 6, 99–108.

Wagner, B.P., Nedelcu, J., and Martin, E. (2002). Delayed Postischemic Hypothermia Improves Long-Term Behavioral Outcome after Cerebral Hypoxia-Ischemia in Neonatal Rats. *Pediatr. Res.* 51, 354–360.

Legend to the figures and tables

Figure 1. (A) Average weights \pm S.E.M. of hypoxic and sham rats starting from P7 (one-day prior the intervention). (B) Brain lesion induced by acute (24 and 72h) and chronic hypoxia-ischemia (4 weeks).

Table 1. Average days \pm S.E.M. of appearance of physical and neurological reflexes in sham and HI rats. $*P < 0.05$, $**P < 0.01$, $***P < 0.001$ $****P < 0.0001$ vs. control rats.

Figure 2. Effect of neonatal HI on Open field performance in sham and HI rats; (A) number of crossing (B) Frequency of entry to the center, (C) representative traces of sham and HI rat movement during the open field test. (D) number of rearing. Statistical analysis: Two way ANOVA and Multiple Comparison test ($**P < 0.01$, $***P < 0.001$, $****P < 0.0001$). Test duration: 10 min. N= 13 Male HI, 6 Female HI, 8 Male Sham, 7 Female Sham.

Figure 3. Effect of neonatal HI on Rota-rod performance. (A) number of falls during the habituation session, (B) latency of falls during the test session. Statistical analysis: Two-way ANOVA and Multiple Comparison test $****P < 0.0001$. N= 13 Male HI, 6 Female HI, 8 Male Sham, 7 Female Sham.

Figure 4. Effect of neonatal HI on MWM performance after 30 days. (A) Mean escape latency during the 4 days of training (B) Cumulative distance to platform during the training and the test days. Statistical analysis: Two-way ANOVA and Tukey's multiple comparison test $****P < 0.0001$. N= 13 Male HI, 6 Female HI, 8 Male Sham, 7 Female Sham.

Figure 5. Motor function was assessed with a CatWalk gait analysis system (A) maximum contact area, (B) stand and (C) swing speed. Statistical analysis: Two-way ANOVA and Tukey's multiple comparison test ($*P < 0.05$, $**P < 0.01$, $***P < 0.001$, $****P < 0.0001$). RF, right fore; RH, right hind; LF, left fore; LH, left hind limbs.

Figure 6. Cytokine/Chemokine levels in Plasma. The amount of IFN- γ , IL-1 β , IL-6, M-CSF (CSF1), MCP-1 (CCL2), MIP-1 α (CCL3), MIP-3 α (CCL20), RANTES (CCL5), and TNF- α in plasma in sham and HI groups are reported. Results are presented as individual values (pg/mL) and the mean \pm SD is also shown. Statistical analysis: one-way ANOVA

and Tukey's multiple comparison test (* $P<0.05$, ** $P<0.01$, *** $P<0.001$, **** $P<0.0001$). F: female, M: male. (the group of 24h and 72h male and female are pooled)

Figure 7. Cytokine/Chemokine levels in CSF. The amount of EPO, IFN- γ , IL-5, IL-17A, M-CSF (CSF1), MCP-1 (CCL2), MIP-3 α (CCL20), RANTES (CCL5), and VEGF. in CSF in Sham and HI groups are reported. Results are presented as individual values (pg/mL) and the mean \pm SD is also shown. Statistical analysis: one-way ANOVA and Tukey's multiple comparison test (* $P<0.05$, ** $P<0.01$, *** $P<0.001$, **** $P<0.0001$).

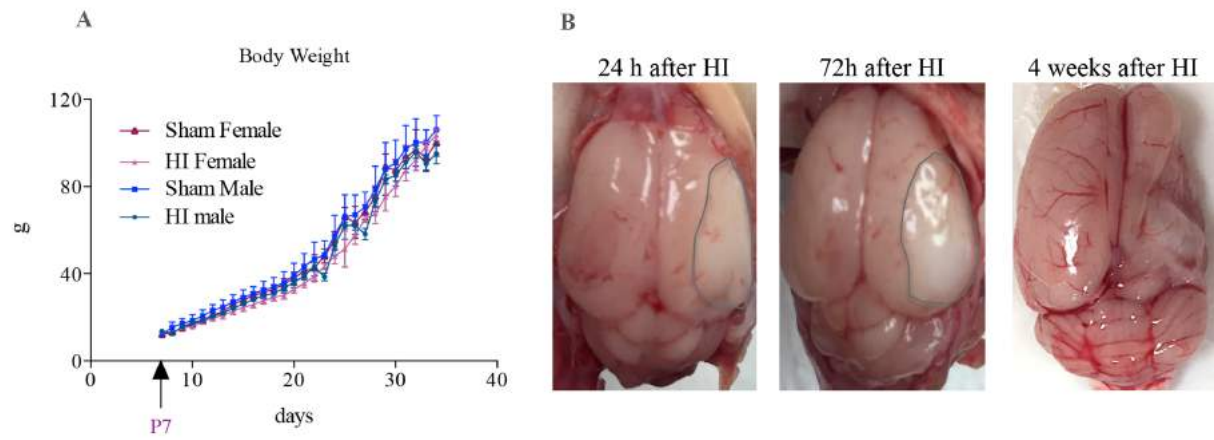


Figure 1

	Days of appearance	
	Sham	HI
Left eye opening	14.1 ± 0.1	14.7 ± 0.2
Right eye opening	14.1 ± 0.1	21.6 ± 0.8****
Ear unfolding	13.9 ± 0.9	14.1 ± 0.1
righting reflex	8	8
negative geotaxis	11.3 ± 0.4	12.5 ± 0.7**
crossed extensor reflex	8	8
Eylid reflex	15.2 ± 0.4	15.6 ± 0.8
Ear twitch reflex	15.6 ± 0.6	17 ± 0.2**
auditory startle	10.4 ± 0.1	12.6 ± 0.8**
Forelimb placing	8	8
Hindlimb placing	17.8 ± 0.8	18.1 ± 0.1
Limb grasping	10.2 ± 0.1	11.7 ± 0.3*
gait	9.2 ± 0.2	12.6 ± 0.8****

Table 1

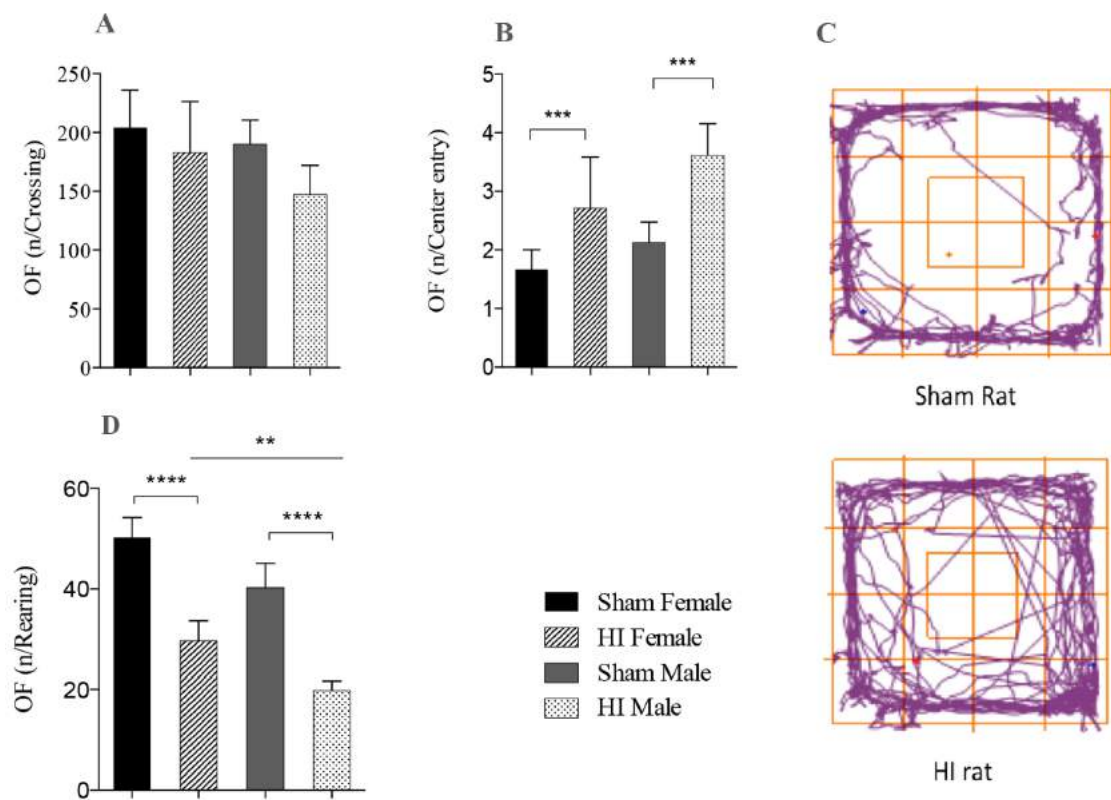


Figure 2

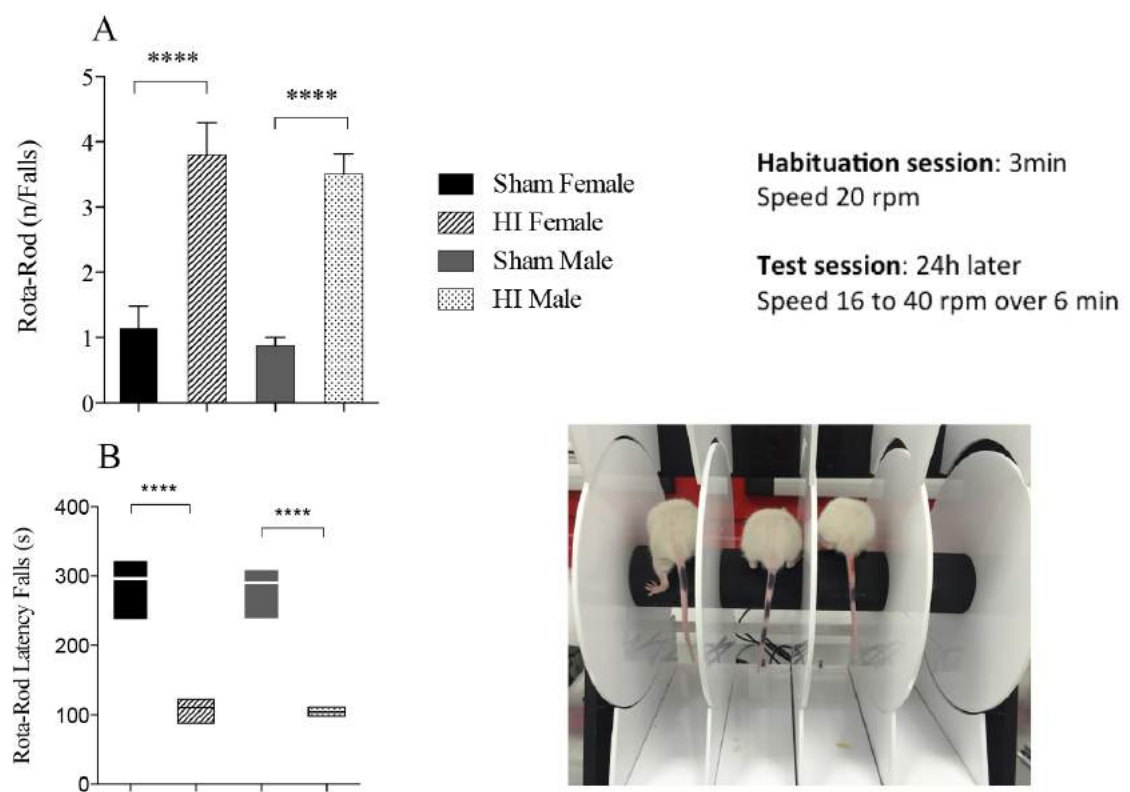


Figure 3

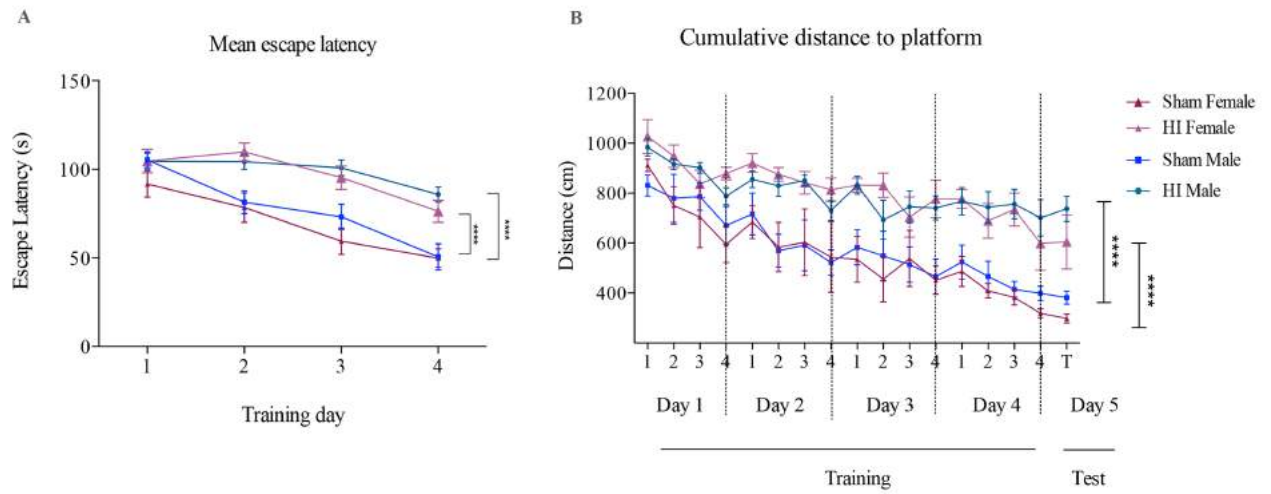


Figure 4

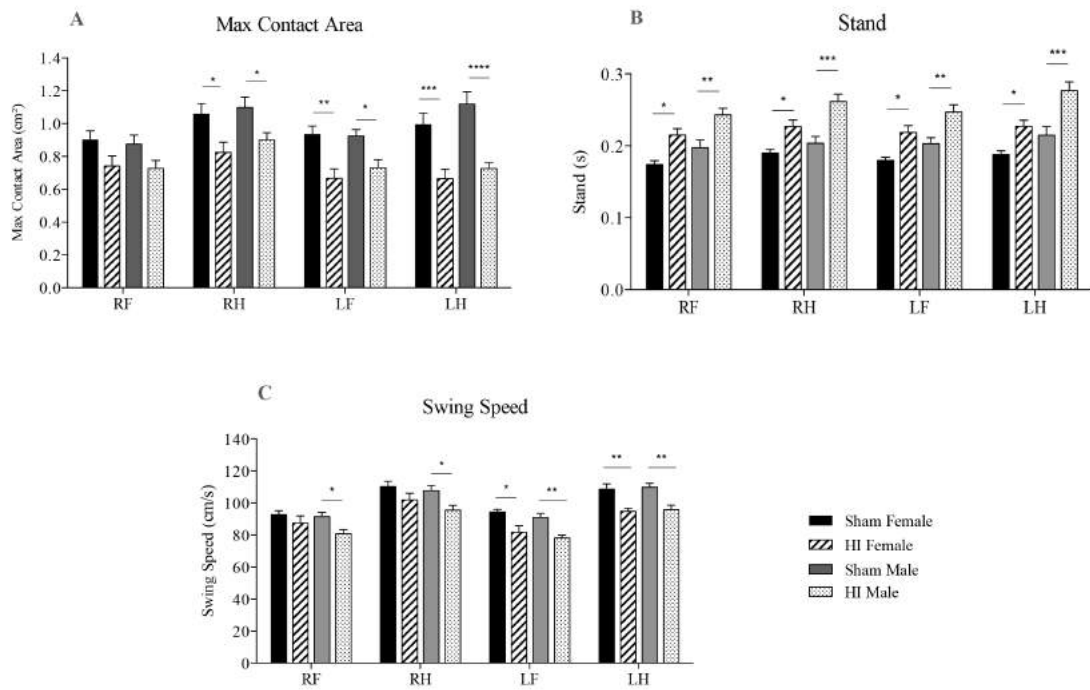


Figure 5

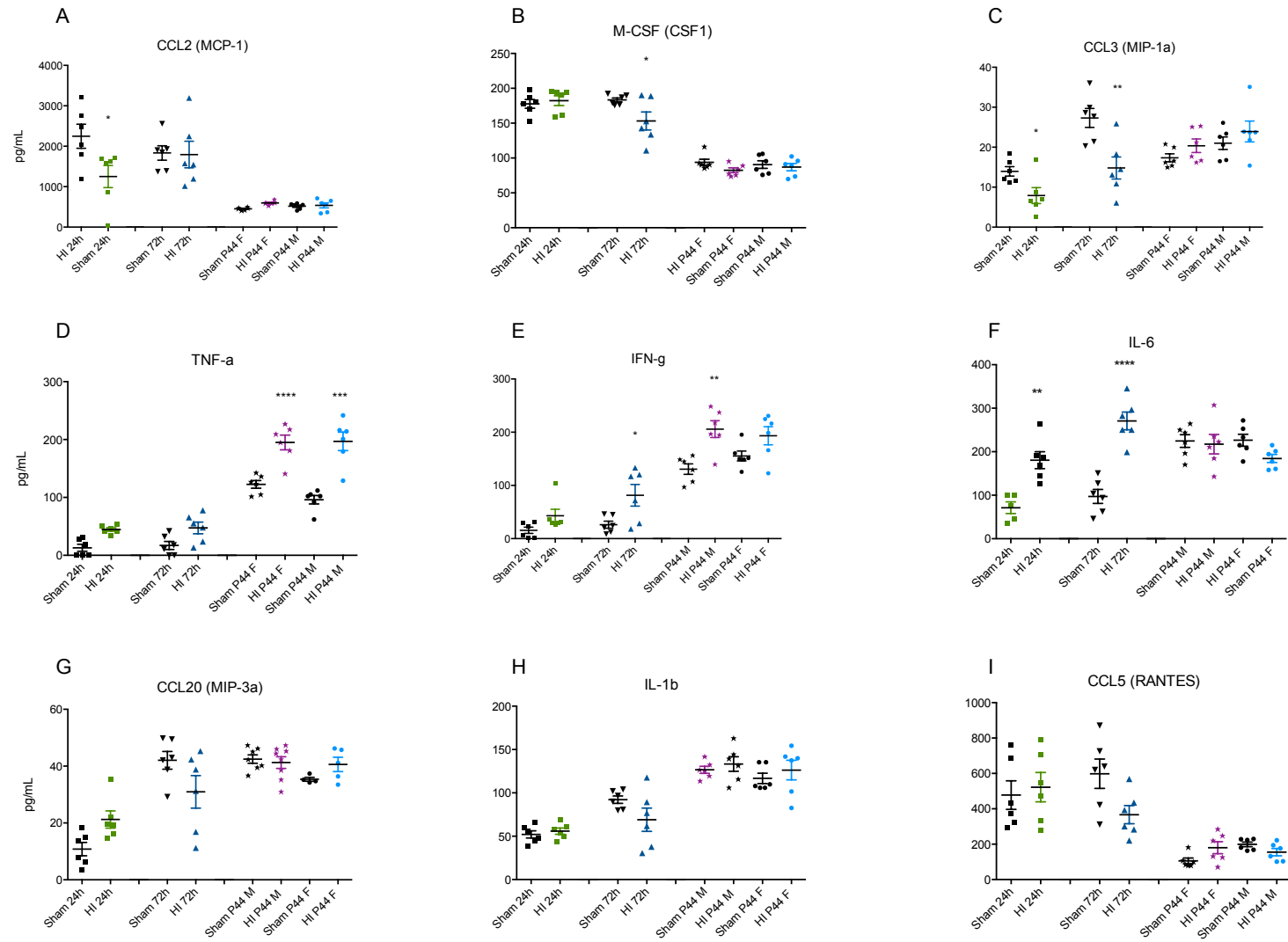


Figure 6

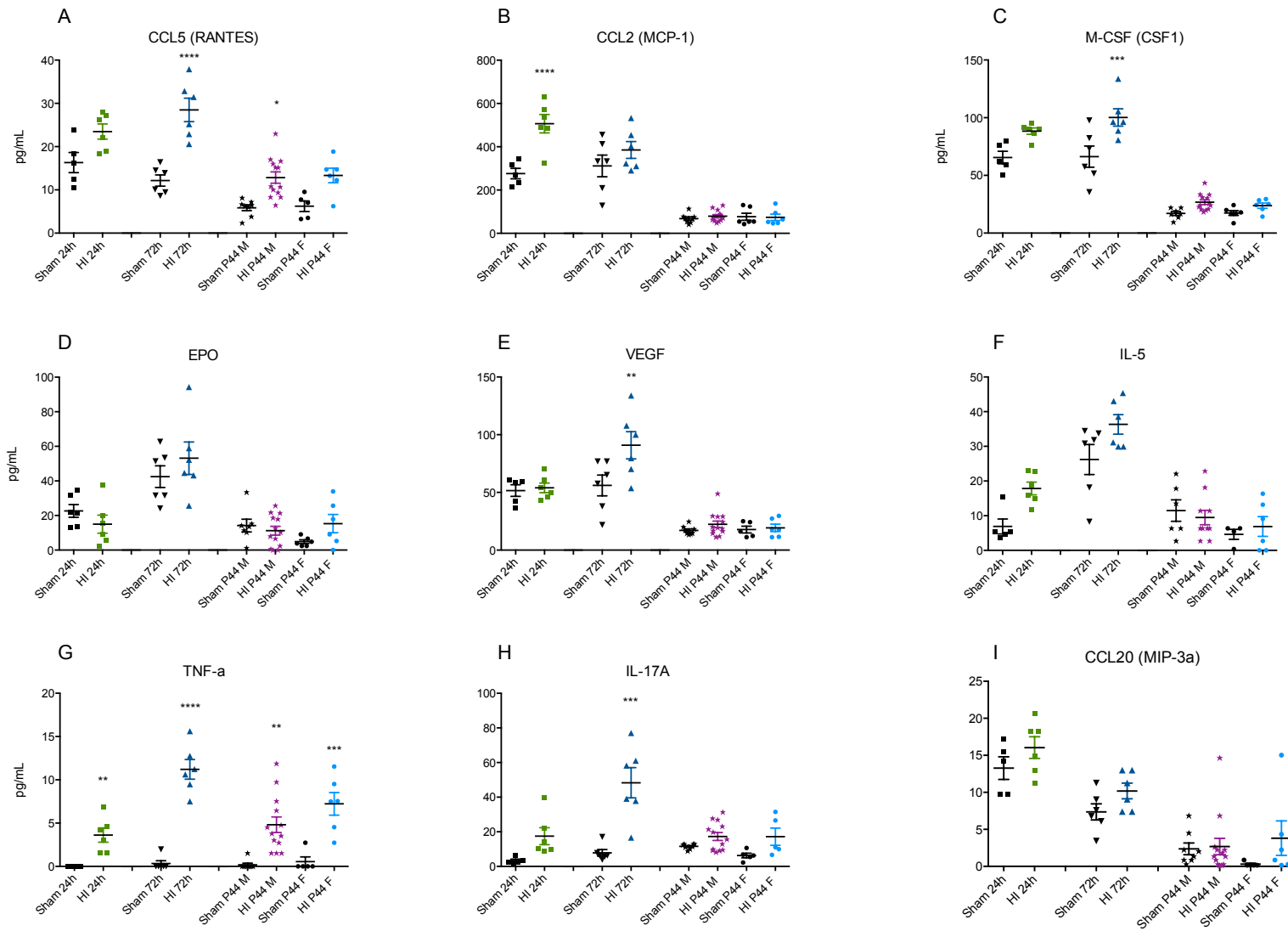


Figure 7

CONCLUSION

Neurological insults and disease leading to extensive neurodegeneration, exemplified by MS or HI, represent major unmet needs for therapeutic interventions. Characterization and targeting of the processes that initiate specific disease pathologies are clearly important areas for investigation. The inchoate evidence for both protective and pathogenic roles of microglia and the activation of common inflammation pathways in these cells in several neurodegenerative disorders supports the hypothesis that glia-induced inflammation is an aspect of pathology. Although inhibition of neuroinflammation may not alter the underlying cause of disease, it may decrease the production of factors that contribute to neurotoxicity and demyelination, thus resulting in a clinical benefit.

A common link between neurodegenerative conditions is the chronic activation of innate immune responses counting also those intermediated by microglia. Such activation can trigger toxic pathways leading to progressive degeneration. Yet, microglia are also crucial for governing inflammatory processes, such as repair and regeneration mechanisms. The adaptive immune response is implicated in neurodegenerative diseases contributing to tissue damage, but in several cases, mediators used by the immune system to resolve inflammation, mediate neuroprotection and repair are also used by the CNS for growth and development. This common language is demonstrated by the role of microglia, and the role of cytokines and chemokines during development of the brain.

Notwithstanding the fact that the CNS is an immune-privileged site, innate and adaptive immune responses do frequently take place in the CNS. They are indispensable to eliminate infectious agents, as well as for clearing debris and endorsing tissue repair. Despite these helpful roles of immune responses, such responses must remain under tight control to avoid any damage to the CNS. The BBB and the powerful immune-regulatory functions act together to protect such control. Microglia are actively maintained in a quiescent state, and the influx and local activation of peripheral immune cells is severely limited. Despite these measures, chronic immune activation is a pathological hallmark of neurodegenerative disorders.

A better consideration of the endogenous protective pathways will certainly disclose ways to harness reparative processes, and so improve control over chronic inflammatory neurodegenerative disorders.

REFERENCES

- Abbott, N.J., Rönnbäck, L., and Hansson, E. (2006). Astrocyte-endothelial interactions at the blood-brain barrier. *Nat. Rev. Neurosci.* 7, 41–53.
- Aderem, A., and Underhill, D.M. (1999). Mechanisms of phagocytosis in macrophages. *Annu. Rev. Immunol.* 17, 593–623.
- Aharoni, R. (2013). New findings and old controversies in the research of multiple sclerosis and its model experimental autoimmune encephalomyelitis. *Expert Rev. Clin. Immunol.* 9, 423–440.
- Albertsson, A.-M., Bi, D., Duan, L., Zhang, X., Leavenworth, J.W., Qiao, L., Zhu, C., Cardell, S., Cantor, H., Hagberg, H., et al. (2014). The immune response after hypoxia-ischemia in a mouse model of preterm brain injury. *J. Neuroinflammation* 11.
- Albert-Weissenberger, C., Sirén, A.-L., and Kleinschnitz, C. (2013). Ischemic stroke and traumatic brain injury: the role of the kallikrein-kinin system. *Prog. Neurobiol.* 101–102, 65–82.
- Aloisi, F. (2001). Immune function of microglia. *Glia* 36, 165–179.
- Amor, S., Puentes, F., Baker, D., and van der Valk, P. (2010). Inflammation in neurodegenerative diseases. *Immunology* 129, 154–169.
- Bacon, K., Baggiolini, M., Broxmeyer, H., Horuk, R., Lindley, I., Mantovani, A., Matsushima, K., Murphy, P., Nomiyama, H., Oppenheim, J., et al. (2002). Chemokine/chemokine receptor nomenclature. *J. Interferon Cytokine Res.* 22, 1067–1068.
- Baeten, K.M., and Akassoglou, K. (2011). Extracellular matrix and matrix receptors in blood-brain barrier formation and stroke. *Dev. Neurobiol.* 71, 1018–1039.
- Baggiolini, M. (2001). Chemokines in pathology and medicine. *J. Intern. Med.* 250, 91–104.
- Balduini, W., De Angelis, V., Mazzoni, E., and Cimino, M. (2000). Long-lasting behavioral alterations following a hypoxic/ischemic brain injury in neonatal rats. *Brain Res.* 859, 318–325.
- Banati, R.B., Gehrman, J., Schubert, P., and Kreutzberg, G.W. (1993). Cytotoxicity of microglia. *Glia* 7, 111–118.
- Banerjee, S., and Bhat, M.A. (2007). Neuron-glia interactions in blood-brain barrier formation. *Annu. Rev. Neurosci.* 30, 235–258.
- Banks, W.A. (2016). From blood-brain barrier to blood-brain interface: new opportunities for CNS drug delivery. *Nat. Rev. Drug Discov.* 15, 275–292.

- Barker, R.A., and Cicchetti, F. (2014). Innate immunity and neurodegenerative disorders (Frontiers E-books).
- Barnett, M.H., and Prineas, J.W. (2004). Relapsing and remitting multiple sclerosis: pathology of the newly forming lesion. *Ann. Neurol.* *55*, 458–468.
- Becher, B., Spath, S., and Goverman, J. (2017a). Cytokine networks in neuroinflammation. *Nat. Rev. Immunol.* *17*, 49–59.
- Becher, B., Spath, S., and Goverman, J. (2017b). Cytokine networks in neuroinflammation. *Nat. Rev. Immunol.* *17*, 49–59.
- Benbow, U., and Brinckerhoff, C.E. (1997). The AP-1 site and MMP gene regulation: what is all the fuss about? *Matrix Biol. J. Int. Soc. Matrix Biol.* *15*, 519–526.
- Ben-Nun, A., Kaushansky, N., Kawakami, N., Krishnamoorthy, G., Berer, K., Liblau, R., Hohlfeld, R., and Wekerle, H. (2014). From classic to spontaneous and humanized models of multiple sclerosis: impact on understanding pathogenesis and drug development. *J. Autoimmun.* *54*, 33–50.
- Bjartmar, C., Wujek, J.R., and Trapp, B.D. (2003). Axonal loss in the pathology of MS: consequences for understanding the progressive phase of the disease. *J. Neurol. Sci.* *206*, 165–171.
- Blankesteijn, M., and Altara, R. (2014). Inflammation in Heart Failure (Academic Press).
- Brown, C.M., Mulcahey, T.A., Filipek, N.C., and Wise, P.M. (2010). Production of Proinflammatory Cytokines and Chemokines During Neuroinflammation: Novel Roles for Estrogen Receptors α and β . *Endocrinology* *151*, 4916–4925.
- Bustamante, A., Simats, A., Vilar-Bergua, A., García-Berrocso, T., and Montaner, J. (2016). Blood/Brain Biomarkers of Inflammation After Stroke and Their Association With Outcome: From C-Reactive Protein to Damage-Associated Molecular Patterns. *Neurotherapeutics* *13*, 671–684.
- Butovsky, O., Madore, C., and Weiner, H. (2017). Microglial Biology and Physiology. In *Neuroimmune Pharmacology*, T. Ikezu, and H.E. Gendelman, eds. (Springer International Publishing), pp. 167–199.
- Butt, A.M. (2006). Neurotransmitter-mediated calcium signalling in oligodendrocyte physiology and pathology. *Glia* *54*, 666–675.
- Calza, L., Fernandez, M., Giuliani, A., Aloe, L., and Giardino, L. (2002). Thyroid hormone activates oligodendrocyte precursors and increases a myelin-forming protein and NGF content in the spinal cord during experimental allergic encephalomyelitis. *Proc. Natl. Acad. Sci. U. S. A.* *99*, 3258–3263.
- Campbell, I.L., Krucker, T., Steffensen, S., Akwa, Y., Powell, H.C., Lane, T., Carr, D.J., Gold, L.H., Henriksen, S.J., and Siggins, G.R. (1999). Structural and functional neuropathology in transgenic mice with CNS expression of IFN- α . *Brain Res.* *835*, 46–61.

- Carvey, P.M., Hendey, B., and Monahan, A.J. (2009). The Blood Brain Barrier in Neurodegenerative Disease: A Rhetorical Perspective. *J. Neurochem.* *111*, 291–314.
- CHEN, W.-W., ZHANG, X., and HUANG, W.-J. (2016). Role of neuroinflammation in neurodegenerative diseases (Review). *Mol. Med. Rep.* *13*, 3391–3396.
- Chen, W.-W., Zhang, X., and Huang, W.-J. (2016). Role of neuroinflammation in neurodegenerative diseases (Review). *Mol. Med. Rep.* *13*, 3391–3396.
- Cherry, J.D., Olschowka, J.A., and O'Banion, M.K. (2014). Neuroinflammation and M2 microglia: the good, the bad, and the inflamed. *J. Neuroinflammation* *11*, 98.
- Chou, I.-C., Trakht, T., Signori, C., Smith, J., Felt, B.T., Vazquez, D.M., and Barks, J.D.E. (2001). Behavioral/Environmental Intervention Improves Learning After Cerebral Hypoxia-Ischemia in Rats. *Stroke* *32*, 2192–2197.
- Chu, T., Shields, L.B.E., Zhang, Y.P., Feng, S.-Q., Shields, C.B., and Cai, J. (2017). CXCL12/CXCR4/CXCR7 Chemokine Axis in the Central Nervous System: Therapeutic Targets for Remyelination in Demyelinating Diseases. *The Neuroscientist* 1073858416685690.
- Clause, K.C., and Barker, T.H. (2013). Extracellular matrix signaling in morphogenesis and repair. *Curr. Opin. Biotechnol.* *24*, 830–833.
- Compston, A., and Coles, A. (2002). Multiple sclerosis. *Lancet Lond. Engl.* *359*, 1221–1231.
- Constantinescu, C.S., Farooqi, N., O'Brien, K., and Gran, B. (2011a). Experimental autoimmune encephalomyelitis (EAE) as a model for multiple sclerosis (MS). *Br. J. Pharmacol.* *164*, 1079–1106.
- Constantinescu, C.S., Farooqi, N., O'Brien, K., and Gran, B. (2011b). Experimental autoimmune encephalomyelitis (EAE) as a model for multiple sclerosis (MS). *Br. J. Pharmacol.* *164*, 1079–1106.
- Conway, J.G., McDonald, B., Parham, J., Keith, B., Rusnak, D.W., Shaw, E., Jansen, M., Lin, P., Payne, A., Crosby, R.M., et al. (2005). Inhibition of colony-stimulating-factor-1 signaling in vivo with the orally bioavailable cFMS kinase inhibitor GW2580. *Proc. Natl. Acad. Sci. U. S. A.* *102*, 16078–16083.
- Dendrou, C.A., Fugger, L., and Friese, M.A. (2015). Immunopathology of multiple sclerosis. *Nat. Rev. Immunol.* *15*, 545–558.
- Denes, A., Vidyasagar, R., Feng, J., Narvainen, J., McColl, B.W., Kauppinen, R.A., and Allan, S.M. (2007). Proliferating resident microglia after focal cerebral ischaemia in mice. *J. Cereb. Blood Flow Metab. Off. J. Int. Soc. Cereb. Blood Flow Metab.* *27*, 1941–1953.
- Descamps, F.J., Martens, E., and Opdenakker, G. (2002). Analysis of Gelatinases in Complex Biological Fluids and Tissue Extracts. *Lab. Invest.* *82*, 1607–1608.

- Dheen, S.T., Kaur, C., and Ling, E.-A. (2007). Microglial activation and its implications in the brain diseases. *Curr. Med. Chem.* 14, 1189–1197.
- Dinarello, C.A. (2007). Historical Review of Cytokines. *Eur. J. Immunol.* 37, S34–S45.
- Dringen, R. (2005). Oxidative and antioxidative potential of brain microglial cells. *Antioxid. Redox Signal.* 7, 1223–1233.
- Du, Q., and Geller, D.A. (2010). Cross-Regulation Between Wnt and NF- κ B Signaling Pathways. *Forum Immunopathol. Dis. Ther.* 1, 155–181.
- Eklind, S., Mallard, C., Leverin, A.L., Gilland, E., Blomgren, K., Mattsby-Baltzer, I., and Hagberg, H. (2001). Bacterial endotoxin sensitizes the immature brain to hypoxic--ischaemic injury. *Eur. J. Neurosci.* 13, 1101–1106.
- Engelhardt, B. (2008). Immune cell entry into the central nervous system: Involvement of adhesion molecules and chemokines. *J. Neurol. Sci.* 274, 23–26.
- Engelhardt, B., and Liebner, S. (2014). Novel insights into the development and maintenance of the blood–brain barrier. *Cell Tissue Res.* 355, 687–699.
- Enzinger, C., and Fazekas, F. (2015). Measuring Gray Matter and White Matter Damage in MS: Why This is Not Enough. *Front. Neurol.* 6.
- Faulkner, J.R., Herrmann, J.E., Woo, M.J., Tansey, K.E., Doan, N.B., and Sofroniew, M.V. (2004). Reactive astrocytes protect tissue and preserve function after spinal cord injury. *J. Neurosci. Off. J. Soc. Neurosci.* 24, 2143–2155.
- da Fonseca, A.C.C., Matias, D., Garcia, C., Amaral, R., Geraldo, L.H., Freitas, C., and Lima, F.R.S. (2014). The impact of microglial activation on blood-brain barrier in brain diseases. *Front. Cell. Neurosci.* 8.
- Frantz, C., Stewart, K.M., and Weaver, V.M. (2010). The extracellular matrix at a glance. *J Cell Sci* 123, 4195–4200.
- Fricker, M., Neher, J.J., Zhao, J.-W., Théry, C., Tolkovsky, A.M., and Brown, G.C. (2012). MFG-E8 mediates primary phagocytosis of viable neurons during neuroinflammation. *J. Neurosci. Off. J. Soc. Neurosci.* 32, 2657–2666.
- Frohman, E.M., Racke, M.K., and Raine, C.S. (2006). Multiple sclerosis--the plaque and its pathogenesis. *N. Engl. J. Med.* 354, 942–955.
- Fu, R., Shen, Q., Xu, P., Luo, J.J., and Tang, Y. (2014). Phagocytosis of Microglia in the Central Nervous System Diseases. *Mol. Neurobiol.* 49, 1422–1434.
- Fukuda, S., Fini, C.A., Mabuchi, T., Koziol, J.A., Eggleston, L.L., and del Zoppo, G.J. (2004). Focal cerebral ischemia induces active proteases that degrade microvascular matrix. *Stroke* 35, 998–1004.

Gendelman, H.E., and Masliah, E. (2017). Innate and Adaptive Immunity in Health and Disease. In *Neuroimmune Pharmacology*, T. Ikezu, and H.E. Gendelman, eds. (Springer International Publishing), pp. 3–4.

Ginhoux, F., Lim, S., Hoeffel, G., Low, D., and Huber, T. (2013). Origin and differentiation of microglia. *Front. Cell. Neurosci.* 7, 45.

Glass, C.K., Saijo, K., Winner, B., Marchetto, M.C., and Gage, F.H. (2010). Mechanisms Underlying Inflammation in Neurodegeneration. *Cell* 140, 918–934.

Gomes-Leal, W. (2012). Microglial physiopathology: how to explain the dual role of microglia after acute neural disorders? *Brain Behav.* 2, 345–356.

Gómez-Nicola, D., Fransen, N.L., Suzzi, S., and Perry, V.H. (2013). Regulation of microglial proliferation during chronic neurodegeneration. *J. Neurosci. Off. J. Soc. Neurosci.* 33, 2481–2493.

Graeber, M.B., Li, W., and Rodriguez, M.L. (2011). Role of microglia in CNS inflammation. *FEBS Lett.* 585, 3798–3805.

Groom, J.R., Richmond, J., Murooka, T.T., Sorensen, E.W., Sung, J.H., Bankert, K., von Andrian, U.H., Moon, J.J., Mempel, T.R., and Luster, A.D. (2012). CXCR3 Chemokine Receptor-Ligand Interactions in the Lymph Node Optimize CD4⁺ T Helper 1 Cell Differentiation. *Immunity* 37, 1091–1103.

Guan, Z., Kuhn, J.A., Wang, X., Colquitt, B., Solorzano, C., Vaman, S., Guan, A.K., Evans-Reinsch, Z., Braz, J., Devor, M., et al. (2016). Injured sensory neuron-derived CSF1 induces microglial proliferation and DAP12-dependent pain. *Nat. Neurosci.* 19, 94–101.

Guerreiro-Cacais, A.O., Laaksonen, H., Flytzani, S., N'diaye, M., Olsson, T., and Jagodic, M. (2015). Translational utility of experimental autoimmune encephalomyelitis: recent developments. *J. Inflamm. Res.* 8, 211–225.

Hagberg, H., Mallard, C., Ferriero, D.M., Vannucci, S.J., Levison, S.W., Vexler, Z.S., and Gressens, P. (2015). The role of inflammation in perinatal brain injury. *Nat Rev Neurol* 11, 192–208.

Halleskog, C., Mulder, J., Dahlström, J., Mackie, K., Hortobágyi, T., Tanila, H., Kumar Puli, L., Färber, K., Harkany, T., and Schulte, G. (2011). WNT signaling in activated microglia is proinflammatory. *Glia* 59, 119–131.

Hallmann, R., Zhang, X., Di Russo, J., Li, L., Song, J., Hannocks, M.-J., and Sorokin, L. (2015). The regulation of immune cell trafficking by the extracellular matrix. *Curr. Opin. Cell Biol.* 36, 54–61.

Hanisch, U.-K., Lyons, S.A., Prinz, M., Nolte, C., Weber, J.R., Kettenmann, H., and Kirchhoff, F. (1997). Mouse Brain Microglia Express Interleukin-15 and Its Multimeric Receptor Complex Functionally Coupled to Janus Kinase Activity. *J. Biol. Chem.* 272, 28853–28860.

Hansen, J.T., and Koeppen, B.M. (2002). Netter's Atlas of Human Physiology (Icon Learning Systems).

Harry, G.J., and Kraft, A.D. (2008). Neuroinflammation and Microglia: Considerations and approaches for neurotoxicity assessment. *Expert Opin. Drug Metab. Toxicol.* 4, 1265–1277.

Hashimoto, D., Chow, A., Noizat, C., Teo, P., Beasley, M.B., Leboeuf, M., Becker, C.D., See, P., Price, J., Lucas, D., et al. (2013). Tissue-resident macrophages self-maintain locally throughout adult life with minimal contribution from circulating monocytes. *Immunity* 38, 792–804.

Hattori, T., Sato, Y., Kondo, T., Ichinohashi, Y., Sugiyama, Y., Yamamoto, M., Kotani, T., Hirata, H., Hirakawa, A., Suzuki, S., et al. (2015). Administration of Umbilical Cord Blood Cells Transiently Decreased Hypoxic-Ischemic Brain Injury in Neonatal Rats. *Dev. Neurosci.* 37, 95–104.

Hedtjörn, M., Mallard, C., and Hagberg, H. (2004). Inflammatory gene profiling in the developing mouse brain after hypoxia-ischemia. *J. Cereb. Blood Flow Metab. Off. J. Int. Soc. Cereb. Blood Flow Metab.* 24, 1333–1351.

Hellström Erkenstam, N., Smith, P.L.P., Fleiss, B., Nair, S., Svedin, P., Wang, W., Boström, M., Gressens, P., Hagberg, H., Brown, K.L., et al. (2016). Temporal Characterization of Microglia/Macrophage Phenotypes in a Mouse Model of Neonatal Hypoxic-Ischemic Brain Injury. *Front. Cell. Neurosci.* 10.

Hemmer, B., Cepok, S., Nessler, S., and Sommer, N. (2002). Pathogenesis of multiple sclerosis: an update on immunology. *Curr. Opin. Neurol.* 15, 227–231.

Hensley, K., Mhatre, M., Mou, S., Pye, Q.N., Stewart, C., West, M., and Williamson, K.S. (2006). On the relation of oxidative stress to neuroinflammation: lessons learned from the G93A-SOD1 mouse model of amyotrophic lateral sclerosis. *Antioxid. Redox Signal.* 8, 2075–2087.

Hess, D.C., Abe, T., Hill, W.D., Studdard, A.M., Carothers, J., Masuya, M., Fleming, P.A., Drake, C.J., and Ogawa, M. (2004). Hematopoietic origin of microglial and perivascular cells in brain. *Exp. Neurol.* 186, 134–144.

Hickey, W.F., Cohen, J.A., and Burns, J.B. (1987). A quantitative immunohistochemical comparison of actively versus adoptively induced experimental allergic encephalomyelitis in the Lewis rat. *Cell. Immunol.* 109, 272–281.

Hilaire, J., and Gendelman, H.E. (2017). Macrophages, Microglia and Dendritic Cell Function. In *Neuroimmune Pharmacology*, T. Ikezu, and H.E. Gendelman, eds. (Springer International Publishing), pp. 155–166.

Hoepfner, D.J., Hengartner, M.O., and Schnabel, R. (2001). Engulfment genes cooperate with ced-3 to promote cell death in *Caenorhabditis elegans*. *Nature* 412, 202–206.

- Hosono, T., Kamo, A., Hakotani, S., Minato, K., Akeno, H., Taguchi, Y., Miyano, A., and Iseki, T. (2010). Effect of hypothermia on motor function of adult rats after neonatal hyperthermic hypoxic–ischemic brain insult. *Eur. J. Appl. Physiol.* *109*, 35–39.
- Houser, B. (2012). Bio-Rad's Bio-Plex® suspension array system, xMAP technology overview. *Arch. Physiol. Biochem.* *118*, 192–196.
- Ikezu, T., and Gendelman, H. (2017). *Neuroimmune Pharmacology* (Springer).
- Ingber, D.E. (2006). Mechanical control of tissue morphogenesis during embryological development. *Int. J. Dev. Biol.* *50*, 255–266.
- Jana, N., Basu, A., and Tandon, P.N. (2016). *Inflammation: the Common Link in Brain Pathologies* (Springer).
- Káradóttir, R., and Attwell, D. (2007). Neurotransmitter receptors in the life and death of oligodendrocytes. *Neuroscience* *145*, 1426–1438.
- Karperien, A., Ahammer, H., and Jelinek, H.F. (2013). Quantitating the subtleties of microglial morphology with fractal analysis. *Front. Cell. Neurosci.* *7*.
- Kennedy, D.W., and Abkowitz, J.L. (1997). Kinetics of central nervous system microglial and macrophage engraftment: analysis using a transgenic bone marrow transplantation model. *Blood* *90*, 986–993.
- Kettenmann, H., Hanisch, U.-K., Noda, M., and Verkhratsky, A. (2011). Physiology of microglia. *Physiol. Rev.* *91*, 461–553.
- Kim, S.R. (2015). Inhibition of microglial activation and induction of neurotrophic factors by flavonoids: a potential therapeutic strategy against Parkinson's disease. *Neural Regen. Res.* *10*, 363–364.
- Kim, Y.-K., Na, K.-S., Myint, A.-M., and Leonard, B.E. (2016). The role of pro-inflammatory cytokines in neuroinflammation, neurogenesis and the neuroendocrine system in major depression. *Prog. Neuropsychopharmacol. Biol. Psychiatry* *64*, 277–284.
- Kivisäkk, P., Imitola, J., Rasmussen, S., Elyaman, W., Zhu, B., Ransohoff, R.M., and Khoury, S.J. (2009). Localizing CNS immune surveillance: Meningeal APCs activate T cells during EAE. *Ann. Neurol.* *65*, 457–469.
- Klapal, L., Igelhorst, B.A., and Dietzel-Meyer, I.D. (2016). Changes in Neuronal Excitability by Activated Microglia: Differential Na⁺ Current Upregulation in Pyramid-Shaped and Bipolar Neurons by TNF- α and IL-18. *Front. Neurol.* *7*.
- Klein, T., and Bischoff, R. (2011). Physiology and pathophysiology of matrix metalloproteases. *Amino Acids* *41*, 271–290.
- Kopatz, J., Beutner, C., Welle, K., Bodea, L.G., Reinhardt, J., Claude, J., Linnartz-Gerlach, B., and Neumann, H. (2013). Siglec-h on activated microglia for recognition and engulfment of glioma cells. *Glia* *61*, 1122–1133.

- Koudriavtseva, T., and Mainero, C. (2016). Neuroinflammation, neurodegeneration and regeneration in multiple sclerosis: intercorrelated manifestations of the immune response. *Neural Regen. Res.* *11*, 1727–1730.
- Kryczek, I., Wei, S., Keller, E., Liu, R., and Zou, W. (2007). Stroma-derived factor (SDF-1/CXCL12) and human tumor pathogenesis. *Am. J. Physiol. - Cell Physiol.* *292*, C987–C995.
- Lalancette-Hébert, M., Swarup, V., Beaulieu, J.M., Bohacek, I., Abdelhamid, E., Weng, Y.C., Sato, S., and Kriz, J. (2012). Galectin-3 Is Required for Resident Microglia Activation and Proliferation in Response to Ischemic Injury. *J. Neurosci.* *32*, 10383–10395.
- Larochelle, C., Alvarez, J.I., and Prat, A. (2011). How do immune cells overcome the blood–brain barrier in multiple sclerosis? *FEBS Lett.* *585*, 3770–3780.
- Lassmann, H. (2009). [Clinical and pathological topics of multiple sclerosis]. *Rinsho Shinkeigaku* *49*, 715–718.
- Lassmann, H., Brück, W., and Lucchinetti, C. (2001). Heterogeneity of multiple sclerosis pathogenesis: implications for diagnosis and therapy. *Trends Mol. Med.* *7*, 115–121.
- Lassmann, H., van Horssen, J., and Mahad, D. (2012). Progressive multiple sclerosis: pathology and pathogenesis. *Nat. Rev. Neurol.* *8*, 647–656.
- Lau, L.W., Cua, R., Keough, M.B., Haylock-Jacobs, S., and Yong, V.W. (2013). Pathophysiology of the brain extracellular matrix: a new target for remyelination. *Nat. Rev. Neurosci.* *14*, 722–729.
- Lawson, L.J., Perry, V.H., and Gordon, S. (1992). Turnover of resident microglia in the normal adult mouse brain. *Neuroscience* *48*, 405–415.
- Leblond, A.-L., Klinkert, K., Martin, K., Turner, E.C., Kumar, A.H., Browne, T., and Caplice, N.M. (2015a). Systemic and Cardiac Depletion of M2 Macrophage through CSF-1R Signaling Inhibition Alters Cardiac Function Post Myocardial Infarction. *PloS One* *10*, e0137515.
- Leblond, A.-L., Klinkert, K., Martin, K., Turner, E.C., Kumar, A.H., Browne, T., and Caplice, N.M. (2015b). Systemic and Cardiac Depletion of M2 Macrophage through CSF-1R Signaling Inhibition Alters Cardiac Function Post Myocardial Infarction. *PLoS ONE* *10*, e0137515.
- Lee, H.K., Chaboub, L.S., Zhu, W., Zollinger, D., Rasband, M.N., Fancy, S.P.J., and Deneen, B. (2015). Daam2-PIP5K Is a Regulatory Pathway for Wnt Signaling and Therapeutic Target for Remyelination in the CNS. *Neuron* *85*, 1227–1243.
- Ling, E.A. (1976). Some aspects of amoeboid microglia in the corpus callosum and neighbouring regions of neonatal rats. *J. Anat.* *121*, 29–45.
- Liu, F., and McCullough, L.D. (2013). Inflammatory responses in hypoxic ischemic encephalopathy. *Acta Pharmacol. Sin.* *34*, 1121–1130.
- Liu, L., and Duff, K. (2008). A technique for serial collection of cerebrospinal fluid from the cisterna magna in mouse. *J. Vis. Exp. JoVE*.

- Lorentzen, J.C., Issazadeh, S., Storch, M., Mustafa, M.I., Lassman, H., Linington, C., Klareskog, L., and Olsson, T. (1995). Protracted, relapsing and demyelinating experimental autoimmune encephalomyelitis in DA rats immunized with syngeneic spinal cord and incomplete Freund's adjuvant. *J. Neuroimmunol.* *63*, 193–205.
- Lossinsky, A.S., and Shivers, R.R. (2004). Structural pathways for macromolecular and cellular transport across the blood-brain barrier during inflammatory conditions. Review. *Histol. Histopathol.* *19*, 535–564.
- Louhimies, S. (2002). Directive 86/609/EEC on the protection of animals used for experimental and other scientific purposes. *Altern. Lab. Anim. ATLA* *30 Suppl 2*, 217–219.
- Lu, P., Takai, K., Weaver, V.M., and Werb, Z. (2011). Extracellular Matrix Degradation and Remodeling in Development and Disease. *Cold Spring Harb. Perspect. Biol.* *3*.
- Lue, L.-F., Kuo, Y.-M., Beach, T., and Walker, D.G. (2010). Microglia Activation and Anti-inflammatory Regulation in Alzheimer's Disease. *Mol. Neurobiol.* *41*, 115–128.
- Lull, M.E., and Block, M.L. (2010). Microglial activation and chronic neurodegeneration. *Neurotherapeutics* *7*, 354–365.
- Luster, A.D. (1998). Chemokines - Chemotactic cytokines that mediate inflammation. *N. Engl. J. Med.* *338*, 436–445.
- Malemud, C.J. (2006). Matrix metalloproteinases (MMPs) in health and disease: an overview. *Front. Biosci. J. Virtual Libr.* *11*, 1696–1701.
- Masure, S., Proost, P., Van Damme, J., and Opdenakker, G. (1991). Purification and identification of 91-kDa neutrophil gelatinase. Release by the activating peptide interleukin-8. *Eur. J. Biochem.* *198*, 391–398.
- Matsumoto, Y., Ohmori, K., and Fujiwara, M. (1992). Microglial and astroglial reactions to inflammatory lesions of experimental autoimmune encephalomyelitis in the rat central nervous system. *J. Neuroimmunol.* *37*, 23–33.
- Mayeux, R. (2004). Biomarkers: Potential Uses and Limitations. *NeuroRx* *1*, 182–188.
- McCandless, E.E., Piccio, L., Woerner, B.M., Schmidt, R.E., Rubin, J.B., Cross, A.H., and Klein, R.S. (2008). Pathological expression of CXCL12 at the blood-brain barrier correlates with severity of multiple sclerosis. *Am. J. Pathol.* *172*, 799–808.
- McFarland, A.J., Anoopkumar-Dukie, S., Arora, D.S., Grant, G.D., McDermott, C.M., Perkins, A.V., and Davey, A.K. (2014). Molecular Mechanisms Underlying the Effects of Statins in the Central Nervous System. *Int. J. Mol. Sci.* *15*, 20607–20637.
- Mesplès, B., Plaisant, F., Fontaine, R.H., and Gressens, P. (2005). Pathophysiology of neonatal brain lesions: lessons from animal models of excitotoxicity. *Acta Paediatr. Oslo Nor.* *1992 94*, 185–190.

- Messina, S., and Patti, F. (2014). Gray Matters in Multiple Sclerosis: Cognitive Impairment and Structural MRI. *Mult. Scler. Int.* 2014.
- Minagar, A. (2015). Multiple Sclerosis: A Mechanistic View (Academic Press).
- Morrison, D.K. (2012). MAP Kinase Pathways. *Cold Spring Harb. Perspect. Biol.* 4, a011254.
- Mortola, J.P., and Dotta, A. (1992). Effects of hypoxia and ambient temperature on gaseous metabolism of newborn rats. *Am. J. Physiol.* 263, R267-272.
- Muller, W.A. (2009). Mechanisms of Transendothelial Migration of Leukocytes. *Circ. Res.* 105, 223–230.
- Muneer, A. (2016). Bipolar Disorder: Role of Inflammation and the Development of Disease Biomarkers. *Psychiatry Investig.* 13, 18–33.
- Murphy, P.M., Baggiolini, M., Charo, I.F., Hébert, C.A., Horuk, R., Matsushima, K., Miller, L.H., Oppenheim, J.J., and Power, C.A. (2000). International Union of Pharmacology. XXII. Nomenclature for Chemokine Receptors. *Pharmacol. Rev.* 52, 145–176.
- Nathan, C. (2002). Points of control in inflammation. *Nature* 420, 846–852.
- Nathan, C., and Ding, A. (2010). Nonresolving Inflammation. *Cell* 140, 871–882.
- Nayak, D., Roth, T.L., and McGavern, D.B. (2014). Microglia Development and Function. *Annu. Rev. Immunol.* 32, 367–402.
- Neher, J.J., Neniskyte, U., Zhao, J.-W., Bal-Price, A., Tolkovsky, A.M., and Brown, G.C. (2011). Inhibition of microglial phagocytosis is sufficient to prevent inflammatory neuronal death. *J. Immunol. Baltim. Md 1950* 186, 4973–4983.
- Nencini, P., Romani, I., Borsini, W., and Inzitari, D. (2013). Fabry Disease and Acute Ischemic Stroke: A Prospective Study in Unselected Adults of Both Gender (P04.069). *Neurology* 80, P04.069-P04.069.
- Neumann, J., Sauerzweig, S., Röncke, R., Gunzer, F., Dinkel, K., Ullrich, O., Gunzer, M., and Reymann, K.G. (2008). Microglia cells protect neurons by direct engulfment of invading neutrophil granulocytes: a new mechanism of CNS immune privilege. *J. Neurosci. Off. J. Soc. Neurosci.* 28, 5965–5975.
- Neuwelt, E.A., Bauer, B., Fahlke, C., Fricker, G., Iadecola, C., Janigro, D., Leybaert, L., Molnár, Z., O'Donnell, M.E., Povlishock, J.T., et al. (2011). Engaging neuroscience to advance translational research in brain barrier biology. *Nat. Rev. Neurosci.* 12, 169–182.
- Obermeier, B., Daneman, R., and Ransohoff, R.M. (2013). Development, maintenance and disruption of the blood-brain barrier. *Nat. Med.* 19, 1584–1596.
- O'Brien, K., Gran, B., and Rostami, A. (2010). T-cell based immunotherapy in experimental autoimmune encephalomyelitis and multiple sclerosis. *Immunotherapy* 2, 99–115.

- Olmos-Alonso, A., Schetters, S.T.T., Sri, S., Askew, K., Mancuso, R., Vargas-Caballero, M., Holscher, C., Perry, V.H., and Gomez-Nicola, D. (2016). Pharmacological targeting of CSF1R inhibits microglial proliferation and prevents the progression of Alzheimer's-like pathology. *Brain* 139, 891–907.
- Piskunov, A.K. (2010). Neuroinflammation biomarkers. *Neurochem. J.* 4, 55–63.
- Podbielska, M., Banik, N.L., Kurowska, E., and Hogan, E.L. (2013). Myelin Recovery in Multiple Sclerosis: The Challenge of Remyelination. *Brain Sci.* 3, 1282–1324.
- Prinz, M., and Priller, J. (2014). Microglia and brain macrophages in the molecular age: from origin to neuropsychiatric disease. *Nat. Rev. Neurosci.* 15, 300–312.
- Proost, P., Wuyts, A., and van Damme, J. (1996). The role of chemokines in inflammation. *Int. J. Clin. Lab. Res.* 26, 211–223.
- Ransohoff, R.M., Kivisäkk, P., and Kidd, G. (2003). Three or more routes for leukocyte migration into the central nervous system. *Nat. Rev. Immunol.* 3, 569–581.
- Redzic, Z. (2011). Molecular biology of the blood-brain and the blood-cerebrospinal fluid barriers: similarities and differences. *Fluids Barriers CNS* 8, 3.
- Rezai-Zadeh, K., Gate, D., and Town, T. (2009). CNS Infiltration of Peripheral Immune Cells: D-Day for Neurodegenerative Disease? *J. Neuroimmune Pharmacol.* 4, 462–475.
- Rm, R., D, S., A, V., Ne, B., and A, B.-O. (2015). Neuroinflammation: Ways in Which the Immune System Affects the Brain., Neuroinflammation: Ways in Which the Immune System Affects the Brain. *Neurother. J. Am. Soc. Exp. Neurother. Neurother.* 12, 12, 896, 896–909.
- Robinson, A.P., Harp, C.T., Noronha, A., and Miller, S.D. (2014). The experimental autoimmune encephalomyelitis (EAE) model of MS: utility for understanding disease pathophysiology and treatment. *Handb. Clin. Neurol.* 122, 173–189.
- Rojas, J.J., Deniz, B.F., Miguel, P.M., Diaz, R., Hermel, É. do E.-S., Achaval, M., Netto, C.A., and Pereira, L.O. (2013). Effects of daily environmental enrichment on behavior and dendritic spine density in hippocampus following neonatal hypoxia–ischemia in the rat. *Exp. Neurol.* 241, 25–33.
- Rumajogee, P., Bregman, T., Miller, S.P., Yager, J.Y., and Fehlings, M.G. (2016). Rodent Hypoxia–Ischemia Models for Cerebral Palsy Research: A Systematic Review. *Front. Neurol.* 7.
- Sabeh, F., Ota, I., Holmbeck, K., Birkedal-Hansen, H., Soloway, P., Balbin, M., Lopez-Otin, C., Shapiro, S., Inada, M., Krane, S., et al. (2004). Tumor cell traffic through the extracellular matrix is controlled by the membrane-anchored collagenase MT1-MMP. *J. Cell Biol.* 167, 769–781.
- Saliba, E., and Henrot, A. (2001). Inflammatory mediators and neonatal brain damage. *Biol. Neonate* 79, 224–227.

Santonen, T., Aitio, A., Fowler, B.A., and Nordberg, M. (2015). Chapter 8 - Biological Monitoring and Biomarkers. In *Handbook on the Toxicology of Metals (Fourth Edition)*, (San Diego: Academic Press), pp. 155–171.

Sasaki, T., Fässler, R., and Hohenester, E. (2004). Laminin: the crux of basement membrane assembly. *J. Cell Biol.* *164*, 959–963.

Sawada, M., Suzumura, A., Yamamoto, H., and Marunouchi, T. (1990). Activation and proliferation of the isolated microglia by colony stimulating factor-1 and possible involvement of protein kinase C. *Brain Res.* *509*, 119–124.

Schmitt, A., Malchow, B., Hasan, A., and Fallkai, P. (2014). The impact of environmental factors in severe psychiatric disorders. *Front. Neurosci.* *8*.

Schmitz, J., Owyang, A., Oldham, E., Song, Y., Murphy, E., McClanahan, T.K., Zurawski, G., Moshrefi, M., Qin, J., Li, X., et al. (2005). IL-33, an interleukin-1-like cytokine that signals via the IL-1 receptor-related protein ST2 and induces T helper type 2-associated cytokines. *Immunity* *23*, 479–490.

Shimizu, T., Smits, R., and Ikenaka, K. (2016). Microglia-Induced Activation of Noncanonical Wnt Signaling Aggravates Neurodegeneration in Demyelinating Disorders. *Mol. Cell. Biol.* *36*, 2728–2741.

Sierra, A., Abiega, O., Shahraz, A., and Neumann, H. (2013). Janus-faced microglia: beneficial and detrimental consequences of microglial phagocytosis. *Front. Cell. Neurosci.* *7*, 6.

Skundric, D.S. (2005). Experimental models of relapsing-remitting multiple sclerosis: current concepts and perspective. *Curr. Neurovasc. Res.* *2*, 349–362.

Smith, M.E. (1999). Phagocytosis of myelin in demyelinating disease: a review. *Neurochem. Res.* *24*, 261–268.

Song, J., Wu, C., Zhang, X., and Sorokin, L.M. (2013). In Vivo Processing of CXCL5 (LIX) by Matrix Metalloproteinase (MMP)-2 and MMP-9 Promotes Early Neutrophil Recruitment in IL-1 β -Induced Peritonitis. *J. Immunol.* *190*, 401–410.

Song, J., Wu, C., Korpos, E., Zhang, X., Agrawal, S.M., Wang, Y., Faber, C., Schäfers, M., Körner, H., Opdenakker, G., et al. (2015). Focal MMP-2 and MMP-9 activity at the blood-brain barrier promotes chemokine-induced leukocyte migration. *Cell Rep.* *10*, 1040–1054.

Sorokin, L. (2010). The impact of the extracellular matrix on inflammation. *Nat. Rev. Immunol.* *10*, 712–723.

Sparacio, S.M., Zhang, Y., Vilcek, J., and Benveniste, E.N. (1992). Cytokine regulation of interleukin-6 gene expression in astrocytes involves activation of an NF- κ B-like nuclear protein. *J. Neuroimmunol.* *39*, 231–242.

Stadelmann, C. (2011). Multiple sclerosis as a neurodegenerative disease: pathology, mechanisms and therapeutic implications. *Curr. Opin. Neurol.* *24*, 224–229.

- Stamatovic, S.M., Keep, R.F., and Andjelkovic, A.V. (2008). Brain Endothelial Cell-Cell Junctions: How to “Open” the Blood Brain Barrier. *Curr. Neuropharmacol.* 6, 179–192.
- Stoll, G., and Jander, S. (1999). The role of microglia and macrophages in the pathophysiology of the CNS. *Prog. Neurobiol.* 58, 233–247.
- Stone, S., and Flamme, A.C.L. (2016). Type II Activation of Macrophages and Microglia by Immune Complexes Enhances Th17 Biasing in an IL-6-Independent Manner. *PLOS ONE* 11, e0164454.
- Streit, W.J., Walter, S.A., and Pennell, N.A. (1999). Reactive microgliosis. *Prog. Neurobiol.* 57, 563–581.
- Streit, W.J., Mrak, R.E., and Griffin, W.S.T. (2004). Microglia and neuroinflammation: a pathological perspective. *J. Neuroinflammation* 1, 14.
- ‘t Hart, B.A., van Kooyk, Y., Geurts, J.J.G., and Gran, B. (2015). The primate autoimmune encephalomyelitis model; a bridge between mouse and man. *Ann. Clin. Transl. Neurol.* 2, 581–593.
- Takao, K., Tanda, K., Nakamura, K., Kasahara, J., Nakao, K., Katsuki, M., Nakanishi, K., Yamasaki, N., Toyama, K., Adachi, M., et al. (2010). Comprehensive Behavioral Analysis of Calcium/Calmodulin-Dependent Protein Kinase IV Knockout Mice. *PLOS ONE* 5, e9460.
- Tang, Y., and Le, W. (2016). Differential Roles of M1 and M2 Microglia in Neurodegenerative Diseases. *Mol. Neurobiol.* 53, 1181–1194.
- Tanuma, N., Sakuma, H., Sasaki, A., and Matsumoto, Y. (2006). Chemokine expression by astrocytes plays a role in microglia/macrophage activation and subsequent neurodegeneration in secondary progressive multiple sclerosis. *Acta Neuropathol. (Berl.)* 112, 195–204.
- Thameem Dheen, S., Kaur, C., and Ling, E.-A. (2007). Microglial Activation and its Implications in the Brain Diseases. *Curr. Med. Chem.* 14, 1189–1197.
- Theocharis, A.D., Skandalis, S.S., Gialeli, C., and Karamanos, N.K. (2016). Extracellular matrix structure. *Adv. Drug Deliv. Rev.* 97, 4–27.
- Trapp, B.D., and Nave, K.-A. (2008). Multiple sclerosis: an immune or neurodegenerative disorder? *Annu. Rev. Neurosci.* 31, 247–269.
- Turner, M.D., Nedjai, B., Hurst, T., and Pennington, D.J. (2014). Cytokines and chemokines: At the crossroads of cell signalling and inflammatory disease. *Biochim. Biophys. Acta BBA - Mol. Cell Res.* 1843, 2563–2582.
- Van den Steen, P.E., Wuyts, A., Husson, S.J., Proost, P., Van Damme, J., and Opdenakker, G. (2003). Gelatinase B/MMP-9 and neutrophil collagenase/MMP-8 process the chemokines human GCP-2/CXCL6, ENA-78/CXCL5 and mouse GCP-2/LIX and modulate their physiological activities. *Eur. J. Biochem.* 270, 3739–3749.

- Varatharaj, A., and Galea, I. (2017). The blood-brain barrier in systemic inflammation. *Brain. Behav. Immun.* *60*, 1–12.
- Vezzani, A., and Friedman, A. (2011). Brain inflammation as a biomarker in epilepsy. *Biomark. Med.* *5*, 607–614.
- Wang, S., Zhang, H., and Xu, Y. (2016). Crosstalk between microglia and T cells contributes to brain damage and recovery after ischemic stroke. *Neurol. Res.* *38*, 495–503.
- Wang, W., Lu, R., Feng, D.-Y., Liang, L.-R., Liu, B., and Zhang, H. (2015a). Inhibition of microglial activation contributes to propofol-induced protection against post-cardiac arrest brain injury in rats. *J. Neurochem.* *134*, 892–903.
- Wang, W.-Y., Tan, M.-S., Yu, J.-T., and Tan, L. (2015b). Role of pro-inflammatory cytokines released from microglia in Alzheimer's disease. *Ann. Transl. Med.* *3*.
- Wu, C., Ivars, F., Anderson, P., Hallmann, R., Vestweber, D., Nilsson, P., Robenek, H., Tryggvason, K., Song, J., Korpos, E., et al. (2009). Endothelial basement membrane laminin alpha5 selectively inhibits T lymphocyte extravasation into the brain. *Nat. Med.* *15*, 519–527.
- Zigmond, M.J., Coyle, J.T., and Rowland, L.P. (2014). *Neurobiology of Brain Disorders: Biological Basis of Neurological and Psychiatric Disorders* (Elsevier).